# Impact of Wildfire on Annual Water Yield in Large Watersheds

A Dissertation

Presented in Partial Fulfillment of the Requirements for the

Degree of Doctor of Philosophy

with a

Major in Civil Engineering

in the

College of Graduate Studies

University of Idaho

by

Sangki Lee

Major Professor: Daniele Tonina, Ph.D.

Committee Members: Charles Luce, Ph.D.; Elowyn Yager, Ph.D., P.G.;

Peter Goodwin, Ph.D., P.E.

Department Administrator: Patricia J. S. Colberg, Ph.D., P.E.

May 2020

**Authorization to Submit Dissertation**

This dissertation of Sangki Lee, submitted for the degree of Doctor of Philosophy with a Major in Civil Engineering and titled "Impact of Wildfire on Annual Water Yield in Large Watersheds," has been reviewed in final form. Permission, as indicated by the signatures and dates below, is now granted to submit final copies to the College of Graduate Studies for approval.

Major Professor: _____ Date: _____
Daniele Tonina, Ph.D.

Committee Members: _____ Date: _____
Charles Luce, Ph.D.

_____ Date: _____
Elowyn Yager, Ph.D., P.G.

_____ Date: _____
Peter Goodwin, Ph.D., P.E.

Department Administrator: _____ Date: _____
Patricia J. S. Colberg, Ph.D., P.E.

## Abstract

Available studies on the effects of wildfire on water yield were conducted in small size watersheds (<10km$^2$) and little is known on the scalability of those findings to large watersheds. However, the frequency and occurrence of wildfires that burn large watersheds (>100km$^2$) have been increasing in the last decades, resulting on the need to predict their impacts on watershed hydrology. The impact of wildfire on watershed annual water yield is constrained by a complex interaction among several processes, which include hydrologic, geologic, ecologic, climatic alterations. This study investigates short- and long-term responses of annual water yield changes due to wildfire in large watersheds within a paired watershed framework. We, also, propose a new theoretical approach based on the Budyko framework to predict the change in annual water yield due to wildfires, which was originally proposed to explore alterations of water and energy balance within burned watersheds. Long-term responses of annual water yield were predicted by analyzing residuals between annual water yields measured in the field and estimated with paired watershed regression models. Paired watershed analyses were applied to 34 pairs between 11 burned watersheds and 8 unburned watersheds in the Salmon River and Payette River basin (Central Idaho USA), Yellowstone National Park (Wyoming, USA), and Klamath River basin (California, USA). The Budyko framework was conducted in 8 burned watersheds for 10 wildfires, were statistically significant from paired watershed analyses. The Budyko framework was applied both at the yearly time scale (one point for each year) and as originally developed as time averaged (one point for pre and one for post-fire period). This study employed (1) a simple linear model with evaporative index (AET/P) and (2) *Fu* [1981]'s equation with relative evaporative index (1-Q/P). Results show that annual water yield generally increases after wildfires that burned more than 10% of drainage area with negligible and undetectable changes for smaller burned areas. Exceptions to this trend are for watersheds whose hydrological system is dominated by baseflows (with large ground water storage) and those whose wildfire mainly burned short vegetation. Annual water yield tends to return toward pre-fire condition following the Kuczera's curve, which is related with changes in water demand following

regrowth or resuccession of burned trees/vegetation. Post-fire annual water yield increased with burned area, and this correlation was more evident in Mediterranean than in arid climate regions. Post-fire change in annual water yield increases proportionally with drainage area in small watersheds, but this relationship is limited in large watersheds. Results of the Budyko framework show decrease in evapotranspiration rate in most burned watersheds. Reduction in evapotranspiration results in an increase of annual water yield. On the other hand, increase in evaporative index was detected in burned watershed where trees grew quickly during the post-fire period. Climatic conditions can affect the hydrological response during post-fire. Weather condition is an important factor for estimating the annual water yield responses against wildfire. Budyko framework shows that wildfire impact is mitigated under wet weather condition or enhanced under dry weather condition. Results of paired watershed analysis and Budyko framework show a good agreement that post-fire annual water yield responses are strongly correlated with changes in evapotranspiration rate associated with tree mortality or regrowth rate.

**Acknowledgements**

I would like to thank my advisor, Dr. Daniele Tonina. I am happy that I have him as my advisor during my graduate studies. His consistent and insightful guidance and continual support have helped me to overcome all of obstacles that I had during my studies. His knowledge as well as passion will continue to inspire me in my future carrier. I would specially like to thank my committee members, Dr. Charles Luce, Dr. Elowyn Yager, Dr. Peter Goodwin for their support and assistance throughout the entire process. I also give special thanks to my colleagues for valuable discussions.

Sangki Lee

**Dedication**

to my family

to Dr. Sangil Lee

with all the love and appreciation

## Table of Contents

## List of Tables

## List of Figures

# CHAPTER 1: IMPACTS OF WILDFIRES AND BURNED LANDCOVER ON ANNUAL WATER YIELD IN LARGE WATERSHEDS USING PAIRED WATERSHED ANALYSIS

**Abstract**

The frequency and occurrence of wildfires in large watersheds (>100 $km^2$) has been increasing in recent decades. The majority of studies on the effects of wildfire on water yield have been conducted in small size watersheds (<10 $km^2$) and questions remain regarding transferability to large watersheds. This study investigates the response of annual water yield shortly after wildfire and during recovery in large watersheds using a paired-watershed framework. Long-term responses of annual water yield were studied by analyzing residuals between annual water yields measured in the field and estimated with paired-watershed regression models. Analyses were applied to 34 pairs drawn from 11 burned watersheds and 8 unburned watersheds in the Salmon Payette River basins of Central Idaho USA, the Yellowstone National Park (Wyoming, USA) and Klamath River basin in northern California, USA. Results show that annual water yield generally increases after wildfires that burned more than 10% of drainage area with more than 5% of forest suffering permanent mortality. Conversely, decreases in annual water year were observed for watersheds where permanent tree mortality was negligible (<5%) and where wildfire mainly burned short vegetation. Post-fire annual water yield tends to return toward pre-fire condition over time, related to changes in water demand following regrowth of burned landcover. Post-fire annual water yield increased with extent of wildfire within the basin. The magnitude of the impact of wildfire on annual water yield in large watersheds is less than in small watersheds for a given fraction of basin burned.

**Key words:** Wildfire, Annual Water Yield, Paired Watershed Analysis, Long-term response, Size effect

## 1 Introduction

Wildfires occur more often, and its extent and severity has increased in the western US (Morgan *et al.*, 2008; Dillon *et al.*, 2011; Dennison *et al.*, 2014). Frequency and extent of wildfire have increased in North America along with the frequency and severity of droughts (Dennison *et al.*, 2014; Littell *et al.*, 2016). Exhaustion of soil and atmospheric moisture enhances the flammability and availability of land surface fuel, which consequently increases the probability of wildfires (Swetnam and Betancourt, 1998). Wildfire is a key agent for hydrological and geomorphological processes (Bart and Hope, 2010; Lane *et al.*, 2010; Vieira *et al.*, 2015; Zhou *et al.*, 2015) and is fundamental for forest ecosystem (Dudgeon, 2000; Pringle, 2003; Luce *et al.*, 2012; Shakesby *et al.*, 2016) as it re-starts the ecosystem cycle. It burns forest, kills0 animals, and deteriorates stream water quality due to increased inputs of debris and sediments (Luce *et al.*, 2012; Smith *et al.*, 2012; Moody *et al.*, 2013; Shakesby *et al.*, 2016). It alters hydrological components such as soil repellency (Scott and Van Wyk, 1990; Martin and Moody, 2001; Varela *et al.*, 2005), evapotranspiration (Helvey, 1980; Wine and Cadol, 2016), peak time and discharge (Versini *et al.*, 2013; Mahat *et al.*, 2016) and annual water yield (Berndt, 1971; Helvey, 1980; Martin and Moody, 2001; Bart, 2016; Hallema *et al.*, 2018).

Altered hydrologic cycle (i.e., evaporation, transpiration, infiltration and precipitation) is the fundamental cause for post-fire annual water yield changes from pre-fire conditions (Adams *et al.*, 2012). Previous studies showed that impacts of wildfire on each hydrologic component are greatly interconnected with climate change, landcover type and/or regrowth or re-succession of burned landcover processes (Bart and Hope, 2010; Lane *et al.*, 2010; Vieira *et al.*, 2015; Zhou *et al.*, 2015). Significant amount of reduction in forested area due to permanent tree mortality following wildfire results in annual water yield increases due to reduced water demand through vegetation consumption (evapotranspiration). In the long-term, as re-growing or/and re-generation of burned vegetation occurs, annual water yield is expected to approach pre-wildfire conditions due to vegetation water demand.

Adequate estimation of annual water yield is essential for sustainable development of both human society and ecosystems (Bales *et al.*, 2006; Liu *et al.*, 2008); thus, better understanding about post-fire response of annual water yield is required for proper water resources management plan. This is much needed in large (>100 $km^2$) and very large (>1,000 $km^2$) watersheds where limited information is available on post-fire response of annual water yield. Detailed mechanisms of post-fire alterations are well understood from both numerical modeling and field data analysis in small watersheds. In these watersheds, fire-induced changes in annual water yield have been associated to burned land cover induced changes in evapotranspiration rate (Scott, 1993; Hessling, 1999; Lane *et al.*, 2006; Stoof *et al.*, 2012; Bart and Tague, 2017) caused by tree/vegetation mortality and their regrowth (Kuczera, 1987; Lane *et al.*, 2010). Mature vegetation and regrowth of young vegetation are key factors influencing annual water yield (Helvey, 1980; Hibbert, 1983; Brooks *et al.*, 1997), such that permanent tree mortality after wildfire or their replacement by short vegetation results in a decrease in water demand. As a result, post-fire annual water yield increases as reported by Helvey (1980) due to post-fire reduction of evapotranspiration in a burned watershed in north central Washington. Conversely, fast regrowth may lead to decrease in annual water yield after wildfire as documented in the Cascade crest, Oregon, after wildfire burned needle leaf trees (Berndt, 1971). On the other hand, water yield increased due to decreased infiltration capacity in Los Alamos, New Mexico, whose forest type is mixed with needle leaf and broad leaf trees such as Ponderosa pine, Douglas-fir, Aspen and Juniper (Martin and Moody, 2001).

Other studies on the impact of changes of land cover type like timber harvest or agriculture may provide information on fire-induced water yield response. Bosch and Hewlett (1982) and (Stednick, 1996) synthesized that the amount of increased annual water yield and percentage of cover loss by logging are linearly correlated in small experimental watersheds (<10$km^2$). Here we will test if this also holds for large watersheds, where the evaluation of the post-fire responses of annual water yield is challenging due to increase complexity of alterations in hydrologic components (Thanapakpawin *et al.*, 2007; Wei and Zhang, 2010) and spatial and temporal variability of disturbances (Wilk *et al.*, 2001). Similarly, wildfire as a

disturbance may be affected by more challenging difficulties as logging because large wildfire may be highly heterogeneous as severity and distribution.

Analysis of the post-fire alterations in the hydrologic cycle is more difficult in large than small watersheds due to limitations in accurate observations of hydrologic or geologic variables. Large wildfires have more spatial heterogeneity in terms of wildfire location, burned forest type and severity than small wildfire resulting in more difficulties in documenting, surveying and controlling wildfires in large watersheds. Post-fire response of annual water yield can be misunderstood in large watersheds due to increased complexity and uncertainty of hydrologic components (Thanapakpawin *et al.*, 2007; Wei and Zhang, 2010). Further, climatic variability together with burned land cover and vegetation regrowth distributions plays an important role on post-fire response of annual water yield as the spatial scale of watersheds gets larger (Hallema *et al.*, 2018; Wine *et al.*, 2018). Consequently, these heterogeneities may lead to different alterations of the hydrologic cycle in large watersheds compared to those in small watersheds, such that upscaling our understanding gained from small-scale to large watersheds may be difficult.

Consequently, impacts of wildfire on annual water yield in large watersheds, whose drainage area is larger than several hundred square kilometers are getting recently more attention (Luce *et al.*, 2012; Wine and Cadol, 2016; Hallema *et al.*, 2018), and their findings show inconsistent post-fire response of annual water yield. Luce *et al.* (2012) found increase in post-fire annual water yield in the Middle Fork of the Boise River watershed (A=2,150 $km^2$), whereas Wine and Cadol (2016) reported statistically insignificant changes in post-fire annual water yield in the Gila watersheds in New Mexico (A=4,807 $km^2$). Most recently, Hallema *et al.* (2018) showed a general increasing trend in post-fire annual water yield from watersheds whose drainage area ranges from 10 to 100,000 $km^2$ using a complex analytical model with a limitation in terms of engineering simplicity.

The objective of this study is to expand the knowledge of the impact of wildfire on annual water yield in large watersheds based on measured data. This study examined changes in annual water yield at the short term after wildfire in large watersheds throughout the

United States by employing paired watershed analysis, which provides data-based information about post-fire response of annual water yield. It examined the effects of landcover composition of pre-fire period and permanent tree mortality on post-fire response in annual water yield. To examine the effect of burned forest type, this study developed a simple analytical model for the estimation of post-fire response of annual water yield linked with fractions of pre-fire forested area and post-fire permanently dead forest. It also assessed long-term behavior of post-fire annual water yield, which is a function of burned landcover and their regrowth. It also evaluated the effect of spatial scale of burned watersheds for post-fire response of annual water yield.

## 2 Study Sites and Data Acquisition

### 2.1 Study Sites

We selected large wildfire burned watersheds (>100 $km^2$) in the western U.S., as study sites, considering availability of pre and post discharge records of both burned and nearby unburned (control) watersheds (Figure 1.1). Burned and control watersheds were categorized based on a threshold of 10% of burned area of the total drainage area during a water year. A total of 11 burned watersheds and 8 control watersheds were identified (Table 1.1). Control and burned watersheds were paired considering data availability near the time of major wildfires (Figure 1.2).

The upper and lower watersheds of the Klamath River basin (NCA; Figure 1.1) are in alpine highland and Mediterranean climate regions, respectively. Watersheds in the central Idaho area (CID; Figure 1.1) are in a semi-arid mountain climate region. The Yellowstone National Park watersheds (YNP; Figure 1.1) are in an alpine highland climate region. NCA is located at elevation ranges about 150 ~ 4,300m, and CID and YNP are located at elevation rages about 1,000~3,500m (Table 1.1). The study sites are dominated by needle leaf forest (~70%; Figure 1.3; Figure 1.5) and partially covered by shrub and short vegetation (~30%; Figure 1.3; Figure 1.5).

Despite numerous watersheds having gauge data in these areas (Figure 1.1), only a few were suitable for analysis considering length and continuity of record, particularly around major fire years, or upstream regulation. In central Idaho, we used basins CID0, CID1, CID2, CID3, CID6, CID7, and CID8; in Northern California, we used NCA0, NCA1, NCA2, and NCA3; and in Yellowstone National Park we used YNP0, YNP1, YNP2, YNP5, YNP6, YNP7, and YNP10). Most of the central Idaho (CID0, CID1, CID2, CID7, and CID8) watersheds and northern California (NCA0, NCA1, and NCA3) watersheds and all of the Yellowstone National Park watersheds were headwater watersheds independent of one another. In central Idaho, CID2 is upstream of CID3, and CID4 and CID5 are upstream of CID6; and in northern California, NCA0 and NCA1 are upstream of NCA2.

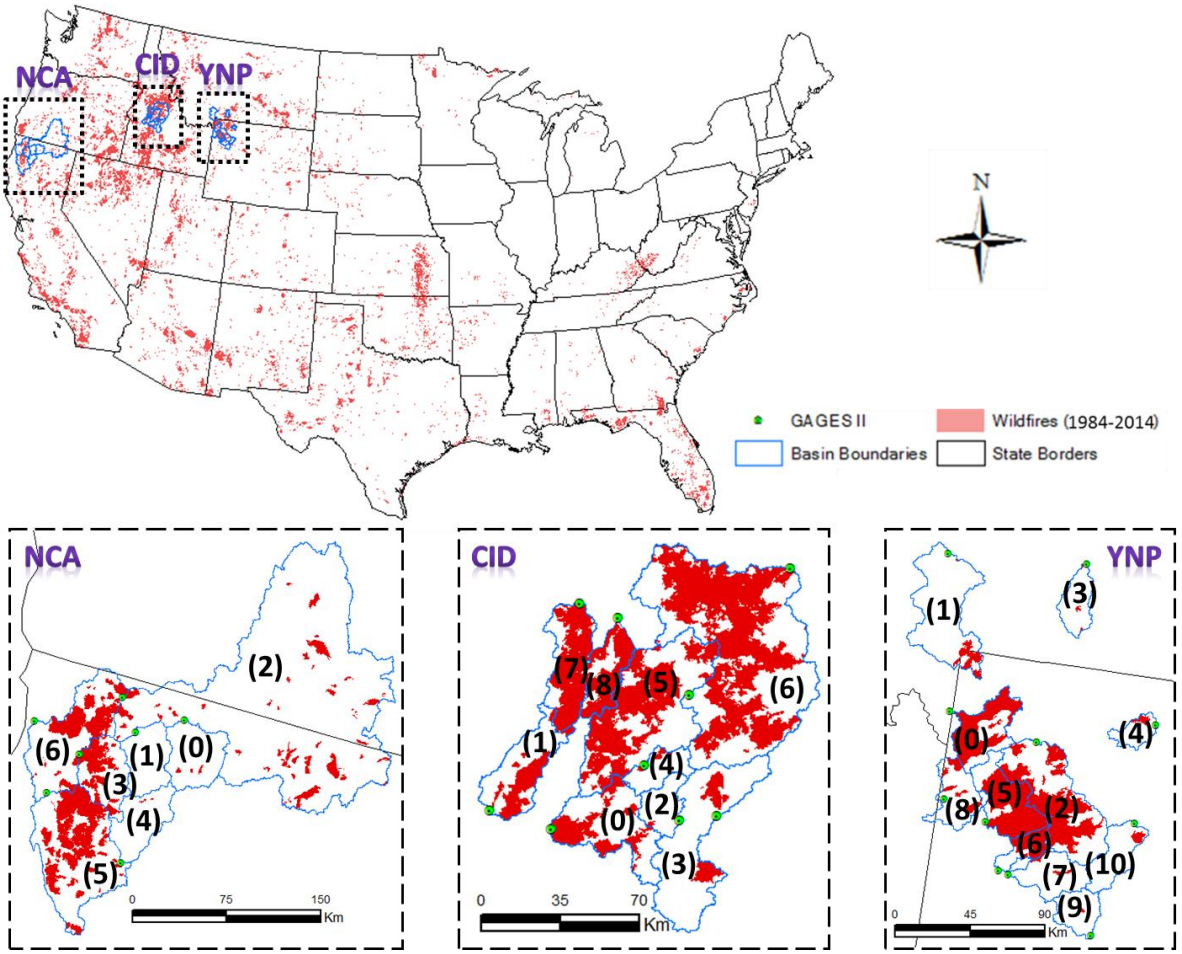


**Figure 1.1** Wildfires between 1984 and 2014 in study sites: NCA (the Klamath River Basin in Oregon-California), CID (Rocky Mountains in central Idaho) and YNP (the Yellowstone National Park).

**Table 1.1** Summary of watersheds and wildfires. Shaded and open rows indicate burned and control watersheds, respectively. CID4; YNP3, 4, 8 and 9 from Figure 1.1 were excluded due to lack of discharge data around wildfire year. NCA4 and its downstream watersheds NCA5 and 6 from Figure 1.1 were excluded due to dam regulation in NCA4. Gauge information is listed in Supplementary Table 1.1.

| Site | Water-shed ID | Gauge ID | Drainage Area ($km^2$) | Gauge E.L. (m) | Elevation Range (m) | | | | Cumulative Burned Area by 2014 (%) |
|---|---|---|---|---|---|---|---|---|---|
| | | | | | Watershed | | Wildfire | | |
| | | | | | min | max | min | max | |
| CID | 0 | 13235000 | 1163.2 | 1155.2 | 1148 | 3213 | 1164 | 2862 | 35.4 |
| | 1 | 13237920 | 874.8 | 926.6 | 912 | 2583 | 917 | 2583 | 34.6 |
| | 2 | 13295000 | 376.4 | 1896.4 | 1891 | 3222 | 2243 | 2894 | 1.7 |
| | 3 | 13296500 | 2090.9 | 1798.3 | 1798 | 3288 | 1859 | 3072 | 9.6 |
| | 5 | 13309220 | 2696.6 | 1335.0 | 1331 | 2981 | 1405 | 2981 | 49.9 |
| | 6 | 13310199 | 7451.0 | 926.6 | 921 | 3160 | 921 | 3014 | 54.1 |
| | 7 | 13310700 | 853.1 | 1143.0 | 1143 | 2786 | 1143 | 2786 | 89.9 |
| | 8 | 13313000 | 561.9 | 1419.1 | 1417 | 2777 | 1417 | 2777 | 86.7 |
| YNP | 0 | 06037500 | 1126.3 | 2026.0 | 2024 | 2875 | 2024 | 2862 | 67.3 |
| | 1 | 06043500 | 2120.4 | 1582.0 | 1581 | 3420 | 2090 | 3021 | 6.7 |
| | 2 | 06186500 | 2516.1 | 2374.0 | 2350 | 3679 | 2350 | 3296 | 51.1 |
| | 5 | 13010065 | 1222.3 | 2073.1 | 2070 | 3121 | 2070 | 3121 | 74.9 |
| | 6 | 13011500 | 404.1 | 2048.3 | 2043 | 3071 | 2465 | 3071 | 66.3 |
| | 7 | 13011900 | 851.8 | 2076.0 | 2066 | 3449 | 2336 | 3111 | 5.5 |
| | 10 | 06280300 | 794.0 | 1894.0 | 1889 | 3776 | 2273 | 3246 | 5.1 |
| NCA | 0 | 11517500 | 2047.3 | 616.8 | 616 | 4305 | 851 | 2051 | 1.5 |
| | 1 | 11519500 | 1713.6 | 809.2 | 805 | 2596 | 1598 | 1674 | 0.0 |
| | 2 | 11520500 | 27502.8 | 407.1 | 406 | 4305 | 406 | 2161 | 4.2 |
| | 3 | 11522500 | 1943.1 | 148.9 | 149 | 2680 | 149 | 2337 | 48.5 |

## 2.2 Data Acquisition

### 2.2.1 Annual Water Yield

Discharge data for annual water yield based on water year from 1950 to 2016 was obtained from the USGS National Water Information System (USGS NWIS; http://waterdata.usgs.gov/nwis) (Figure 1.2). Some gauges have missing data for reasons such as site closure or a damaged gauge. Control and burned watersheds were paired considering data availability near the time of major wildfires of each burned watershed:

control CID2 with burned CID0, 1, 6, 7, 8; control CID3 with burned CID0, 1, 5, 7, 8; control YNP1, 7, 10 with burned YNP0, 2, 5, 6; control NCA0, 1, 2 with burned NCA3. A total of 34 pairs of watersheds were selected for the paired watershed analysis.

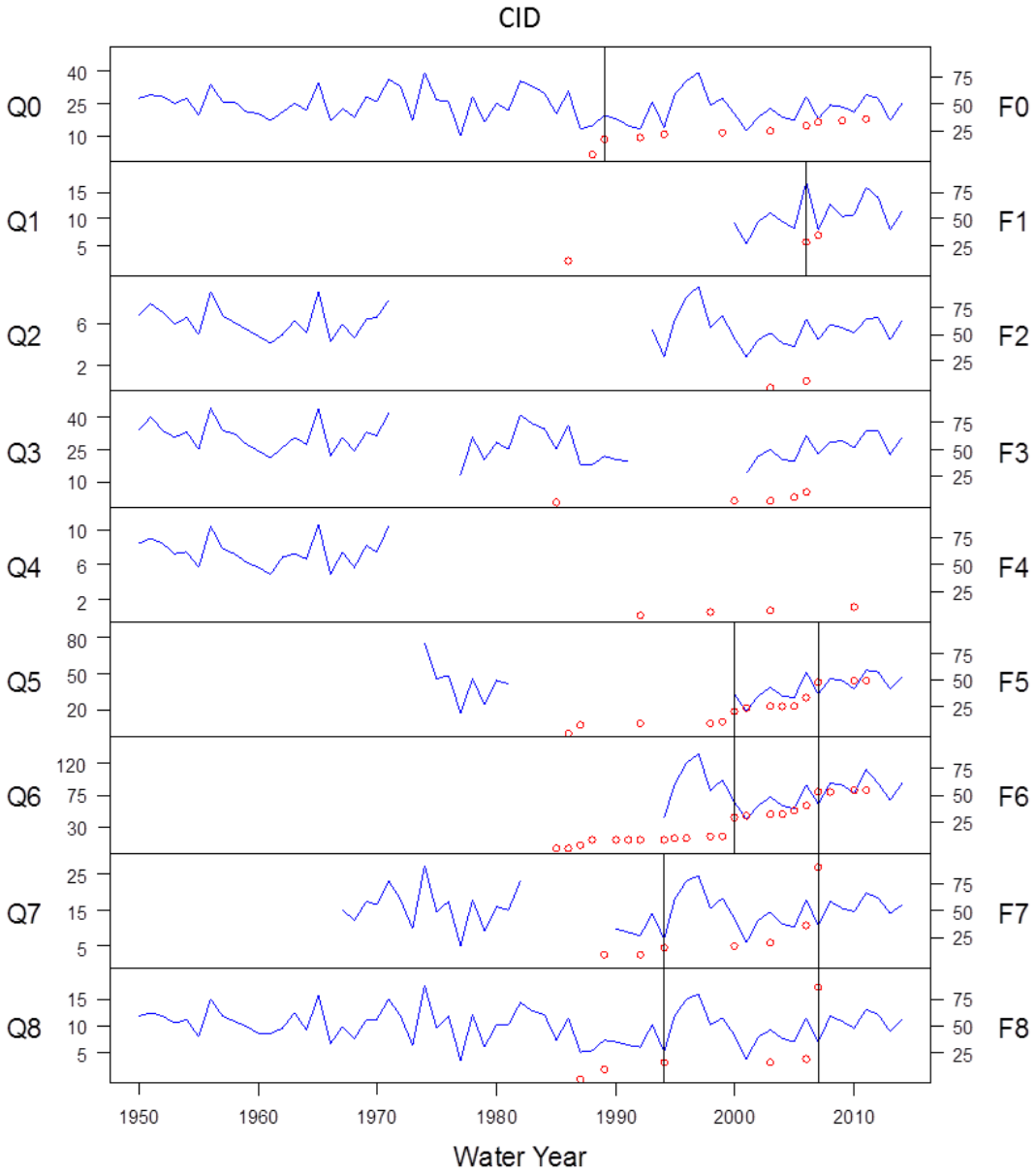


**Figure 1.2** Annual water yield (Q [$m^3/s$]; blue-line) and cumulative percent burned area (F [%]; red-dot) of the study sites (CID, YNP and NCA). Vertical reference lines indicate major wildfire years. 16.9% of CID0 was burned in 1989; 16.5% of CID1 was burned in 2006; 20.6% and 15.0% of CID5 was burned in 2000 and 2007; 17.5% and 12.5% of CID6 was burned in 2000 and 2007; 15.8% and 67.9% of CID7 was burned in 1994 and 2007; and 15.9% and 54.5% of CID8 was burned in 1994 and 2007. 65.9% of YNP0, 40.2% of YNP2, 74.4% of YNP5 and 56.9% of YNP6 were burned in 1988. 19.8% and 26.9% of NCA3 was burned in 1987 and 2008.

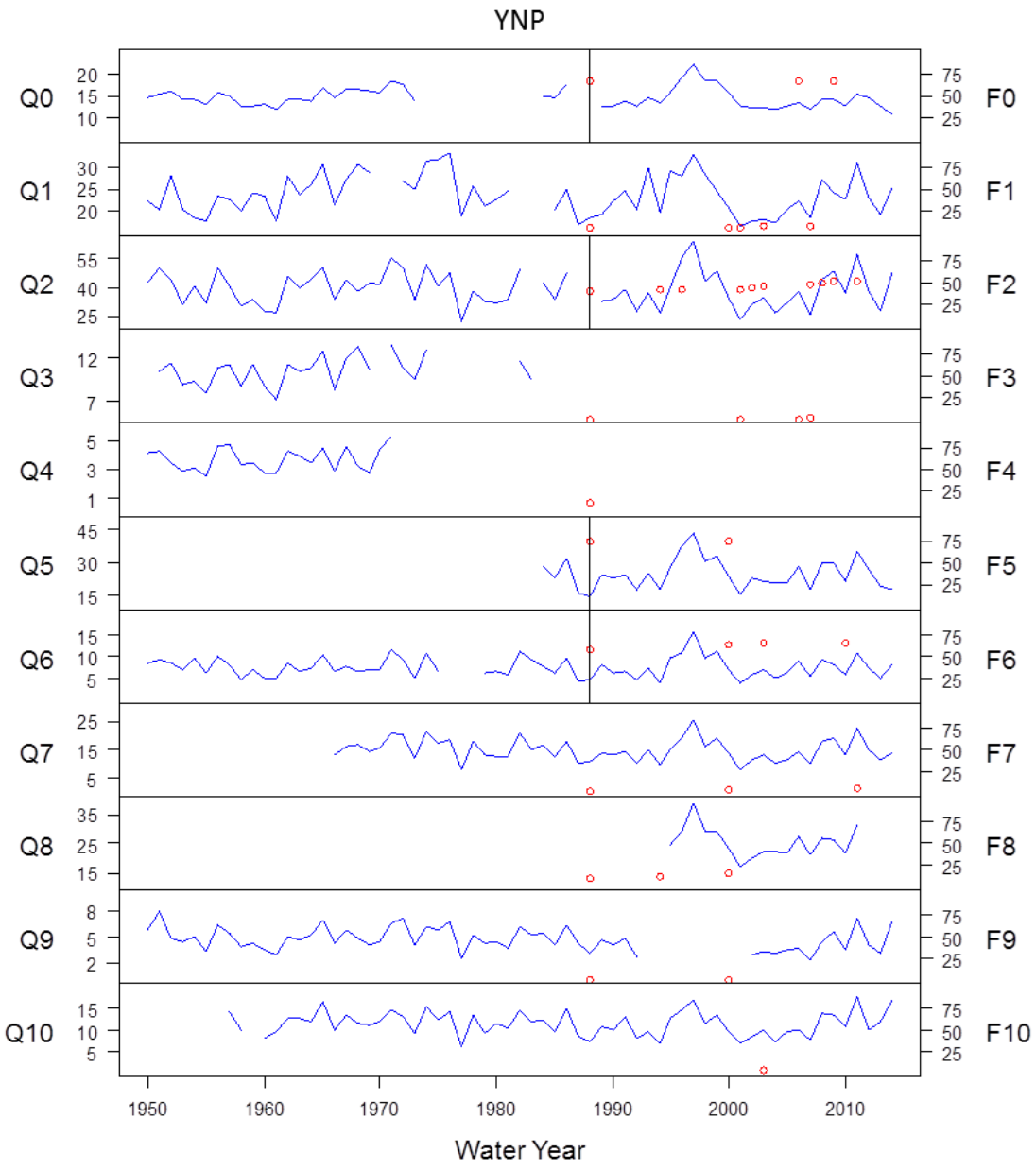


**Figure 1.2** Continue.

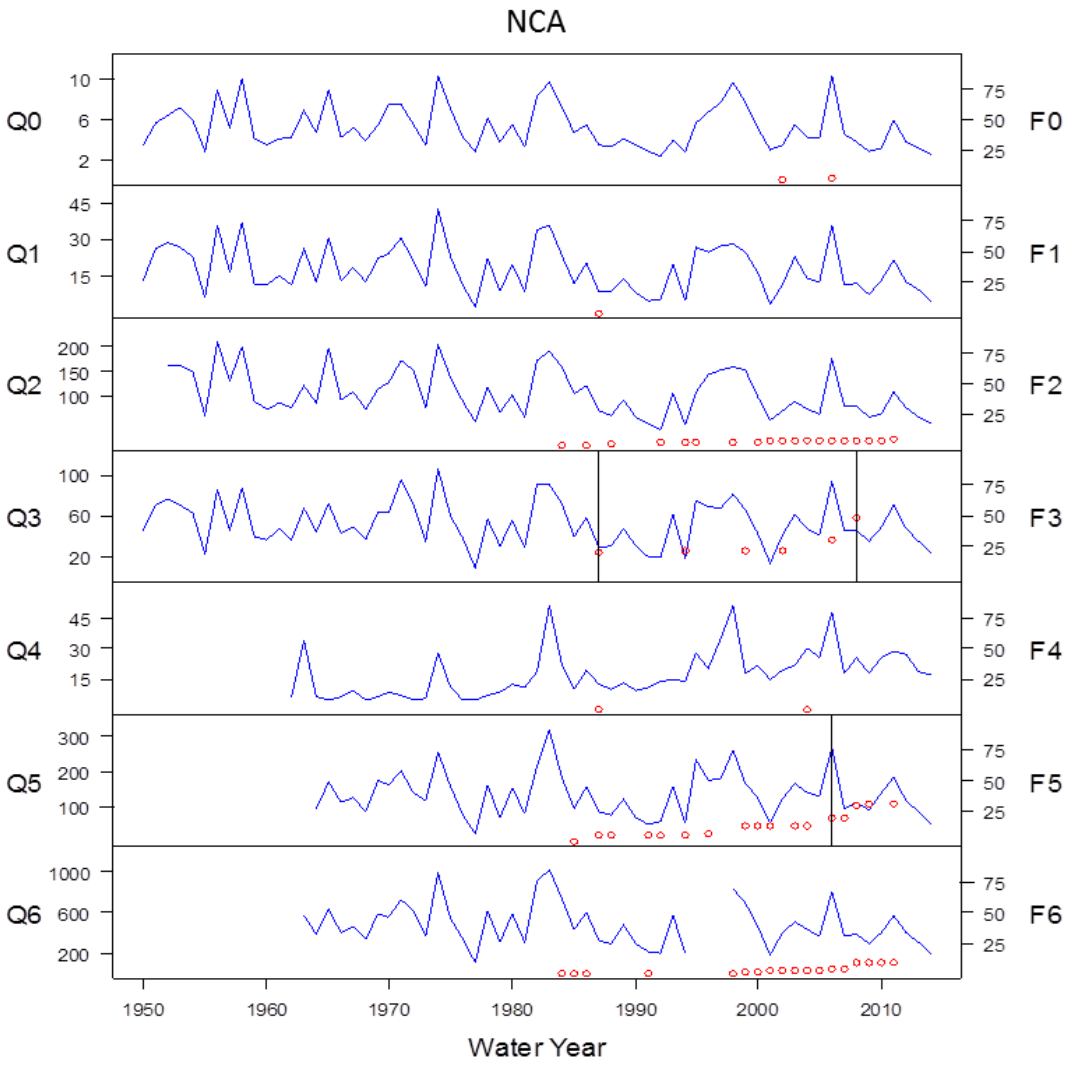


**Figure 1.2** Continue.

### 2.2.2 Historic Wildfire

Historic wildfire extent and event date for wildfires between 1984 and 2014 was obtained from Monitoring Trends in Burn Severity (MTBS; http://www.mtbs.gov) (Figure 1.1; Figure 1.2). All wildfire events between 1984 to 2014 were overlapped in GIS, and total burned area was about 30 to 90% of burned watersheds. Burned area was calculated as the sum of extents of all wildfires within water year divided by total drainage area (%; $km^2/km^2$). We designated burned watersheds as those exceeding 10% burned area by single fire event. Control watersheds (CID2, CID3, YNP1, YNP7, YNP10, NCA0, NCA1 and NCA2) experienced

burning on less than 1% of the total drainage area by individual wildfires during the study period, and cumulative burned area from 1984 to 2014 was less than 10% of drainage area.

### 2.2.3 Landcover Type

We obtained 30 meter resolution National Land Cover Databases (NLCD) for the 1992, 2001, 2006 and 2011 year from the Multi-Resolution Land Characteristics Consortium (MRLC; http://www.mrlc.gov) (Figure 1.3). Because landcover data is not available in every year, wildfires that occurred in 1987, 1988, 1989, 1994, 2000, 2007 and 2008 do not have landcover data immediately before the fire.

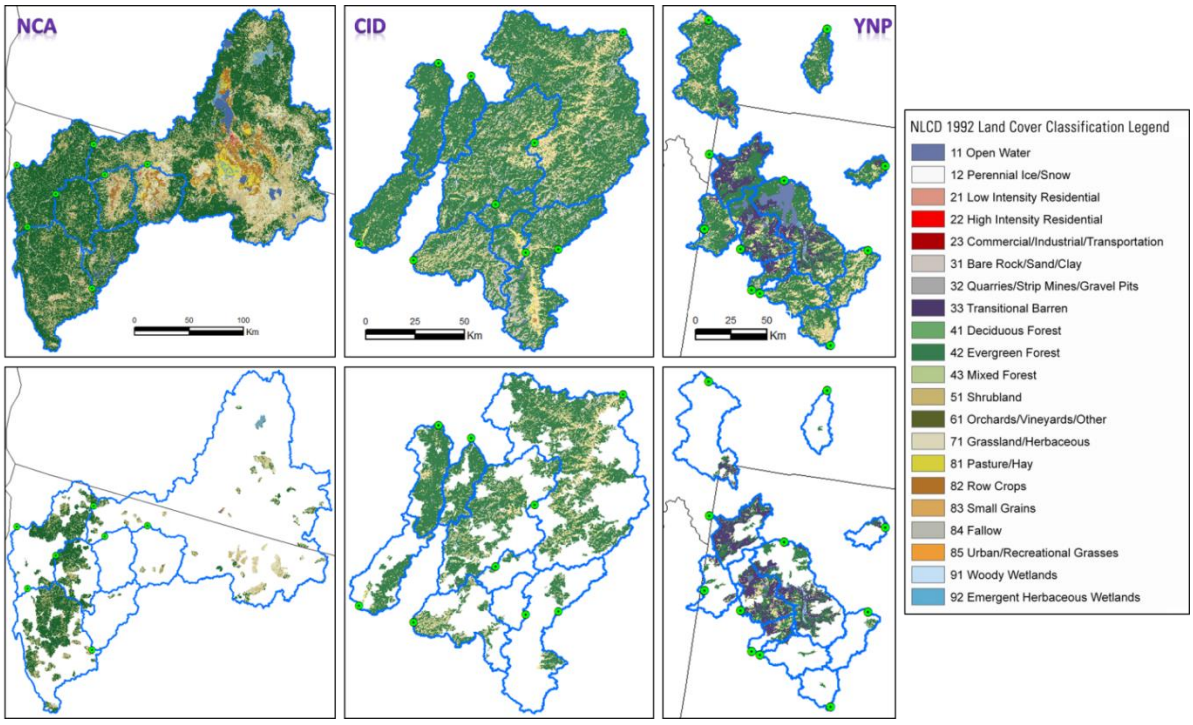


**Figure 1.3** 30-meter resolution landcover measured in 1992 (NLCD 1992; top row), burned landcover corresponds to overlapped wildfire during study period from 1984 to 2014 (bottom row) and landcover classification.

# 3 Methods

## 3.1 Wildfire Impacts on Annual Water Yield

This study investigated wildfire impacts on annual water yield in large-scale watersheds with a paired watershed analysis using multiple linear regression. The paired watershed framework has been applied to hydrologic and ecologic analyses due to its simplicity, and it has been previously used for analysis of water yield responses against wildfires (Campbell *et al.*, 1977; Scott, 1993). It assumes that the post-fire period is long enough that parameters can be estimated assuming stationarity, so we checked the length of the post-fire observation period used for the analysis by looking at the behavior of the residuals. Otherwise, if post-fire conditions return to pre-fire conditions rapidly (within a few years), the model could underestimate the impact of fire.

Paired watershed analysis is useful for detecting changes in a parameter using two nearby watersheds, one as a control and the other as treatment watersheds. Watershed pairs are not required to be identical, but similarity in geology, ecology and climate help produce better models that can more precisely detect change. This study used nearby unburned watersheds as control watersheds within the same climate region of burned watersheds and similar ecologic characteristics (Figure 1.3).

We use multiple linear regression to analyze the data considering equation 1.1:

$$Q_B = a \times Q_C + b \times I + c \qquad (1.1)$$

Where the variables $Q_B$ and $Q_C$ are the annual average discharges of the burned and control watersheds, respectively and $I$ is a fire indicator, whose value is 0 for pre-fire years and 1 for post-fire periods. The fitted parameters are the intercept, *c*, the slope of the relationship in flow between the two watersheds, *a*, and post-fire shift in flow, *b*. Estimation of coefficient, $b$, represents the amount of change in annual water yield due to wildfire: positive/negative values of $b$ indicate increase/decrease in water yield after wildfire, respectively. The statistical significance of $b$ was tested with a *t*-test with a null hypothesis of 0 impact of

wildfire on water yield, *b*=0, with 90% of confidence level. The 90% of confidence level was selected to reduce risk of underestimation of post-fire response of annual water yield. We initially checked for significance of an interaction term (I x Qc), but records were generally short enough that it was not significant for many pairs. Where more than one control watershed was available for a given burned watershed, the best model based on $R^2$ was selected.

### 3.2 Effect of Burned Landcover on Post-fire Response in Annual Water Yield

The NLCD datasets (National Landcover Dataset measured in 1992, 2001, 2006 and 2011) provide landcover composition for the reported year but does not provide information about vegetation age (Figure 1.3). Thus, NLCD does not allow separating the changes due to differential evapotranspiration rates between mature and young tree/vegetation. To work with this limitation, we assumed (1) landcover types of NLCD were initially at a mature stage and (2) that regrowth began right after wildfire. These assumptions can be applicable as changes in annual water yield are related with difference in the fraction of trees between pre- and post-fire period.

We further explored whether post-fire response of annual water yield could be expressed as a function of changes in landcover composition and permanent tree mortality after wildfire on specifically forested area. The annual water yield ($Q$) from a watershed without wildfire ($Q_{pre}$) and with wildfire ($Q_{post}$) for a given hypothetical precipitation ($P$, equal on the two watersheds) can be expressed with equations 1.2 and 1.3 assuming that actual evapotranspiration is the sum of evapotranspiration via forest ($ET_f$) and short vegetation/grass ($ET_g$). Then, fractional changes in annual water yield due to wildfire ($(Q_{post} - Q_{pre})/Q_{pre}$) can be estimated using ecologic ($F$ and $m$), climatic ($P$) and hydrologic ($Q$) information (Equation 1.4; Supplementary Equations S1 – S17).

$$Q_{pre} = P - F \times ET_f - (1 - F) \times ET_g \qquad (1.2)$$

$$Q_{post} = P - (F - m) \times ET_f - \{1 - (F - m)\} \times ET_g \qquad (1.3)$$

where $F$ [%] is the fraction of forest before wildfire, and $m$ [%] is fraction of forest that died and replaced, at least temporarily, by short vegetation after wildfire. Further, $ET_f$ can be expressed as $ET_f = c \times P$ where $c$ is the fraction of precipitation evaporated, and it is conceptually what would be the ordinate axis of the Budyko (1954) relationship for a completely forested watershed. $ET_g$ can be expressed as $ET_g = k \times ET_f$ where $k$ is a relative evaporative capacity of short vegetation compared to forest. Estimation of $k$ is difficult, limiting the direct utility of Equations 1.2 and 1.3 directly. Current knowledge of relative evaporative index of shrub compared to forest is about 0.1 in semi-arid rangeland (Brooks *et al.*, 1997), but our study sites are forested watersheds, so application of a given value of $k$ could generate errors. We further reduced equations 1.2 and 1.3 by calculating the fractional reduction (Supplementary materials). This yields a theoretical expectation of fractional flow change that can be estimated from the forested fraction in the basin (F), its change (m), and a single parameter, c, that is the evaporative index (ET/P) of a conceptually fully forested basin:

$$\frac{\Delta Q}{Q_{pre}} = \frac{Q_{post} - Q_{pre}}{Q_{pre}} = m\left\{\frac{P_{pre}}{Q_{pre}}\frac{(c-1)}{(1-F)} + \frac{1}{1-F}\right\} \qquad (1.4)$$

The parameter $c$ can be inferred by extrapolation between pre-fire forest fraction ($F$) and evaporative index ($ET/P$) of nearby study sties (Supplementary Figure 1.1). This study used a flow-based evaporative index ($1 - \mathrm{Q}/P$) assuming steady-state condition because gridded ET products may have larger uncertainty than Q. 4km-resolution monthly mean precipitation data ($P$) from October 1979 to September 2014 (WY 1980 – 2014) was obtained from the PRISM Climate Group (PRISM; http://prism.oregonstate.edu/). The analysis does not take into account the potential change in precipitation between pre- and post-fire periods but it underscores two fundamental variables that drive watershed response: (1) the original amount of forest cover ($F$) and (2) the total amount of burned and dead forest ($m$).

### 3.3 Long-term Behavior of Post-fire Annual Water Yield

Long-term response of annual water yield mostly depends on changes in water demand by forest regrowth (Kuczera, 1987; Brooks *et al.*, 1997; Lane *et al.*, 2010). This study calculated residuals between observed and estimated annual water yield using the fitted linear models.

$$Residual_i = Q_{B,OBS_i} - Q_{B,EST_i} \quad (1.5)$$

$$Q_{B,EST_i} = a \times Q_{C,OBS_i} + c \quad (1.6)$$

where, *i* is water year, $Q_{B,OBS_i}$ is observed annual water yield in burned watershed, and $Q_{B,EST_i}$ is the estimated annual water yield in burned watershed if it had not been burned. Differences between observed and estimated annual water yield for post-fire period by neglecting wildfire impact (Equation 1.1 with $\mathrm{I} = 0$) quantify the annual change in water yield due to wildfire.

## 4 Results and Discussions

### 4.1 Wildfire Impacts on Annual Water Yield

Most of burned watersheds showed increase in post-fire annual water yield: 1.24 $m^3/s$ of annual water yield was increased (5.5%) in CID0 after wildfire in 1989; 5.82$m^3/s$ of annual water yield was increased (6.4 %) in CID6 after wildfire in 2007; 1.12 $m^3/s$ of annual water yield was increased (8.3 %) in CID7 after wildfire in 2007; 1.09 $m^3/s$ of annual water yield was increased (11.4 %) in CID8 after wildfire in 2007; 0.73 $m^3/s$ of annual water yield was increased (11.5 %) in YNP6 after wildfire in 1988; 6.30 $m^3/s$ of annual water yield was increased (17.2 %) in NCA3 after wildfire in 2008. On the other hand, decrease in post-fire annual water yield was also detected in CID1 and CID6 after wildfires in 2006 and 2000, respectively. 2.67 $m^3/s$ of annual water yield was decreased (-19.3 %) in CID1 after wildfire in 2006. 1.98 $m^3/s$ of annual water yield was decreased (-3.8 %) in CID6 after wildfire in 2000.

This finding is in line with current studies showing increases in annual water yield after wildfire in small watersheds (<10 $km^2$) associated with reduction in evapotranspiration from vegetation (Berndt, 1971; Helvey, 1980; Martin and Moody, 2001). Impact of wildfire on annual water yield can be subdue in baseflow dominated watershed (Kinoshita and Hogue, 2015) as in baseflow dominated YNP0 watershed whose mean baseflow index, BFI, during the study period (1984~2014) is 0.75. This value is significantly larger than the other burned watersheds with BFIs less than 0.45 (Supplementary Table 1.2).

**Table 1.2** Linear regression models of the paired watersheds. Bold numbers represent statistically significant coefficients (confidence level>90%). DF indicates number of data points used for regression model. Other paired watersheds are omitted considering the fitting power of regression models (adjusted $R^2$) in case that has more than one control watersheds in each site. All of results regardless of fitting power are summarized in Supplementary Table 1.3 and Supplementary Figure 1.2.

| Site | Control Water-shed | Burned Watershed (Fire year) | Linear Regression Model | | | | | |
|---|---|---|---|---|---|---|---|---|
| | | | Estimation | | | DF | p-value | Adj. $R^2$ |
| | | | **q** [$m^3/s$] | **a** [-] | **b** [$m^3/s$] | | | |
| CID | 2 | 0 (1989) | 0.52 | 3.98 | 1.24 | 41 | <2.2E-16 | 0.954 |
| | | 6 (2000) | 3.28 | 13.76 | -1.98 | 11 | 4.00E-15 | 0.997 |
| | | 6 (2007) | 2.34 | 13.91 | 5.82 | 11 | 2.89E-08 | 0.950 |
| | 3 | 1 (2006) | -3.53 | 0.62 | -2.67 | 11 | 8.81E-07 | 0.906 |
| | | 7 (2007) | -2.76 | 0.63 | 1.12 | 19 | 9.69E-14 | 0.953 |
| | | 8 (2007) | -0.74 | 0.37 | 1.09 | 42 | <2.2E-16 | 0.930 |
| YNP | 7 | 6 (1988) | -2.15 | 0.61 | 0.73 | 43 | <2.2E-16 | 0.841 |
| NCA | 1 | 3 (2008) | 11.29 | 2.26 | 6.30 | 40 | <2.2E-16 | 0.955 |

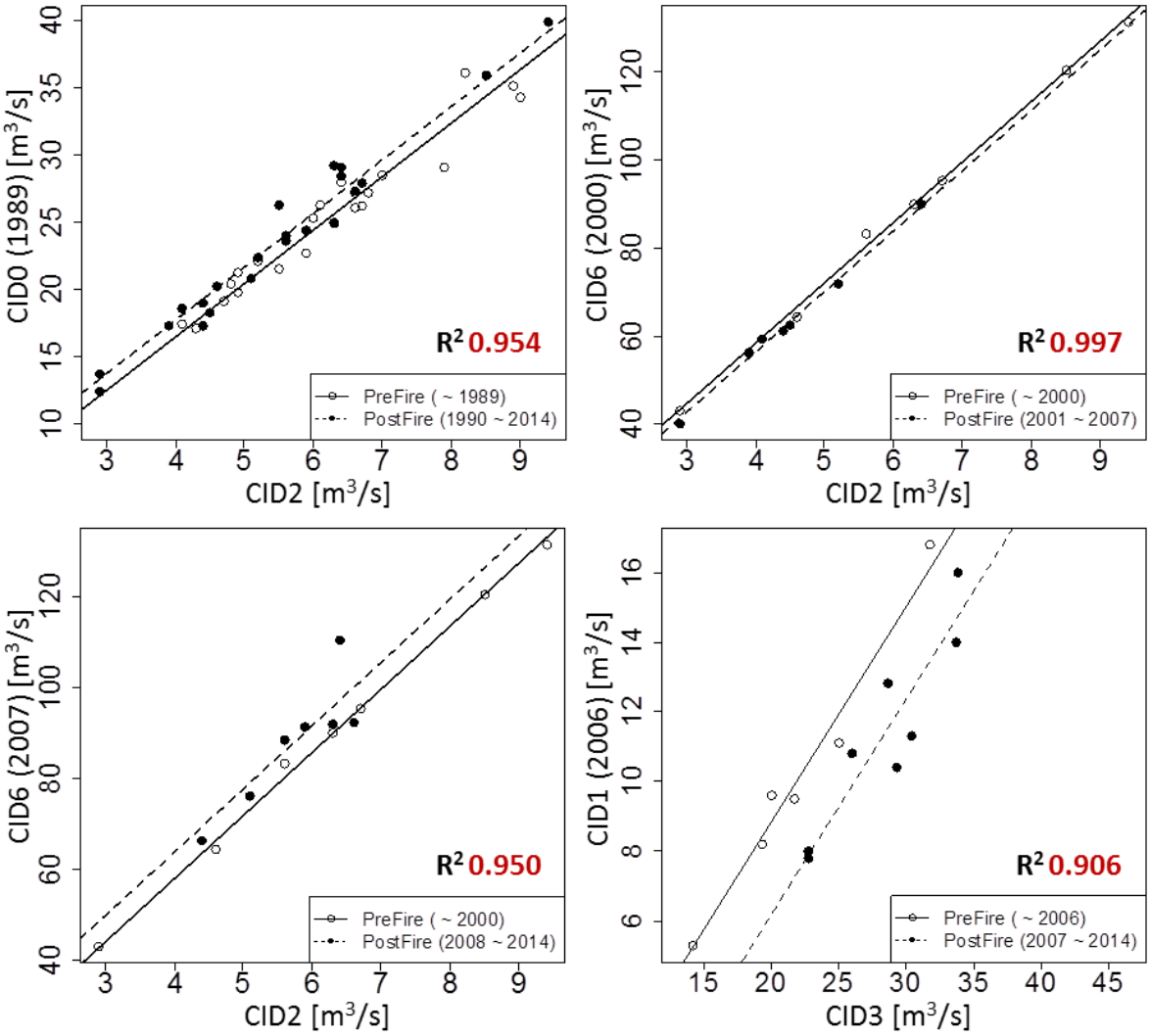


**Figure 1.4** Results of linear regression between burned watersheds (y-axis) and control watersheds (x-axis) summarized in Table 1.2. Continuous and dashed lines indicate linear regression of annual water yield of paired watersheds for pre- and post- wildfire periods, respectively.

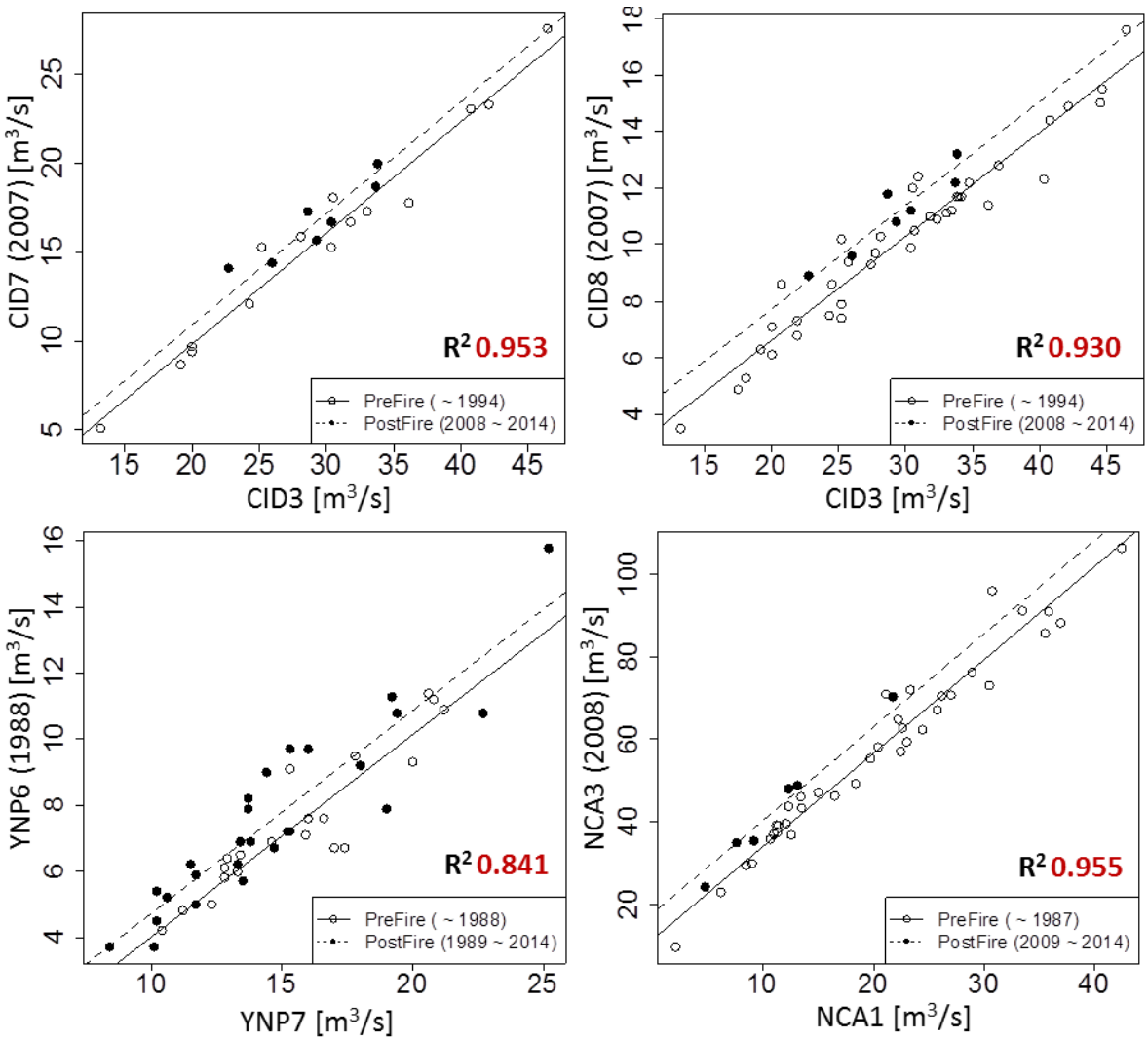


**Figure 1.4** Continue.

## 4.2 Effect of Burned Landcover on Post-fire Response in Annual Water Yield

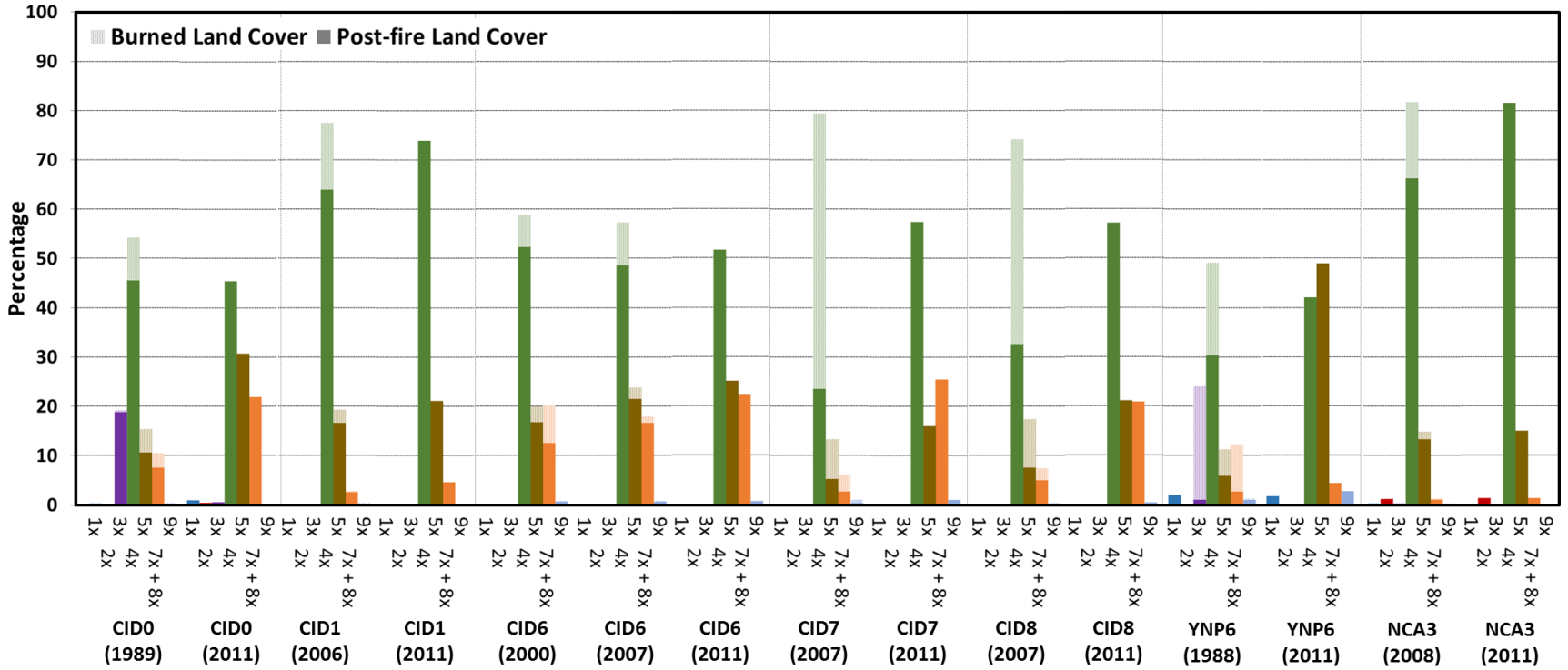


**Figure 1.5** Fraction of burned and unburned land cover type and land cover composition after wildfire which is available recent observation. Solid colored and mosaic bars are percentage of unburned and burned land cover type after wildfire, respectively. Numbers in parenthesis indicate major fire year at each burned watersheds. NLCD 1992 was used for wildfires in 1987, 1988, 1989 and 1994; NLCD 2001 was used for wildfire in 2000; NLCD 2006 was used for wildfires in 2006, 2007 and 2008. 1x (blue): water body and perennial snow, 2x (red): developed area, 3x (purple): barren, 4x (green): forest, 5x (brown): shrubland, 7x+8x (orange): grassland and cultivated crop, 9x (sky blue): wetlands. Calculations of changes in landcover changes are listed in Supplementary Table 1.4.

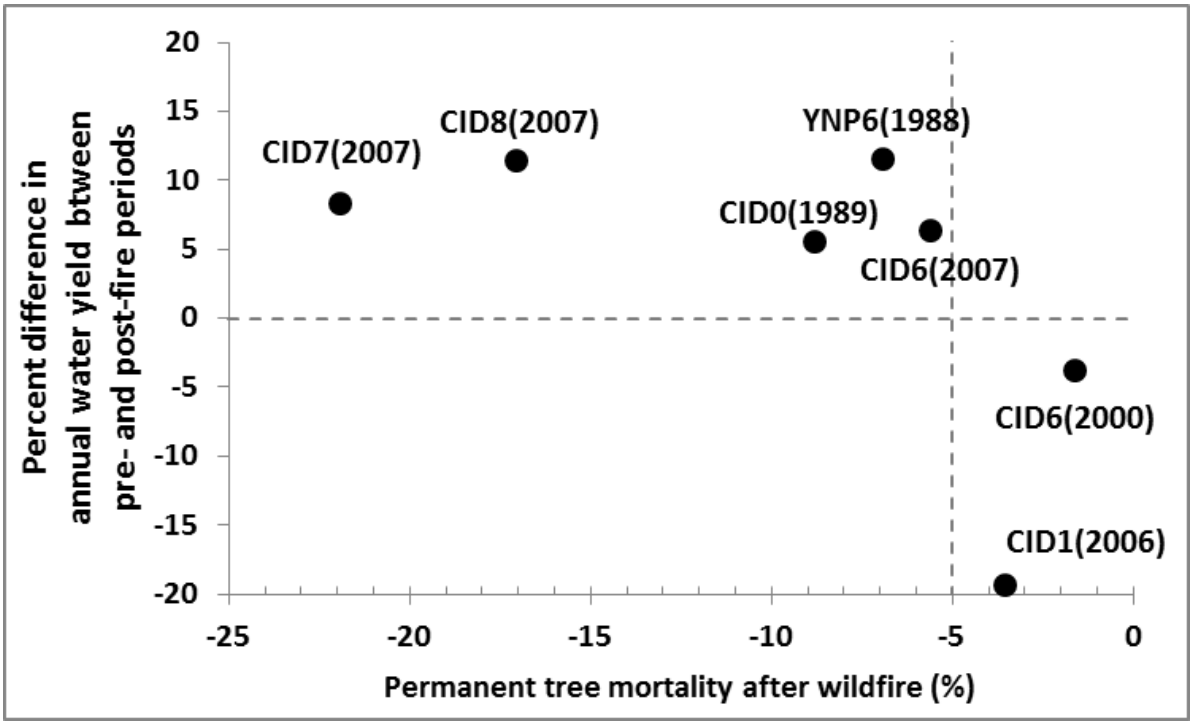


**Figure 1.6** Percent difference in annual water yield between pre- and post-fire periods following permanent tree mortality after wildfire in CID and YNP. Negative value of x-axis indicates permanent reduction in fraction of needle leaf forest. NCA3 was excluded due to its different trend of changes in landcover composition during post-fire that is consistent compared to CID and YNP. Percent difference in annual water yield is difference between observed ($Q_{OBS}$) and estimated discharge ($Q_{EST}$) assuming none of wildfire impact (Equation 1.1 with I=0), and calculated by $\frac{1}{m}\sum_{j}^{m}\frac{Q_{obs,j}-Q_{est,j}}{Q_{est,j}}\times 100-\frac{1}{n}\sum_{i}^{n}\frac{Q_{obs,i}-Q_{est,i}}{Q_{est,i}}\times 100$ where, n and m are number of years of pre- and post-fire periods, respectively; i and j are water year of pre- and post-fire period, respectively.

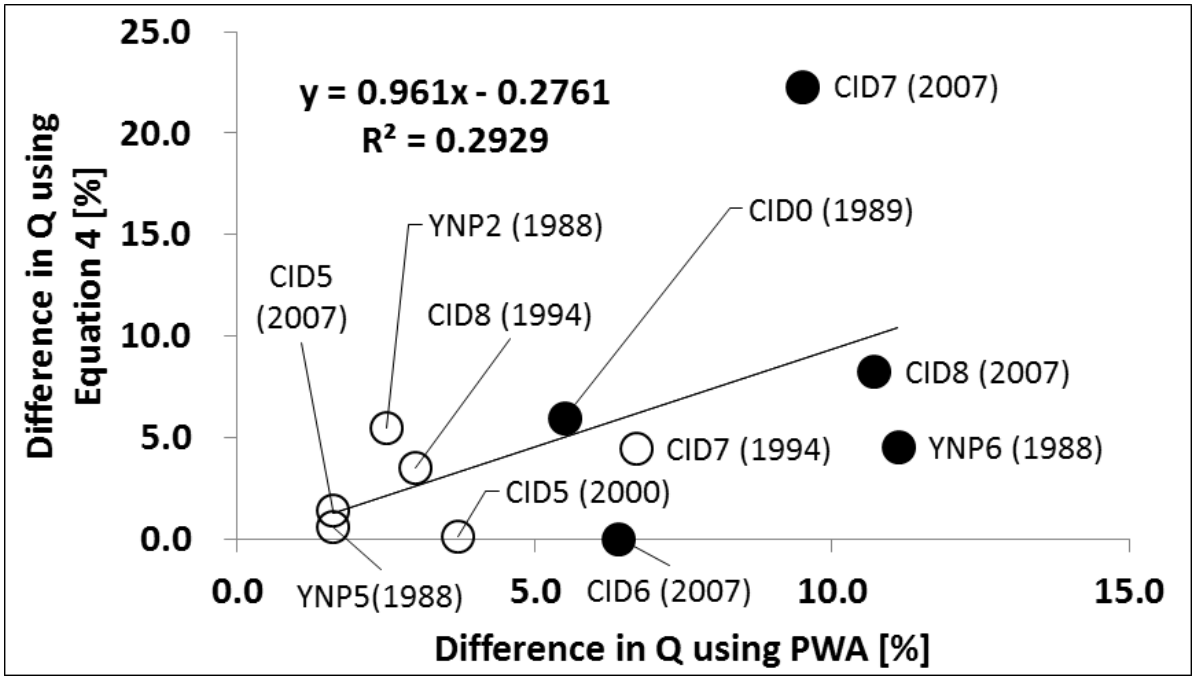


**Figure 1.7** Percent difference in annual water yield between pre- and post-fire periods following permanent tree mortality after wildfire in CID and YNP estimated by the analytical equation (Equation 1.4; y-axis) and the paired watershed analysis (x-axis). Calculations using Equation 1.4 is summarized in Supplementary Table 1.5). Filled markers indicate statistical significance with 90% of confidence level from the paired watershed analysis. NCA3 was excluded due to insufficient watersheds for extrapolating the efficiency coefficient $c$.

### 4.3 Long-term Behavior of Post-fire Annual Water Yield

This study calculated residuals between yield observed and estimated with the pre-fire model to test the long-term effects of wildfires on water yield (Equation 1.1 with I=0; Figure 1.8). Positive residuals represent increased water yield, and negative residuals represent decreased water yield. CID1 (2006), CID6 (2000), CID6 (2007), CID7 (2007), CID8 (2007) and NCA3 (2008) have relatively short post-fire period to capture the entire dynamics of recovery of burned landcover (Figure 1.8). For instance, Kuczera (1987) extimated about 200 years after wildfire for an ash forest to return to pre-fire conditions. Our results show as general trend an increase of annual water yield right after wildfire followed by a decreasing trend. We suggest that this trend is caused by increasing water demand of regrowth of burned vegetation (Kuczera, 1987; Wine and Cadol, 2016). Data for the post-fire periods of these watersheds are short and less than 10 years, such that it is difficult to determine whether the post-fire changes in annual water yield are permanent or an on-going process.

CID0 (1989) and YNP6 (1988) have relatively longer than the other watersheds post-fire record periods of about 20 years (Figure 1.8). CID0 residual trend shows after a sudden increase after wildfire a constant decrease which can be associated with vegetation re-growth (Figure 1.5). Conversely, YNP6 (1988) residuals do show an apparent strong reduction few years after wildfire followed by an increase. This watershed experienced permanent tree mortality, partial regrowth of burned forest, and conversion of barren area to shrub (Figure 1.5). One hypothesis of a lack of trend may be related with different regrowth speed between shrub and tree. Short vegetation grows quickly compared to tree. Assuming conversion of barren area began right after wildfire, quick decrease within 6 years after wildfire may be related with water consumption by succession of shrub, which follows by increase in annual water yield right after wildfire due to permanent tree mortality. Following trend can be interpreted as same manner with what was detected in CID0 (1989).

Although very limited, the residuals of NCA3 (2008) may show a decreasing trend during post-fire period due to increasing water demand by recovery of burned canopy. Although wildfire extent used in this study does not include burn severity, burned landcover in NCA3 can be assumed as canopy burn considering consistent landcover compositions during post-fire period. It took 7 years to return to pre-fire condition (Figure 1.8), which was also found by Wine and Cadol (2016) that 6 years of post-fire recovery period for canopy burned of needle leaf forest.

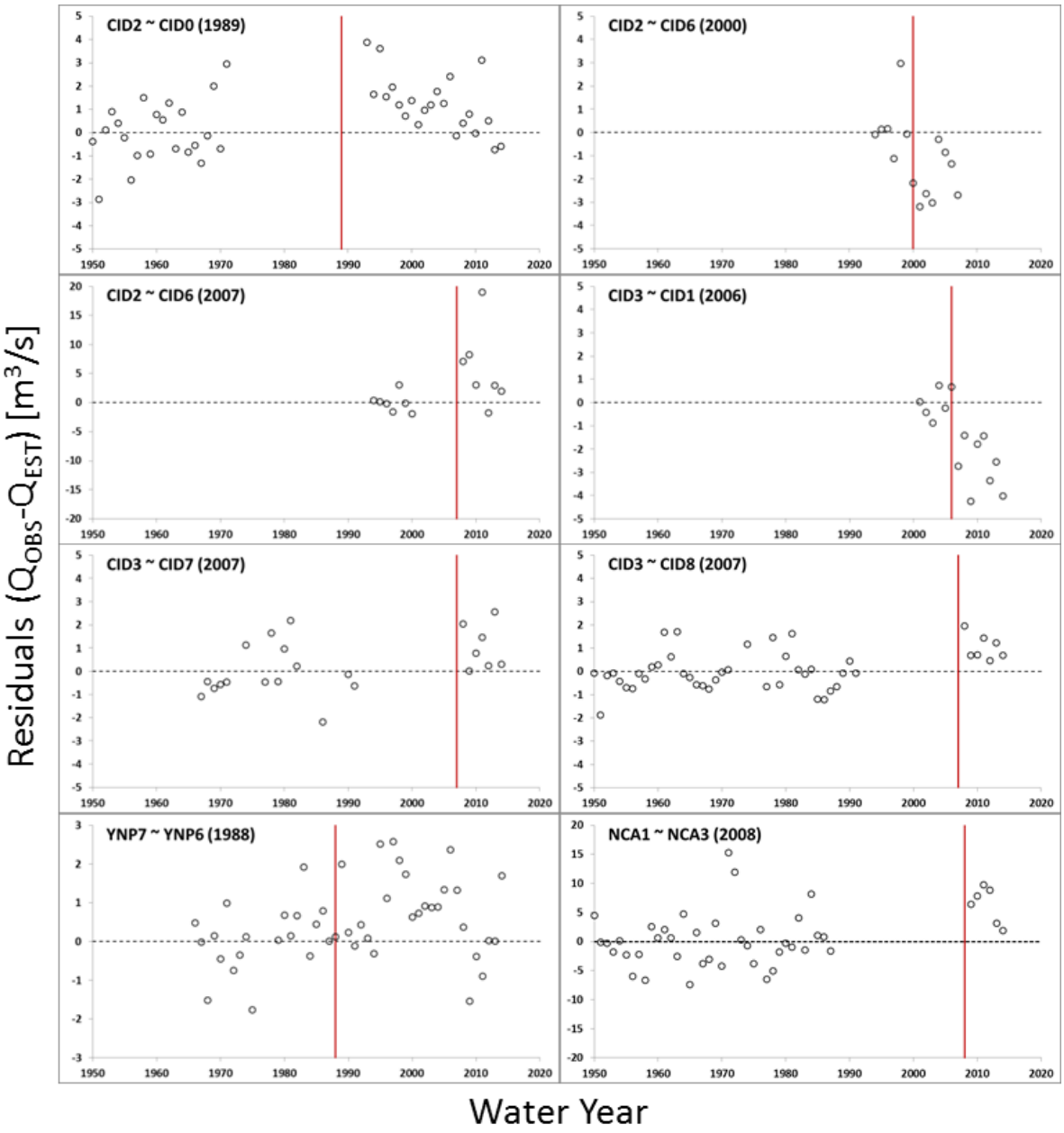


**Figure 1.8** Residuals ($Q_{OBS} – Q_{EST}$) between observed discharges ($Q_{OBS}$) and discharges estimated ($Q_{EST}$) by the linear regression model using I=0 in burned watersheds paired with control watersheds listed in Table 1.2. Residuals of omitted watershed pairs from Table 1.2 considering fitting power of paired watershed analysis are summarized in Supplementary Figure 1.3. Vertical intercepts indicate major wildfire years which correspond to numbers in bracelets.

### 4.4 Effect of Spatial Scale of Burned Watersheds

CID0 (1989), CID6 (2007), CID7 (2007), CID8 (2007), YNP6 (1988) and NCA3 (2008) were selected with statistically significant increase in annual water yield from paired watershed analysis. CID1 (2006) and CID6 (2000) with decrease in post-fire annual water yield were excluded because of a few number of decreasing cases.

Small to large size watersheds (<1,000km$^2$) may burn more than half of drainage area whereas very large watersheds (>1,000km$^2$) are mainly subject to partial-burned (<~30%) where drainage area is larger than 1,000km$^2$ (Figure 1.9A). Positive linear correlation between changes in post-fire annual water yield and percent burned area was not detected even in small watersheds (<10km$^2$) whereas strong positive linear correlation for logging projects was found in small experimental watersheds (Bosch and Hewlett, 1982; Stednick, 1996) (Figure 1.9B; Figure 1.9C). Thus, evapotranspiration changes due to vegetation removal or burn have different effects on annual water yield after logging and wildfire. Interestingly, large watersheds with small burned areas are close to the 1:1 line suggesting that they are quite efficient in responding to the disturbance (Figure 1.9C). However, as burned area increases their efficiency decreases rapidly and remains around 13% regardless of the percent of burned areas (Figure 1.9B).

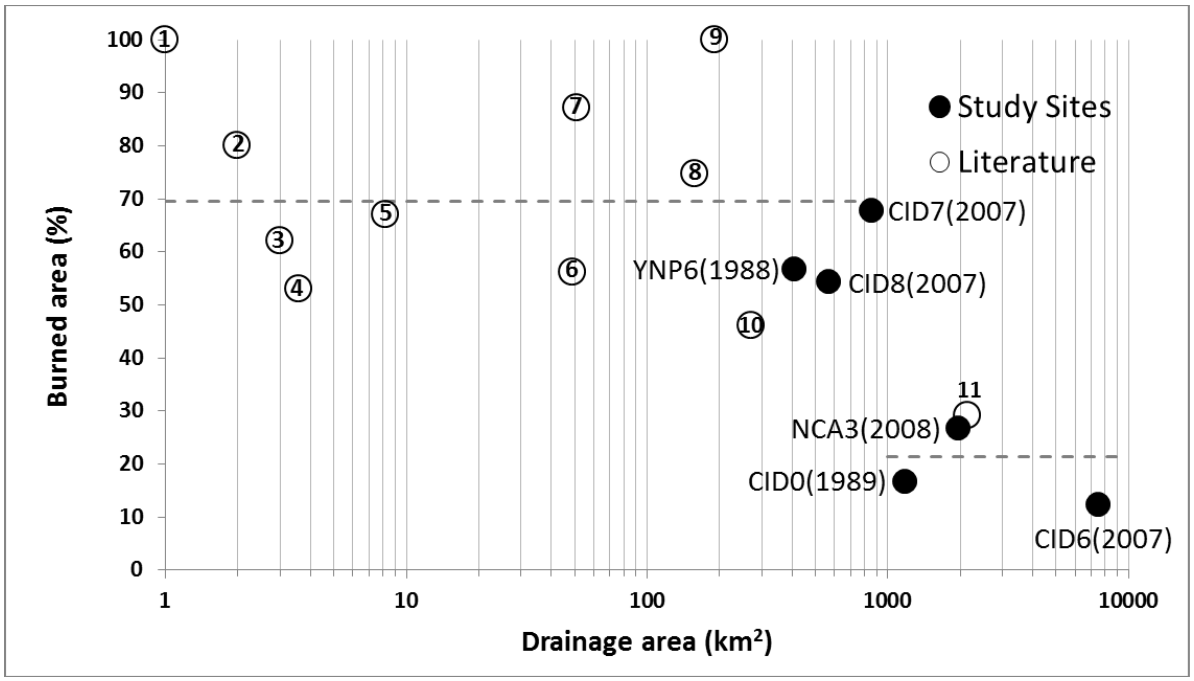


**Figure 1.9A** Percent burned area (%) following drainage area ($km^2$) for the assessment of size effect of impact of wildfire on annual water yield regarding spatial scale of burned watershed. Dashed line indicates mean value. Solid dots represent burned watersheds of this study and numbered circles represent literature review: 1. Stoof *et al.* (2012), 2. Scott (1993), 3. Lane *et al.* (2006), 4 and 5. Mahat *et al.* (2016), 6. Hessling (1999), 7. Kinoshita and Hogue (2015), 8. Bart (2016), 9. Wine and Cadol (2016), 10. Loáiciga *et al.* (2001) and 11. Luce *et al.* (2012).

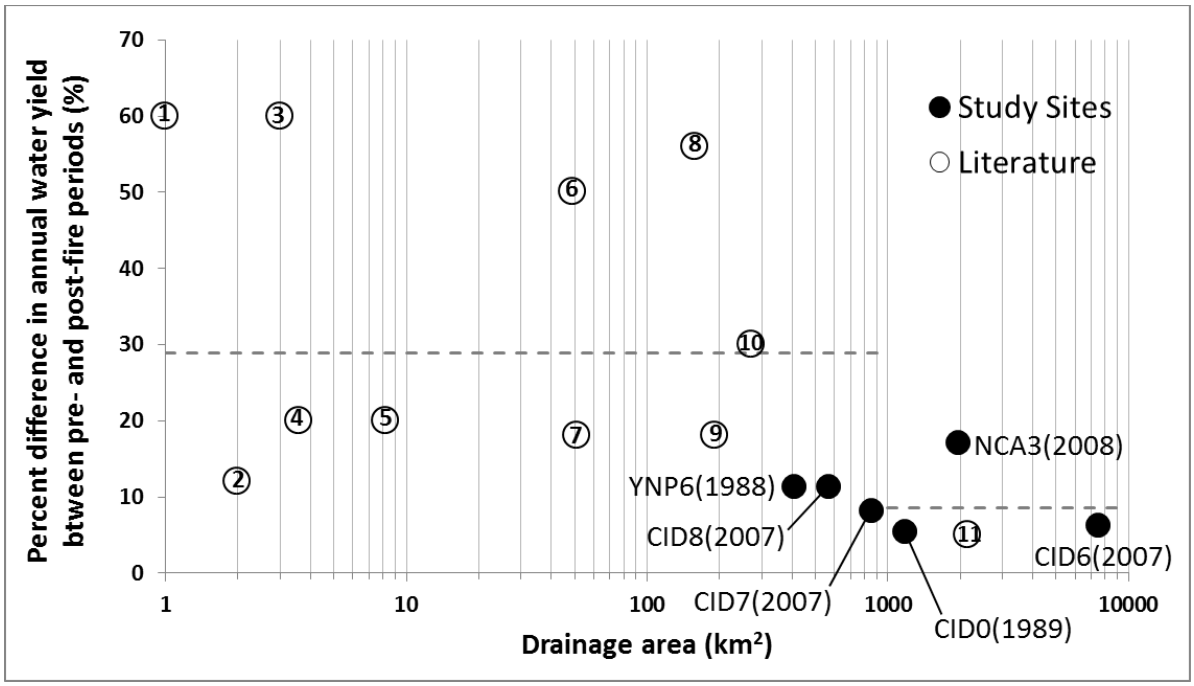


**Figure 1.9B** Percent difference in annual water yield between pre- and post-fire periods (%) following drainage area ($km^2$). Dashed line indicates mean value.

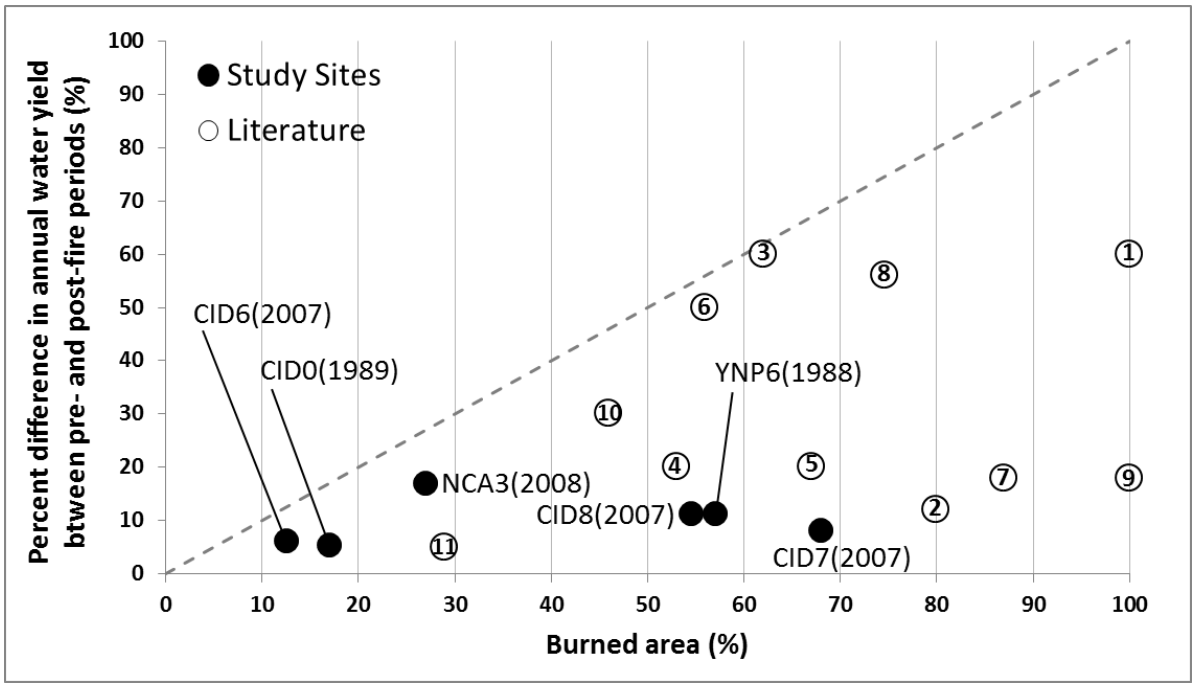


**Figure 1.9C** Percent difference in annual water yield between pre- and post-fire periods (%) following percent burned area (%). Dashed line indicates 1 to 1 line.

## 5 Conclusions

Available studies conducted mostly in small watersheds showed that annual water yield response to wildfire depends on the ecologic and climatic characteristics of the watershed besides the burned land cover type and their regrowth. This study confirmed that these variables also governs the annual water yield response in large watersheds.

Wildfires caused permanent tree mortality mostly in central Idaho watersheds (Salmon and Payette River Basins) and Yellowstone National Park basin, while burned trees began regrow quickly in North California Klamath River basin. Annual water yield increased (5.5% ~ 17.2%) in most burned watersheds due to tree/vegetation mortality but wildfire impacts were quite mitigated compared to small watersheds. On the other hand, annual water yield was predicted to decrease (-3.8% ~ -19.3%) where reduction in fraction of burned needleleaf trees were less than 5%. The long-term responses are still on-going after recent wildfires in the study sites, thus, continued efforts for measurement are required for understanding the long-term behavior. Responses of annual water yield in a long-term context were estimated to follow changes in evapotranspiration rate for two studied watersheds one in Central Idaho (CID0, 1989) and one in Yellowstone National Park (YNP6, 1988) where enough post-fire period data were available.

Burned watersheds produce more water than the pre-fire period due to reduced consumption of water within the watershed. Assessment of wildfire impact on annual water yield is important for proper water resources management plan that accounts for both timing and amount of changes in annual water yield. Although, results of this study showed increase in post-fire annual water yield in general, magnitude of the impact of wildfire in large watersheds is typically lower than what is expected in small watersheds. Current understanding suggests that the reason of this mitigation is due to spatial heterogeneity of burned area and the percent of burned areas per wildfire is constrained to less than 30% in large watersheds (>1,000km$^2$).

**References**

Adams HD, Luce CH, Breshears DD, Allen CD, Weiler M, Hale VC, Smith AMS, Huxman TE. 2012. Ecohydrological consequences of drought- and infestation- triggered tree die-off: insights and hypotheses. Ecohydrology, **5**: 145-159. DOI: 10.1002/eco.233.

Bales RC, Molotch NP, Painter TH, Dettinger MD, Rice R, Jeff D. 2006. Mountain hydrology of the western United States. Water Resources Research, **42**: W08432. DOI: 10.1029/2005WR004387.

Bart R, Hope A. 2010. Streamflow response to fire in large catchments of a Mediterranean-climate region using paired-catchment experiments. Journal of hydrology, **388**: 370-378. DOI: 10.1016/j.jhydrol.2010.05.016.

Bart RR. 2016. A regional estimate of postfire streamflow change in California. Water Resources Research, **52**: 1465-1478. DOI: 10.1002/2014WR016553.

Bart RR, Tague CL. 2017. The impact of wildfire on baseflow recession rates in California. Hydrological Processes, **31**: 1662-1673. DOI: 10.1002/hyp.11141.

Berndt H. 1971. Early effects of forest fire on streamflow characteristics. In: Res. Note PNW-RN-148. Portland, OR: US Department of Agriculture, Forest Service, Pacific Northwest Forest and Range Experiment Station. 11 p, USDA Forest Service, Pacific Northwest Forest and Range Experiment Station.

Bosch JM, Hewlett J. 1982. A review of catchment experiments to determine the effect of vegetation changes on water yield and evapotranspiration. Journal of hydrology, **55**: 3-23. DOI: 10.1016/0022-1694(82)90117-2.

Brooks KN, Ffolliott PF, Gregersen HM, DeBano LF. 1997. Hydrology and the management of watersheds. Iowa State University Press.

Campbell RE, Baker J, Ffolliott PF, Larson FR, Avery CC. 1977. Wildfire effects on a ponderosa pine ecosystem: an Arizona case study. In: USDA For. Serv. Res. Pap. RM-191. Fort Collins, CO: US Department of Agriculture, Forest Service, Rocky Mountain Forest and Range Experimental Station. 12 p., USDA Forest Service.

Dennison PE, Brewer SC, Arnold JD, Moritz MA. 2014. Large wildfire trends in the western United States, 1984–2011. Geophysical Research Letters, **41**: 2928-2933. DOI: 10.1002/2014GL059576.

Dillon GK, Holden ZA, Morgan P, Crimmins MA, Heyerdahl EK, Luce CH. 2011. Both topography and climate affected forest and woodland burn severity in two regions of the western US, 1984 to 2006. Ecosphere, **2**: 1-33. DOI: 10.1890/ES11-00271.1.

Dudgeon D. 2000. Large-scale hydrological changes in tropical Asia: prospects for riverine biodiversity: the construction of large dams will have an impact on the biodiversity of tropical Asian rivers and their associated wetlands. BioScience, **50**: 793-806. DOI: 10.1641/0006-3568(2000)050[0793:LSHCIT]2.0.CO;2.

Hallema DW, Sun G, Caldwell PV, Norman SP, Cohen EC, Liu Y, Bladon KD, McNulty SG. 2018. Burned forests impact water supplies. Nature Communications, **9**: 1307. DOI: 10.1038/s41467-018-03735-6.

Helvey J. 1980. Effects of a north central Washington wildfire on runoff and sediment production. Journal of the American Water Resources Association, **16**: 627-634. DOI: 10.1111/j.1752-1688.1980.tb02441.x.

Hessling M. 1999. Hydrological modelling and a pair basin study of Mediterranean catchments. Physics and Chemistry of the Earth, Part B: Hydrology, Oceans and Atmosphere, **24**: 59-63. DOI: 10.1016/S1464-1909(98)00012-4.

Hibbert AR. 1983. Water yield improvement potential by vegetation management on western rangelands. Journal of the American Water Resources Association, **19**: 375-381. DOI: 10.1111/j.1752-1688.1983.tb04594.x.

Kinoshita AM, Hogue TS. 2015. Increased dry season water yield in burned watersheds in Southern California. Environmental Research Letters, **10**: 014003. DOI: 10.1088/1748-9326/10/1/014003.

Kuczera G. 1987. Prediction of water yield reductions following a bushfire in ash-mixed species eucalypt forest. Journal of hydrology, **94**: 215-236. DOI: 10.1016/0022-1694(87)90054-0.

Lane PN, Feikema PM, Sherwin C, Peel M, Freebairn A. 2010. Modelling the long term water yield impact of wildfire and other forest disturbance in Eucalypt forests. Environmental Modelling & Software, **25**: 467-478. DOI: 10.1016/j.envsoft.2009.11.001.

Lane PN, Sheridan GJ, Noske PJ. 2006. Changes in sediment loads and discharge from small mountain catchments following wildfire in south eastern Australia. Journal of hydrology, **331**: 495-510. DOI: 10.1016/j.jhydrol.2006.05.035.

Littell JS, Peterson DL, Riley KL, Liu Y, Luce CH. 2016. A review of the relationships between drought and forest fire in the United States. Global change biology, **22**: 2353-2369. DOI: 10.1111/gcb.13275.

Liu Y, Gupta H, Springer E, Wagener T. 2008. Linking science with environmental decision making: Experiences from an integrated modeling approach to supporting sustainable water resources management. Environmental Modelling & Software, **23**: 846-858. DOI: 10.1016/j.envsoft.2007.10.007.

Loáiciga HA, Pedreros D, Roberts D. 2001. Wildfire-streamflow interactions in a chaparral watershed. Advances in Environmental Research, **5**: 295-305. DOI: 10.1016/S1093-0191(00)00064-2.

Luce C, Morgan P, Dwire K, Isaak D, Holden Z, Rieman B, Gresswell R, Rinne J, Neville HM, Gresswell R. 2012. Climate change, forests, fire, water, and fish: Building resilient landscapes, streams, and managers. USDA Forest Service.

Mahat V, Silins U, Anderson A. 2016. Effects of wildfire on the catchment hydrology in southwest Alberta. Catena, **147**: 51-60. DOI: 10.1016/j.catena.2016.06.040.

Martin DA, Moody JA. 2001. Comparison of soil infiltration rates in burned and unburned mountainous watersheds. Hydrological Processes, **15**: 2893-2903. DOI: 10.1002/hyp.380.

Moody JA, Shakesby RA, Robichaud PR, Cannon SH, Martin DA. 2013. Current research issues related to post-wildfire runoff and erosion processes. Earth-Science Reviews, **122**: 10-37. DOI: 10.1016/j.earsccirev.2013.03.004.

Morgan P, Heyerdahl EK, Gibson CE. 2008. Multi-season climate synchronized forest fires throughout the 20th century, northern Rockies, USA. Ecology, **89**: 717-728. DOI: 10.1890/06-2049.1.

Pringle C. 2003. What is hydrologic connectivity and why is it ecologically important? Hydrological Processes, **17**: 2685-2689. DOI: 10.1002/hyp.5145.

Scott D. 1993. The hydrological effects of fire in South African mountain catchments. Journal of hydrology, **150**: 409-432. DOI: 10.1016/0022-1694(93)90119-T.

Scott D, Van Wyk D. 1990. The effects of wildfire on soil wettability and hydrological behaviour of an afforested catchment. Journal of hydrology, **121**: 239-256. DOI: 10.1016/0022-1694(90)90234-O.

Shakesby RA, Moody JA, Martin DA, Robichaud PR. 2016. Synthesising empirical results to improve predictions of post-wildfire runoff and erosion response. International journal of wildland fire, **25**: 257-261. DOI: 10.1071/WF16021.

Smith HG, Hopmans P, Sheridan GJ, Lane PN, Noske PJ, Bren LJ. 2012. Impacts of wildfire and salvage harvesting on water quality and nutrient exports from radiata pine and eucalypt forest catchments in south-eastern Australia. Forest ecology and management, **263**: 160-169. DOI: 10.1016/j.foreco.2011.09.002.

Stednick JD. 1996. Monitoring the effects of timber harvest on annual water yield. Journal of hydrology, **176**: 79-95. DOI: 10.1016/0022-1694(95)02780-7.

Stoof CR, Vervoort R, Iwema J, Elsen E, Ferreira A, Ritsema C. 2012. Hydrological response of a small catchment burned by experimental fire. Hydrology and Earth System Sciences, **16**: 267-285. DOI: 10.5194/hess-16-267-2012.

Swetnam TW, Betancourt JL. 1998. Mesoscale disturbance and ecological response to decadal climatic variability in the American Southwest. Journal of climate, **11**: 3128-3147.

Thanapakpawin P, Richey J, Thomas D, Rodda S, Campbell B, Logsdon M. 2007. Effects of landuse change on the hydrologic regime of the Mae Chaem river basin, NW Thailand. Journal of hydrology, **334**: 215-230. DOI: 10.1016/j.jhydrol.2006.10.012.

Varela M, Benito E, De Blas E. 2005. Impact of wildfires on surface water repellency in soils of northwest Spain. Hydrological Processes: An International Journal, **19**: 3649-3657. DOI: 10.1002/hyp.5850.

Versini P-A, Velasco M, Cabello A, Sempere-Torres D. 2013. Hydrological impact of forest fires and climate change in a Mediterranean basin. Natural hazards, **66**: 609-628. DOI: 10.1007/s11069-012-0503-z.

Vieira D, Fernández C, Vega J, Keizer J. 2015. Does soil burn severity affect the post-fire runoff and interrill erosion response? A review based on meta-analysis of field rainfall simulation data. Journal of hydrology, **523**: 452-464. DOI: 10.1016/j.jhydrol.2015.01.071.

Wei X, Zhang M. 2010. Quantifying streamflow change caused by forest disturbance at a large spatial scale: A single watershed study. Water Resources Research, **46**. DOI: 10.1029/2010WR009250.

Wilk J, Andersson L, Plermkamon V. 2001. Hydrological impacts of forest conversion to agriculture in a large river basin in northeast Thailand. Hydrological Processes, **15**: 2729-2748. DOI: 10.1002/hyp.229.

Wine M, Cadol D. 2016. Hydrologic effects of large southwestern USA wildfires significantly increase regional water supply: fact or fiction? Environmental Research Letters, **11**: 085006. DOI: 10.1088/1748-9326/11/8/085006.

Wine ML, Cadol D, Makhnin O. 2018. In ecoregions across western USA streamflow increases during post-wildfire recovery. Environmental Research Letters, **13**: 014010. DOI: 10.1088/1748-9326/aa9c5a.

Zhou Y, Zhang Y, Vaze J, Lane P, Xu S. 2015. Impact of bushfire and climate variability on streamflow from forested catchments in southeast Australia. Hydrological sciences journal, **60**: 1340-1360. DOI: 10.1080/02626667.2014.961923.

# CHAPTER 2: BUDYKO FRAMEWORK: REVEALING THE IMPACTS OF WILDFIRES AND CLIMATE CONDITIONS ON WATERSHED ANNUAL WATER YIELD

**Abstract**

The impact of wildfire on annual water yield, Q, is constrained by a complex interaction among several processes that include hydrologic, ecologic and climatic alterations. Prediction of post-wildfire Q is important because of water demand for energy and food production especially after large wildfire (area>100km$^2$), whose size and frequency has been increasing in the last decades. To address this problem, we propose a novel application of the Budyko framework, which was originally developed to explore alterations of energy and water balance within watersheds. We applied this framework to investigate the impact of wildfire on Q by partitioning precipitation, P, into Q and actual evaporation for 15 large wildfires in 10 large watersheds at both yearly time scale (yearly Q) and as originally developed for long-term averages (a mean value of Q for the pre- and the for post-wildfire period). We apply the model with a flow-based evaporative index (1-Q/P) to constrain measurement uncertainty of evapotranspiration. Results of the Budyko framework support the general observation that post-wildfire Q is larger than pre-wildfire Q. Decrease in post-wildfire Q is detected in watersheds, where burned trees begin regrowth right after wildfire; a process that may cause higher evapotranspiration than in pre-wildfire period. Climatic conditions can affect the hydrological response during post-wildfire period. Both yearly time scale and long-term average approaches show mitigated or enhanced impact of wildfire on Q under post-wildfire wet or dry weather condition, respectively.

**Key words:** Budyko Framework, Annual Water Yield, Wildfire, Climate variability, Evapotranspiration

## 1 Introduction

Appropriate management of water resources is crucial for sustainable use of water for municipal use, food and energy production and ecosystem needs (Bales *et al.*, 2006; Liu *et al.*, 2008). Climate change, anthropogenic activities and their interactions tend to alter hydrologic cycle. Air temperature has been increasing as a result of climate change along with the frequency and severity of wildfires (Morgan *et al.*, 2008; Dillon *et al.*, 2011; Dennison *et al.*, 2014). Intense anthropogenic activities modify landscape, ecology and atmospheric composition, which result in changes in water and energy balance (van der Velde *et al.*, 2014). These disturbances change hydrologic components including evapotranspiration and annual water yield (Berndt, 1971; Helvey, 1980; Martin and Moody, 2001; Bart, 2016). As a result, proper management of water resources has become challenging (Huntington, 2006; Donohue *et al.*, 2011; Wang *et al.*, 2016).

Wildfire is a critical factor that alters hydrologic cycle by affecting infiltration and evapotranspiration (Bart and Hope, 2010; Lane *et al.*, 2010; Adams *et al.*, 2012; Vieira *et al.*, 2015; Zhou *et al.*, 2015) (ET); the latter is associated with tree mortality (decrease in ET) and/or regrowth of burned forest (increase in ET), which, in turn, affect the annual water yield (Brooks *et al.*, 1997). Consequently, wildfire impact on evapotranspiration has a direct effect on post-wildfire response of annual water yield, although its effect is poorly constrained especially for large watershed (drainage area larger than 100 $km^2$) (Helvey, 1980; Lane *et al.*, 2010; Luce *et al.*, 2012).

Paired watershed analysis (Campbell *et al.*, 1977; Scott, 1993; Bart, 2016) and numerical modeling (Lane *et al.*, 2010; Feikema *et al.*, 2013; Sidman *et al.*, 2016) have been usually employed for predicting post-fire response of annual water yield in small watersheds. Paired watershed analysis requires both adjacent control and burned watersheds, whose ecological and hydrological characteristics can be considered similar. However, it is challenging to define or identify proper control watersheds especially when investigating large watershed hydrologic response. On the other hand, numerical modeling use is limited by the large number of variables that need to be characterized to analyze hydrologic alterations. The

difficulties for acquisition of accurate datasets and calibration and validation of numerical models increase significantly as watershed size gets large.

To overcome the limitations of these typical approaches, we propose the use of the Budyko framework to investigate the post-wildfire response of annual water yield especially in large watersheds, those with drainage area large than 100 $km^2$. Budyko (1974) developed a powerful and simple framework to examine water and energy balance of watersheds. This framework enables partitioning of precipitation into annual water yield and evapotranspiration to investigate changes in water and energy balance induced by vegetation cover changes (Budyko, 1974; Zhang *et al.*, 2001; Donohue *et al.*, 2007; Zhang *et al.*, 2016) and other external disturbances such as climate change (Zhang *et al.*, 2004; Yang *et al.*, 2006) and/or anthropogenic activities (Wang and Hejazi, 2011; Jiang *et al.*, 2015).

Here, we suggest that Budyko framework can also be used to evaluate and predict post-wildfire response of annual water yield associated with changes in evapotranspiration. Wildfire is a key ecological and landscape-shaping agent that can cause significant changes in vegetation and, in turn, in evapotranspiration (Scott, 1993; Stoof *et al.*, 2012; Wine and Cadol, 2016). The Budyko framework is well suited for large watershed, where data acquisition for traditional approaches is difficult. Disturbance effect can be detected without the need of control watersheds, because the energy balance variable accounts for potential changes in precipitation conditions (climatic conditions) between pre- and post-wildfire periods. This is important because different weather conditions between pre- and post-wildfire periods may mitigate or enhance the impact of wildfire on annual water yield especially in large watersheds (Wine and Cadol, 2016; Hallema *et al.*, 2018). The Budyko framework uses few variables that are (1) actual evapotranspiration (AET) or annual water yield (Q), (2) potential evapotranspiration (PET) or annual net radiation (RNY) and (3) annual precipitation (P). Our goal is to present the Budyko framework for predicting water yield response due to wildfire and apply it to (1) examine post-fire responses of annual water yield in terms of changes in ET due to wildfire using Fu's equation (Equation 2.1) with water year based evaporative index and dryness index and long-term averaged indices for pre- and

post-fire periods and (2) explore the interaction of post-fire weather condition with impact of wildfire in short- and long-term context.

The long-term time scale (mean averaged over the pre and post wildfire periods) approach enables the assessment of the interaction of post-wildfire weather condition linked with net heat fluxes and availability of water resources in terms of the potential evapotranspiration with the impact of wildfire associated with capability of recovery of burned landcover. On the other hand, the yearly time scale approach enables the assessment of interaction of post-wildfire weather condition considering precipitation-runoff relationship with impact of wildfire. In a short-term context, annual water yield will be less or more than expected under extreme droughts or storms regarding precipitation-runoff relationship.

## 2 The Budyko Framework Revealing the Impacts of Wildfires and Climate Condition

This study adapted the Budyko (1974) framework to analyze the impact of wildfire on annual water yield in terms of changes in actual evapotranspiration (Figure 2.1). The Budyko framework represents hydrological characteristic of watershed in terms of water and energy balance under the assumption of steady state condition, $\mathrm{P} = \mathrm{AET} + \mathrm{Q} + \Delta\mathrm{S}$, where the storage term ΔS is equal to 0 (Budyko, 1974). It has been widely employed for assessments of dynamics of water and energy balance and comparison of watershed characteristics between different periods based on external disturbances (Xu *et al.*, 2014; Jiang *et al.*, 2015) or different regions (Li *et al.*, 2013; Liang and Liu, 2014) with various equations (Fu, 1981; Choudhury, 1999; Zhang *et al.*, 2004; Yang *et al.*, 2008; Donohue *et al.*, 2012). Recent studies showed its applicability in partitioning of precipitation into annual water yield and actual evapotranspiration despite the limitation of the steady-state condition (Donohue *et al.*, 2007; Chen *et al.*, 2013).

This study employed Fu's equation for the Budyko framework with yearly and long-term averaged flow-based evaporative index ($EI_{FB}$; 1-Q/P) and dryness index ($DI$; RNY/P) (Equation 2.1).

$$EI_{FB} = 1 + DI - \left(1 + (DI)^{(\omega+\Delta\omega\times I)}\right)^{1/(\omega+\Delta\omega\times I)} \quad (2.1)$$

where, $EI_{FB}$ and $DI$ are flow-based evaporative index ($1 - \frac{Q}{P}$) and dryness index ($\frac{RNY}{P}$), respectively. The parameter $I$ is a fire indicator with value of 0 and 1 for pre- and post-fire periods, respectively. The coefficient $\omega$ is an empirical parameter that accounts for vegetation, geographical, topographical and soil properties (Greve *et al.*, 2015; Sposito, 2017). A change in $\omega$ between pre ($\omega_{pre}$) and post ($\omega_{post}$) wildfire, $\Delta\omega = \omega_{post} - \omega_{pre}$, indicates altered watershed characteristics after wildfire. Decrease or increase in $\omega$ indicates an increase or a decrease in annual water yield associated with changes in evapotranspiration together with climate variability, respectively.

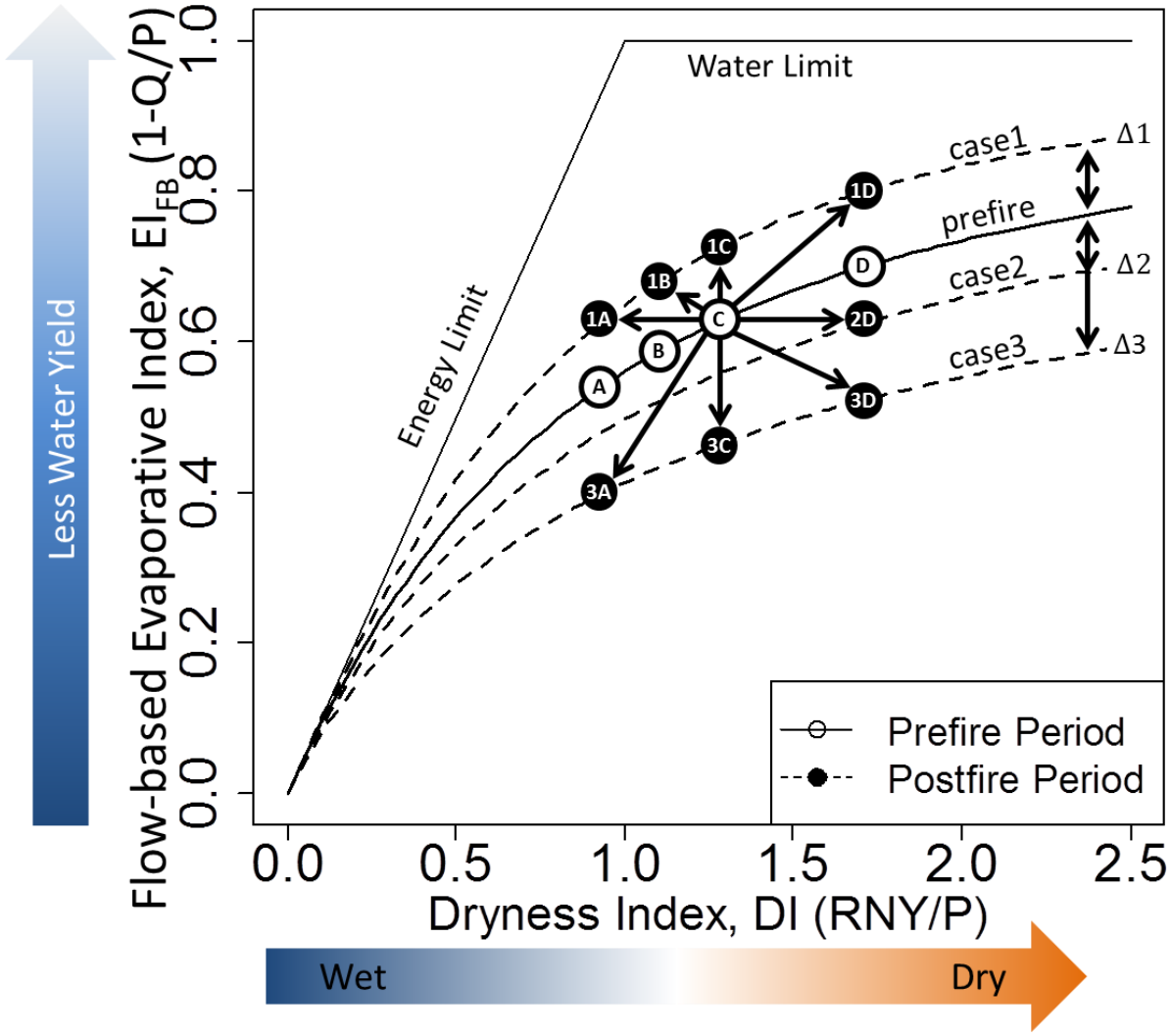


**Figure 2.1** Concept of a new theoretical approach within the Budyko framework for wildfire impact on annual water yield revealing the interaction of weather condition with the impact of wildfire. Circles represent arbitrary cases considering changes in water and energy balance, and curves are Fu's equation correspond to each case.

Upward (case 1) or downward (case 2 or case 3) shift of the Budyko curve after wildfire indicates a decrease or increase in annual water yield, respectively (Figure 2.1). Changes in annual water yield can be directly interpreted as changes in evapotranspiration assuming steady state condition. Increase in post-wildfire evapotranspiration rate indicates an increase in water demand by vegetation recovery, conversely a decrease in post-wildfire evapotranspiration rate indicates a reduction in water demand due to permanent tree mortality. Filled circles in Figure 2.2 show possible scenarios of response of burned watersheds associated with changes in ecological and climatic properties. Cases C show

post-wildfire response of water and energy balance without any impact of climatic conditions between pre- and post-wildfire conditions with case 1C showing an increased evapotranspiration that causes a decrease in annual water yield whereas case 3C a decrease in ET and thus an increase in annual water yield.

The other cases depict a post-fire response of annual water yield and a change between pre- and post-wildfire climatic conditions. Cases 1A, 1B and 1D indicate possible alterations of water and energy balance linked with post-fire weather condition. These cases are expected to occur in burned watersheds, where regeneration/regrowth begins quickly right after wildfire such that evapotranspiration is higher than pre-wildfire period. Long-term behavior of increased ET is likely to be temporary due to vegetation recovery. Upward shifted Budyko curve trends are expected to return toward pre-wildfire condition once regrowth/regeneration of burned landcover is completed.

On the other hand, cases 2 and 3 show decreased ET, which results in increase in annual water yield. Cases 2D, 3A and 3D are expected to occur in burned watersheds with significant amount of permanent tree mortality. Long-term behavior of decreased ET related with burned landcover and its recovery period depend on post-wildfire climatic conditions. Downward shifted Budyko curves tend to return toward pre-fire condition if post-fire climatic conditions are conducive to regrowth/regeneration of burned landcover (Brooks *et al.*, 1997). This may not always happen as post-wildfire drier than pre-fire condition may lend to landcover conversion to short vegetation that consume less water than forest or pre-wildfire landcover. Thus, downward shifted Budyko curve after wildfire may remain decreased in watersheds, where burned forest cover is converted to short vegetation and will not begin regrowth. Water and energy balance will be shifted from D to 2D or 3D when evapotranspiration decreased after wildfire, while weather condition remains the same between pre- and post-fire periods. Strong wildfire impacts on Q may cause a significative departure from the pre-wildfire Budyko curve ($\Delta\omega_{3D} > \Delta\omega_{2D}$).

Right or leftward movements along the Budyko curve exhibits weather conditions and energy balance adjustments of a watershed without significant external disturbances (open circles A, B and D cases).

The new theoretical Budyko framework quantifies the impact of wildfire on evaporative index regarding post-fire wet/dry condition (Figure 2.1). For example, water and energy balance will be shifted from C to 3D or 3A when evapotranspiration decreased significantly due to wildfire and a burned watershed experienced severe droughts (3D) or wet years (3A) during post-fire period. Water and energy balance without wildfire will be shifted from C to D or A under a given change of weather condition. Hence, distance between D~3D and A~3A have the impacts of both wildfire and climate variability on water and energy balance of burned watershed. Figure 2.1 shows that distance between pre and post-wildfire Budyko curves get larger and larger as the watershed get drier. This suggests as observed by other that post-wildfire response of annual water yield is more sensitive under post-fire dry than wet conditions (Zhou *et al.*, 2015; Hallema *et al.*, 2018).

## 3 Study Sites and Data Acquisition

### 3.1 Study Sties

Study sites were selected based on availability of discharge data throughout the Contiguous USA and focused on large watersheds, those with drainage area larger than 100 $km^2$ (Figure 2.1; Table 2.1; Supplementary Table 2.1). Watersheds were considered as burned if wildfire burned at least 10% of the total watershed area within a water year. Those with missing data near the wildfire year, or dominated by groundwater identified with baseflow index lager than 0.5 (BFI>0.5, Supplementary Table 2.1) or with or downstream large reservoirs were excluded from the analysis. This resulted in a total of 10 watersheds (Table 2.1) within the Rocky Mountains in Central Idaho (CID), Yellowstone National Park (YNP) and Klamath River basin in Northern California (NCA).

The CID and YNP watersheds are in semi-arid alpine highland climate region and the NCA basin is in Mediterranean climate region. Elevations of the CID and YNP watersheds range between 1,000 and 3,600 meters and those of NCA between 149 and 2,690 meters. CID and YNP watersheds have needle leaf forest (50 ~ 80%), shrubland (15 ~ 50%) and short vegetation (5 ~ 20%), while NCA has mostly needle leaf forest (>80%) and some shrubland (~15%) as reported by NLCD measured in the years near the major wildfire (MRLC; http://www.mrlc.gov; Supplementary Figure 2.2).

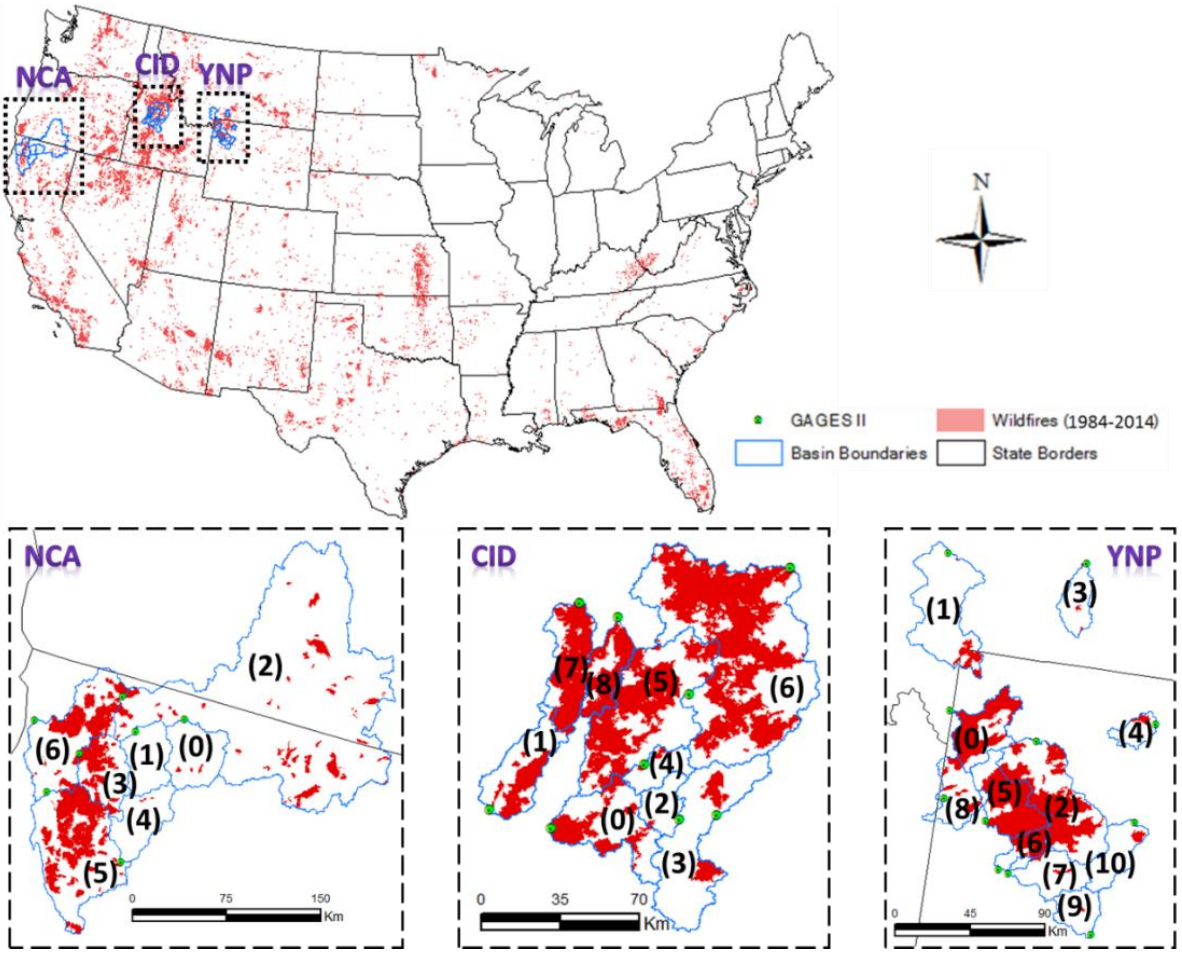


**Figure 2.2** Wildfires between 1984 and 2014 in study sites: (A) NCA, the Klamath River Basin in Oregon-California, (B) CID, central Idaho watersheds and (C) YNP, the Yellowstone National Park.

**Table 2.1** Summary of wildfires and burned watersheds where wildfire impact was statistically significant from paired watershed analysis. Bold numbers indicate water year that wildfire impacts were statistically significant from paired watershed analysis with 90% of confidence level.

| Burned Watershed (wildfire year) | Gauge ID | Drainage Area ($km^2$) | Gauge Elevation (m) | Elevation Range (m) | | | | Cumulative Burned Area by 2014 (%) |
|---|---|---|---|---|---|---|---|---|
| | | | | Watershed | | Wildfire | | |
| | | | | min | max | min | max | |
| CID0 (**1989**) | 13235000 | 1163.2 | 1155.2 | 1148 | 3213 | 1164 | 2862 | 35.4 |
| CID1 (**2006**) | 13237920 | 874.8 | 926.6 | 912 | 2583 | 917 | 2583 | 34.6 |
| CID5 (2000, 2007) | 13309220 | 2696.6 | 1335.0 | 1331 | 2981 | 1405 | 2981 | 49.9 |
| CID6 (**2000, 2007**) | 13310199 | 7451.0 | 926.6 | 921 | 3160 | 921 | 3014 | 54.1 |
| CID7 (1994, **2007**) | 13310700 | 853.1 | 1143.0 | 1143 | 2786 | 1143 | 2786 | 89.9 |
| CID8 (1994, **2007**) | 13313000 | 561.9 | 1419.1 | 1417 | 2777 | 1417 | 2777 | 86.7 |
| YNP2 (1988) | 06186500 | 2516.1 | 2374.0 | 2350 | 3679 | 2350 | 3296 | 51.1 |
| YNP5 (1988) | 13010065 | 1222.3 | 2073.1 | 2070 | 3121 | 2070 | 3121 | 74.9 |
| YNP6 (**1988**) | 13011500 | 404.1 | 2048.3 | 2043 | 3071 | 2465 | 3071 | 66.3 |
| NCA3 (**1987, 2008**) | 11522500 | 1943.1 | 148.9 | 149 | 2680 | 149 | 2337 | 48.5 |

## 3.2 Data Acquisition

### 3.2.1 Annual Water Yield (Q)

Discharge data for quantifying annual water yield (Q; mm/year) within each water year (a water year is from October 1$^{st}$ to September 30$^{th}$ of the following year) was obtained from the USGS National Water Information from water year 1979 to 2014 (WY 1980 - WY 2014) (USGS NWIS; http://waterdata.usgs.gov/nwis) (Supplementary Figure 2.1).

### 3.2.2 Historic Wildfire

Historic wildfire data from 1984 to 2014 was obtained from the Monitoring Trends in Burn Severity (MTBS; http://www.mtbs.gov) (Figure 2.1; Supplementary Figure 2.1). Wildfires extensions were overlapped over the watersheds to quantify the percent burned area, BA, as the ratio between total burned area (sum of extents of all wildfires) and drainage area (Figure 2.1 and Table 2.2). Watersheds burned areas ranged from 12.5% (CID1) to 74.4% (YNP5).

### 3.2.3 Precipitation (P)

Monthly mean precipitation data (P; mm/year) from January 1895 to December 2014 at a 4km-resolution was obtained from PRISM Climate Group (PRISM; http://prism.oregonstate.edu/) (Supplementary Figure 2.3). Site elevation is an important factor for an absolute difference between PRISM data and surface measured precipitation data (Jeton *et al.*, 2006). Percent difference between PRISM P and station measured P is smaller than ±15% in Nevada (USA) below elevation about 2,400 meters (comparison period: 1961-1990 and 1971-2000), and it is expected to be larger above 2,400 meters (Jeton *et al.*, 2006). Elevation range of the study sites ranges between about 100 to 3,600 meters. The following analysis assumes that the PRISM data has approximately a ±15% of estimation error for the study sites.

### 3.2.4 Actual Evapotranspiration (AET)

Monthly mean actual evapotranspiration data (AET; mm/year) from October 1983 to September 2006 (WY 1984 ~ WY 2006) at an 8km-resolution was obtained from the Numerical Terradynamic Simulation Group (NTSG UMT, http://files.ntsg.umt.edu/data/ET_global_monthly_ORIG/Global_8kmResolution/Raster/) (Supplementary Figure 2.3). Root mean square error (RMSE) between tower measured AET and estimated AET is 186.3 mm/year (Zhang *et al.*, 2010). Additionally, AET from October 2006 to September 2014 at a 5km-resolution provided by NASA was obtained from the Numerical Terradynamic Simulation Group (NTSG UMT; http://files.ntsg.umt.edu/data/NTSG_Products/MOD16/MOD16A2_MONTHLY.MERRA_GMAO_1kmALB/GEOTIFF_0.05degree/) (Supplementary Figure 2.3). Mean absolute error (MAE) between tower measured AET and estimated AET is 120.5 mm/year (Running *et al.*, 2017).

Absolute error of satellite based estimated AET for the study period (WY 1984 ~ WY 2014) is about 150 mm/year, and that is about 15% of PRISM precipitation data throughout the study sites. Estimation errors included in P and AET are not negligible considering the order of magnitude of total water balance of the study sites; thus, this study proposed a flow-based

AET (1-Q/P) assuming steady-state condition instead of satellite based AET despite its convenience. Use of flow-based AET and long-term averaged P would minimize the estimation error of the raw data.

### 3.2.5 Net radiation (RNY)

Annual net radiation (RNY) was provided by NOAA NWS NCEP (National Centers for Environmental Prediction) as a surrogate for potential evaporation in terms of energy flux of watershed from October 1979 to September 2014 (WY 1980 ~ WY 2014) at a 19km-resolution (http://app.climateengine.org/) (Supplementary Figure 2.2). This study used RNY instead of potential evapotranspiration (available from January 2000) due to accuracy and data availability for the study periods (WY 1980 ~ WY 2014). RNY is the total energy flux including incoming and outgoing radiation of both short and long wavelengths and represents the energy balance between absorbed, reflected and emitted by earth surface. Hence, RNY is applicable for the dryness index (ratio between available energy and water) of the Budyko framework. RNY is provided as energy flux [MJ/m$^2$/day], and it is converted into equivalent annual evapotranspiration [mm/year].

### 3.2.6 Data Analysis

Impact of wildfire on annual water yield was quantified with different approaches. We analyzed the changes in $\omega$ between pre ($\omega_{pre}$) and post ($\omega_{post}$) wildfire, $\Delta\omega = \omega_{post} - \omega_{pre}$. Statistical significance of $\Delta\omega$ (impact of wildfire) was tested using *t*-test with a null hypothesis that impact of wildfire equals to zero with 90% of confidence level. This study employed 90% of confidence level for the statistical test to minimize risk of underestimation of post-fire response of water and energy balance which may be masked due to climate variability. We quantified the residuals of annual water yield between observed post-fire condition and expected without wildfire annual water year based on pre-wildfire model to examine the long-term trend:

$$\Delta Q_j = Q_{OBS,j} - Q_{EST,j} \qquad (2.2)$$

where *j* is water year after wildfire, and the expected without wildfire annual water yield is quantified from equation 2.1 with the fire indicator *I*=0 and $\omega$ set as for pre-fire period:

$$Q_{EST,j} = P_j \times \left\{ \left(1 + DI_j^{\omega}\right)^{\frac{1}{\omega}} - DI_j \right\}, \quad (2.3)$$

Residuals also account for fire-climate induced changes in annual water yield. The mean residual was quantified to represent the overall change as

$$\Delta Q_m = \frac{1}{\tau} \times \sum_{j=1}^{\tau} \left(\Delta Q_j\right) \quad (2.4)$$

and its relative change in percent

$$\Delta Q_m(\%) = \frac{1}{\tau} \sum_{j}^{\tau} \frac{Q_{obs,j} - Q_{est,j}}{Q_{est,j}} \times 100 \quad (2.5)$$

where $\tau$ is number of available records within the period after wildfire.

Long-term averaged $\overline{EI_{FB}}$ and $\overline{DI}$ were calculated by averaging each raw data of Q, P and RNY first then calculated $1 - \bar{Q}/\bar{P}$ and $\overline{RNY}/\bar{P}$. For $\bar{P}$ and $\overline{RNY}$, observations in water year when discharge data was missing in that water year were excluded to avoid biased result of representative watershed characteristic of water and energy balance.

This study expects to minimize estimation error of PRISM P data by long-term average. Although it is difficult to define that the sample size of PRISM P is large enough, but the long-term averaged P can be expected to minimize the estimation error originated from raw data. The long-term annual water yield change due to wildfire is:

$$\Delta AWY = AWY_{OBS,J} - AWY_{EST,J} \quad (2.6)$$

with

$$AWY_{EST,J} = \left\{ \left( 1 + \left( \frac{RNY_J}{P_J} \right)^{(\omega)} \right)^{\frac{1}{\omega}} - \frac{RNY_J}{P_J} \right\} \times P_J \quad (2.7)$$

where, $J$ indicate post-fire period, $\omega$ is an empirical parameter for pre-fire period, and its relative change in percent as:

$$\Delta AWY(\%) = \frac{AWY_{OBS,J} - AWY_{EST,J}}{AWY_{EST,J}} \times 100 \qquad (2.8)$$

## 4 Results and Discussions

### 4.1 General Watershed Behavior

The average annual precipitation during the study period for CID, YNP and NCA were 970 mm, 859 mm and 1463 mm, respectively (Supplementary Figure 2.3). The wettest and driest water year in CID (based on SPI) produced 1070 mm/year (CID0 in WY 1997) and 293 mm/year (CID8 in WY 1988) (annual water yield), respectively; in YNP produced 1223 mm/year (YNP6 in WY 1997) and 384 mm/year (YNP5 in WY 1988), respectively; and in NCA produced 1457 mm/year (NCA3 in WY 1983) and 386 mm/year (NCA3 in WY 2014), respectively.

The average pre-wildfire annual dryness index ($DI$; $RNY/P$) was 0.96 for CID, 1.29 for YNP and 0.79 for NCA. The average post-wildfire *DI* increased in most burned watersheds except in CID1 (wildfire in 2006), CID7 (1994, 2007), CID8 (1994, 2007) and YNP5 (1988) (Supplementary Figure 2.3; Figure 2.6). Difference in average precipitation for pre- and post-wildfire period in CID and YNP is not notable, whereas it significantly decreased during the first and second post-fire periods in NCA3 from pre-wildfire period (Supplementary Figure 2.3). Decrease in EI in most CID and YNP burned watersheds can be interpreted as reduction in average AET after wildfire due to permanent tree mortality. On the other hand, burned forest quickly re-grew during post-fire periods in NCA3. Increase in the average post-fire annual EI in NCA3 is caused by both increasing water demand by regrowth of burned forest and reduction in precipitation. Increase in EI in NCA3 may be biased due to relatively short pre-wildfire record period (4 years) compared to post-fire period after wildfire in 1987 (21 years) and 2008 (6 years). Also, severe droughts (1991, 1992, 1994, 2001 and 2014) during

post-wildfire period and wet years during pre-wildfire period (1982, 1983 and 1984) may cause the notable difference in EI between pre- and post-wildfire periods.

### 4.2 Flow-based Evaporative Index ($1 - \mathrm{Q}/\mathrm{P}$)

The original Budyko framework and its various applications use actual evapotranspiration (AET) for evaporative index (EI; AET/P) (Budyko, 1974; Fu, 1981; Choudhury, 1999). Global AET data is provided by NASA and it is easy to acquire for data mining. However, its estimation error (about 150 mm/year) is not negligible at the spatial scale of the study sites (100 ~ 10,000 km$^2$). Water and energy balance with a yearly time scale of AET, PET and RNY does not fit to Budyko type equations such as Budyko (1974), Fu (1981), Choudhury (1999), Zhang *et al.* (2004) and Yang *et al.* (2008) but shows linear correlation in our study sites (Supplementary Figure 2.4). Fitted linear equations for pre- and post-wildfire periods are statistically different with 90% of confidence level in CID5 (2007), CID6 (2007), CID7 (2007), CID8 (2007), YNP5 (1988) and YNP6 (1988) (the number in parenthesis following the name of the watershed indicates the year of the wildfire) (Supplementary Table 2.3).

Despite the good performance of linear model using input variables of AET, RNY and P within the study sites for the study periods (Supplementary Table 2.3; Supplementary Figure 2.4), the linear equation may violate water limits under extreme dry weather condition (Supplementary Figure 2.4). Analysis of changes in storage ($\Delta S = P - Q - AET$) shows values of $\Delta S$ about $\pm$300 mm/year throughout the study sites (Supplementary Figure 2.5), which appear to store or leak water during the study period, which should not occur under the assumption of steady state ΔS=0. The change in storage is similar to the accuracy of the AET and P measurements such that we argue that $\Delta S$ is due the uncertainty in measuring AET and P rather than unsteady conditions. Hence, we propose a flow-based evaporative index ($EI_{FB} = 1 - \mathrm{Q}/\mathrm{P}$) instead of $EI$ ($AET/P$) assuming steady-state condition to remove an estimation error of $AET$. Direct measurement of discharge (Q) can be expected to have negligible errors compared to satellite based estimation of AET. For the estimation error of P, we expect to be small because P is in both indices, $1 - \mathrm{Q}/\mathrm{P}$ and $\mathrm{RNY}/\mathrm{P}$ for the yearly time

scale analysis and, long-term averaged value of P can be expected to minimize estimation error.

### 4.3 Budyko Framework with Fu's Equation using yearly time scale of $EI_{FB}$ and $DI$

Fu's equation well fits the water and energy balance with $EI_{FB}$ (Figure 2.3; Table 2.2). Fitted Fu's equations for pre- and post-wildfire periods are statistically different with 90% of confidence level in CID7 (2007) and CID8 (2007) (Table 2.2). The other wildfires do not have statistically significant impact on water and energy balance. Negative $\Delta_\omega$ from CID7 (2007) and CID8 (2007) shows decrease in $EI_{FB}$, which indicates increase in Q (Figure 2.3). This can be interpreted as a reduction in evapotranspiration due to significant amount of permanent tree mortality after wildfire (Supplementary Figure 2.1).

Although non-statistically significant, all the other watersheds showed the same trend as CID7 and CID8 expect CID6 (2000). Increase in $EI_{FB}$ in CID6 after wildfire in 2000 can be interpreted with increasing water demand by quick regrowth of burned forest right after wildfire with negligible amount of permanent tree mortality (<5%; Supplementary Figure 2.1). The Budyko framework shows that water and energy balance tends to converge toward pre-fire Budyko curve 5 years later the wildfire (Figure 2.3 and 2.4), as expected through regrowth of burned landcover declines as forest reaches mature stage (Kuczera, 1987; Lane *et al.*, 2010) and water demand returns to pre-wildfire condition.

In most burned watersheds, water and energy balance tends to return to pre-wildfire condition except CID7 (2007) and CID8 (2007) (Figure 2.3 and 2.4). Gray colored markers represent post-wildfire water years right after wildfire, and they return toward pre-wildfire Budyko curve (solid curve) over time. However, the post-wildfire record period may be short for CID7 (2007) and CID8 (2007) to allow regrowth to pre-fire conditions. Permanent tree mortality was observed in these watersheds after wildfire, and the burned pine tree forest was converted to short vegetation with low water demand (Supplementary Figure 2.1). Post-wildfire Budyko curve may remain lower if reduced water demand persists permanently and the watershed will produce more water compared to pre-fire period.

CID1 (2006) shows increase in post-wildfire annual water yield (Figure 2.3; Table 2.2), although alteration of landcover composition in CID1 (2006) is similar with that in CID6 (2000) (Supplementary Figure 2.1). The amount of permanent tree mortality was not significant (<5%) in CID1 (2006), and quick regrowth began right after wildfire (Supplementary Figure 2.1). This post-wildfire behavior of landcover recovery is supposed to decrease post-wildfire annual water yield as we hypothesized and observed in CID6 (2000). The opposite response of CID1 (2006) compared to CID6 (2000) cannot be explained by post-wildfire weather condition as they are similar to pre-fire period in CID1 (2006) (Figure 2.3; Supplementary Figure 2.3) but potentially to the relatively short pre-wildfire record period of discharge data, which may not represent the pre-wildfire watershed characteristic.

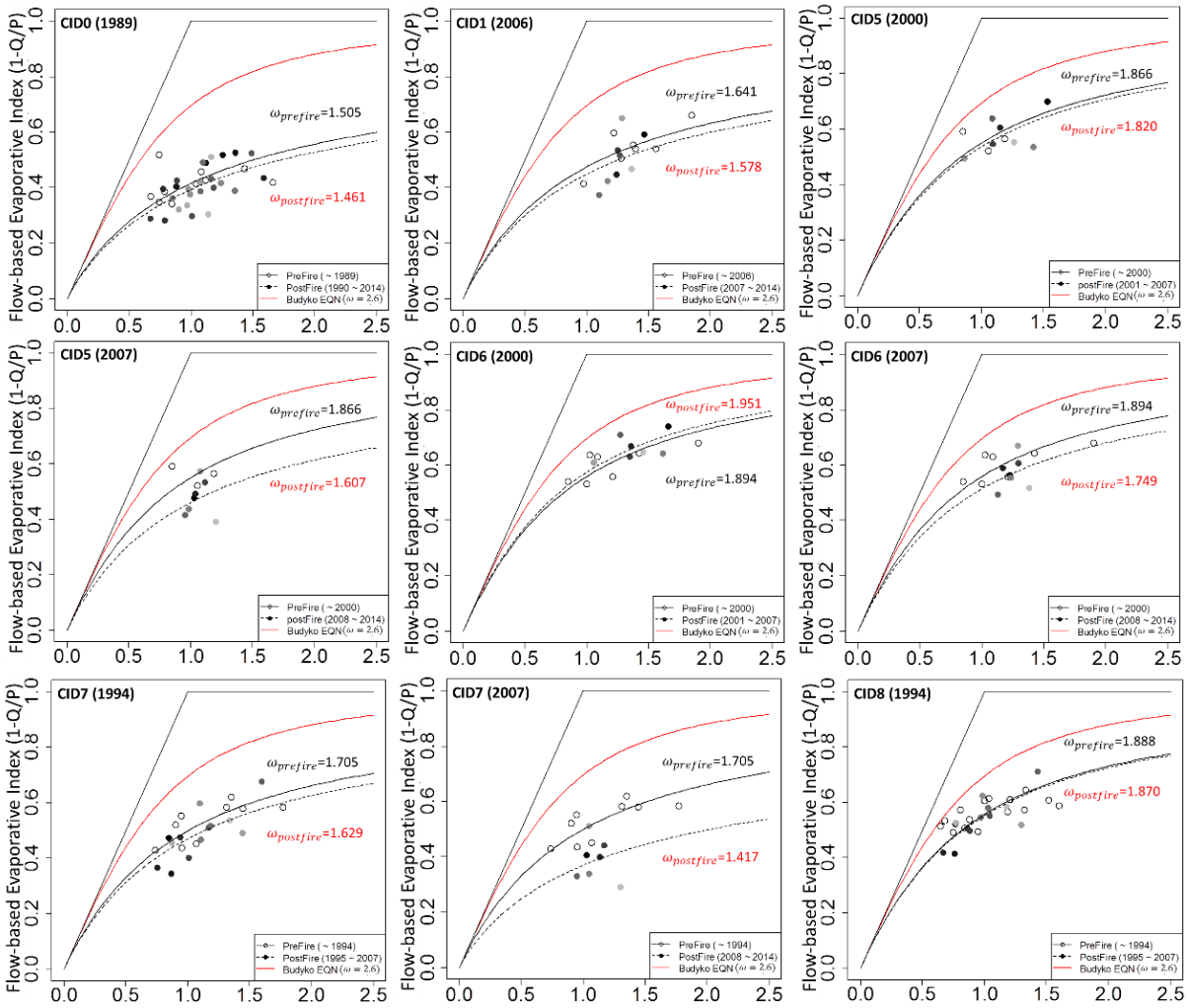


**Figure 2.3** Budyko framework with Fu's equation with flow-based evaporative index ($EI_{FB}$; $1 - Q/P$) and dryness index (RNY/P) from 1980 to 2014 in burned watersheds. Numbers in parenthesis indicate wildfire year. Open circles and filled circles indicate scatter between $EI_{FB}$ and DI during pre- and post-fire period, respectively. Continuous and dashed curves are fitted Fu's equation using non-linear least square method for pre- and post-fire period, respectively. Red colored curve is a Fu's equation for global Budyko curve with $\omega = 2.6$.

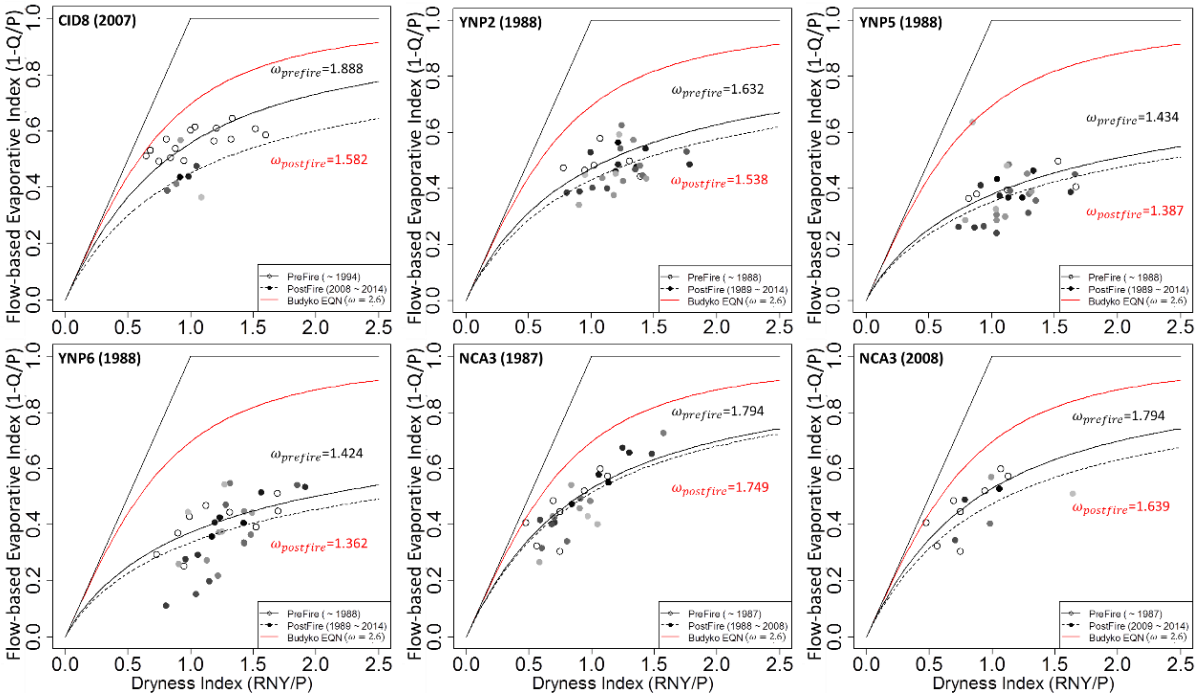


**Figure 2.3** Continue.

**Table 2.2** Summary of post-fire response of annual water yield through the Budyko framework with Fu's equation using yearly data of flow-based EI and DI. Shaded rows indicate statistically significant wildfire impact.

| Watershed (fire year) | Drainage Area (km²) | Burned Area (%) | Budyko Framework with Fu's Equation using yearly data of $\boldsymbol{EI_{FB}}$ and **DI** | | | | |
|---|---|---|---|---|---|---|---|
| | | | Pre-fire | Post-fire | $\Delta\boldsymbol{\omega}$ | $\Delta Q_m$ (mm/yr) | $\Delta Q_m$ (%) |
| CID0 (1989) | 1163.2 | 16.9 | 1.505 | 1.461 | -0.044 | 24.8 | 4.3 |
| CID1 (2006) | 874.8 | 16.5 | 1.641 | 1.578 | -0.063 | 26.4 | 6.2 |
| CID5 (2000) | 2696.6 | 20.6 | 1.866 | 1.820 | -0.046 | 10.8 | 3.6 |
| CID5 (2007) | 2696.6 | 15.0 | 1.866 | 1.607 | -0.259 | 91.2 | 21.1 |
| CID6 (2000) | 7451 | 17.5 | 1.894 | 1.951 | 0.057 | -15.4 | -5.3 |
| CID6 (2007) | 7541 | 12.5 | 1.894 | 1.749 | -0.145 | 41.5 | 12.1 |
| CID7 (1994) | 853.1 | 15.8 | 1.705 | 1.629 | -0.076 | 35.5 | 6.0 |
| CID7 (2007) | 853.1 | 67.9 | 1.705 | 1.417 | -0.288 | 129.8 | 28.1 |
| CID8 (1994) | 561.9 | 15.9 | 1.888 | 1.870 | -0.018 | 5.5 | 0.6 |
| CID8 (2007) | 561.9 | 54.5 | 1.888 | 1.582 | -0.306 | 109.9 | 22.3 |
| YNP2 (1988) | 2516.1 | 40.2 | 1.632 | 1.538 | -0.094 | 37.6 | 9.2 |
| YNP5 (1988) | 1222.3 | 74.4 | 1.434 | 1.387 | -0.047 | 26.3 | 4.8 |
| YNP6 (1988) | 404.1 | 56.9 | 1.424 | 1.362 | -0.062 | 48.4 | 7.1 |
| NCA3 (1987) | 1943.1 | 19.8 | 1.794 | 1.749 | -0.045 | 37.6 | 2.9 |
| NCA3 (2008) | 1943.1 | 26.9 | 1.794 | 1.639 | -0.155 | 59.5 | 12.4 |

The Budyko framework at yearly time scale allows analyzing the long-term response via annual water year residuals. Residuals ($\Delta Q_i$; mm/yr) generally increased compared to pre-fire period (Table 2.2; Figure 2.4) due to reduced evapotranspiration cause by permanent tree mortality. Further, residuals show a noticeable increase in annual water yield during wet years, and a subdue increase or even a decrease in annual water yield during dry water years in all burned watersheds except CID0 in WY 2005 and NCA3 in WY 2014 (Figure 2.4). These results highlight the complex interaction between precipitation, discharge and vegetation. Post-fire weather conditions linked with precipitation-runoff elasticity can mask or enhance wildfire impact on Q. Post-wildfire climatic conditions with precipitations below pre-wildfire average P can mask an increase of annual water yield (Hallema *et al.*, 2018). Whereas, post-fire wet climate with precipitation larger than pre-fire period can amplify or mitigate wildfire impact, where annual water yield increased or decreased due to wildfire, respectively (Hallema *et al.*, 2017). Enhanced amount of increase in annual water yield in WY 2005 in CID0 and in WY 2014 in NCA3 may results of other external impacts besides ecological and climatic variabilities, which is not yet clarified in this study.

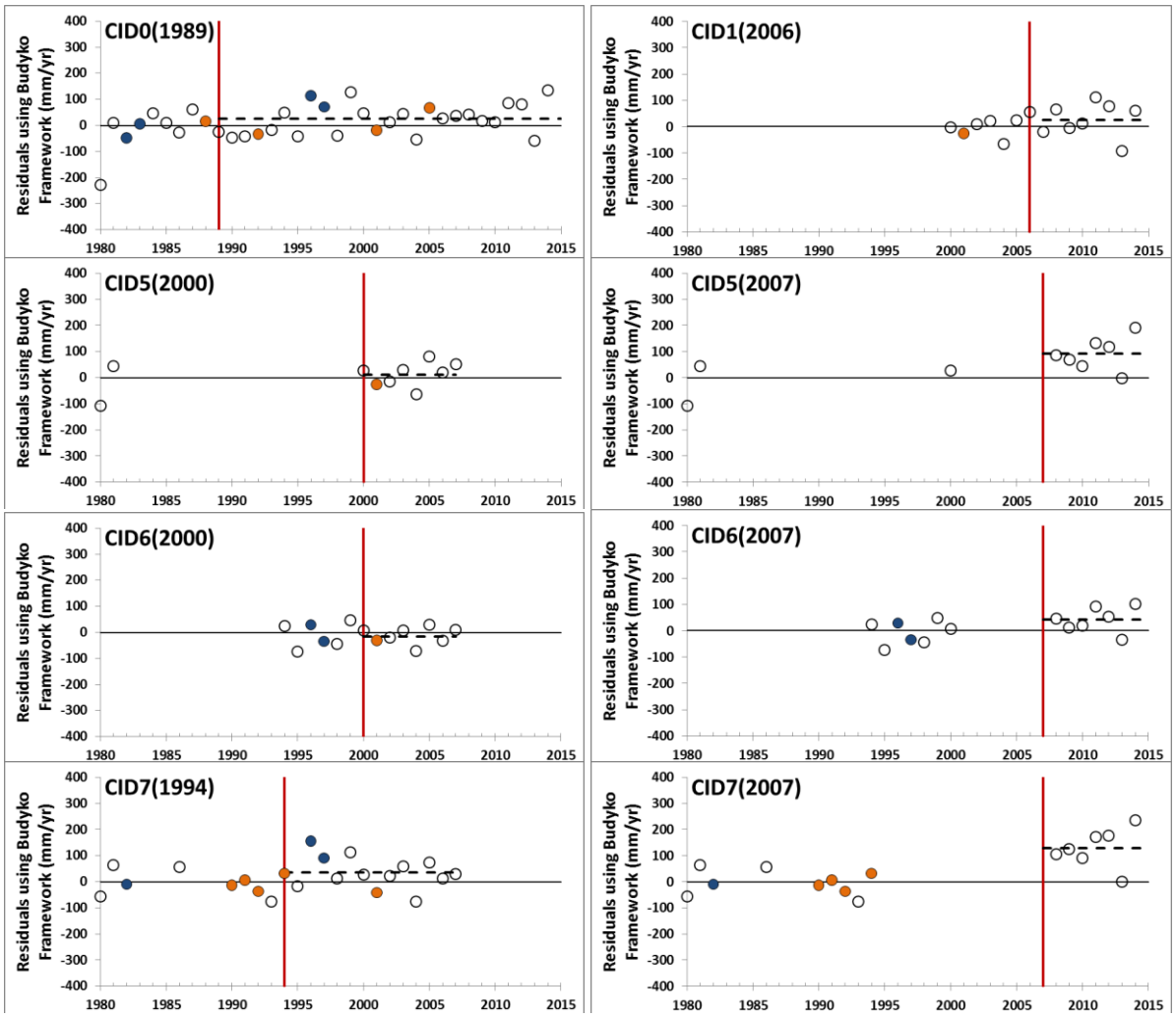


**Figure 2.4** Residuals ($Q_{OBS} - Q_{EST}$) between observed annual water yield ($Q_{OBS}$) and annual water yield estimated by Budyko framework ($Q_{EST}$) with Fu's equation using yearly value of $EI_{FB}$ and $DI$. Dashed line for post-fire period is the residual mean value that corresponds to absolute changes in post-fire annual water yield summarized in Table 2.2 (ΔQ; mm/year). Vertical red lines indicate wildfire years. Blue, orange colored and opened circles indicate wet (SPI>=1), dry (SPI=<-1) and normal (-1<SPI<1) water year based on SPI (Standardized Precipitation Index; (McKee *et al.*, 1993)), respectively.

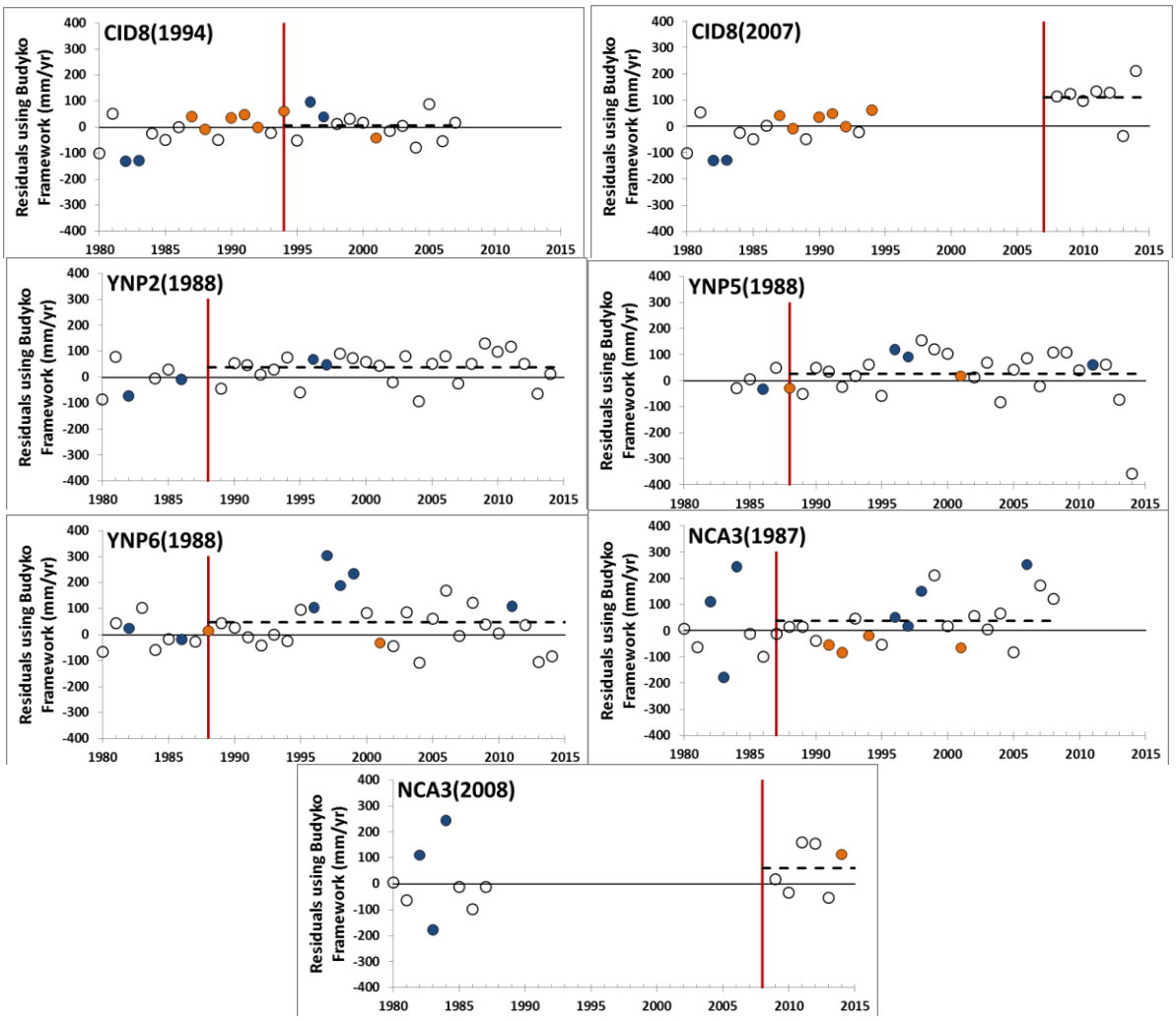


**Figure 2.4** Continued.

Increase in post-fire Q was detected in most burned watersheds. Relationship between $\Delta\omega$ and $\Delta Q_m(\%)$ has a linear correlation regardless of statistical significance of wildfire impact (Figure 2.5). Conversely, $\Delta Q_m(\%)$ did not show notable dependence from spatial scale when plotted versus burned area (%; Figure 2.6A) or drainage area ($km^2$; Figure 2.6B). This result may be biased by the small number of study sites, which may not be sufficient to represent the post-fire response of annual water yield and a large sample may identify a trend.

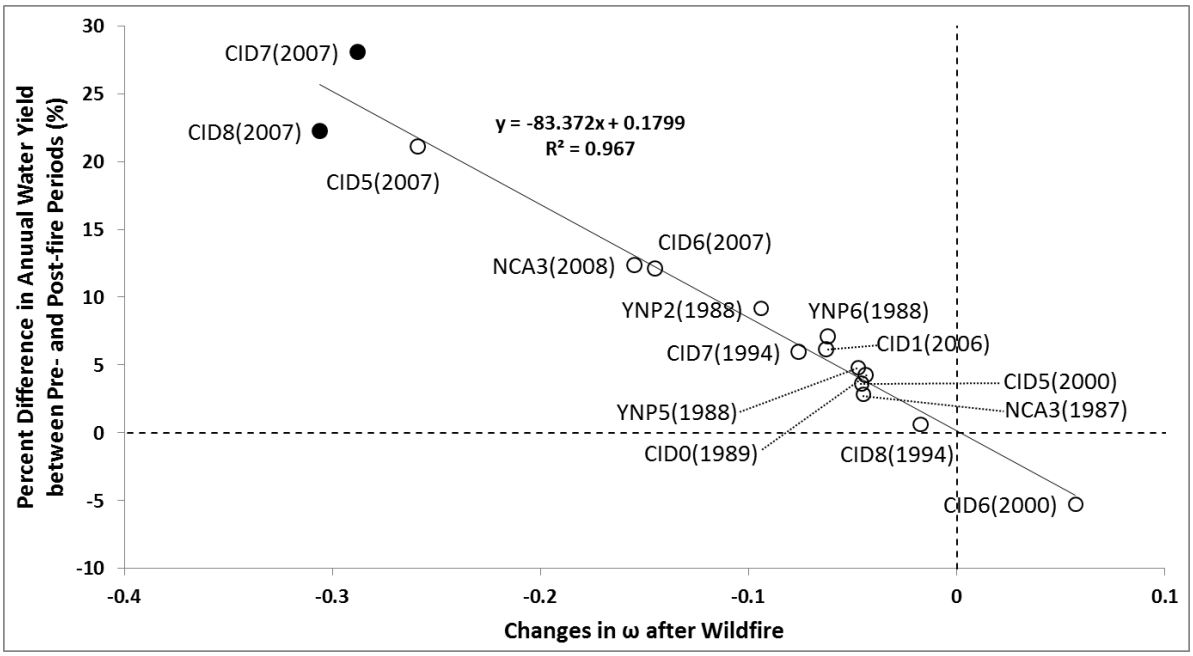


**Figure 2.5** Relationship between $\Delta\omega$ and $\Delta Q_m$(%). Numbers in bracelets indicate wildfire year. Filled markers, CID7 (2007) and CID8 (2007), indicate statistically significant impact of wildfire.

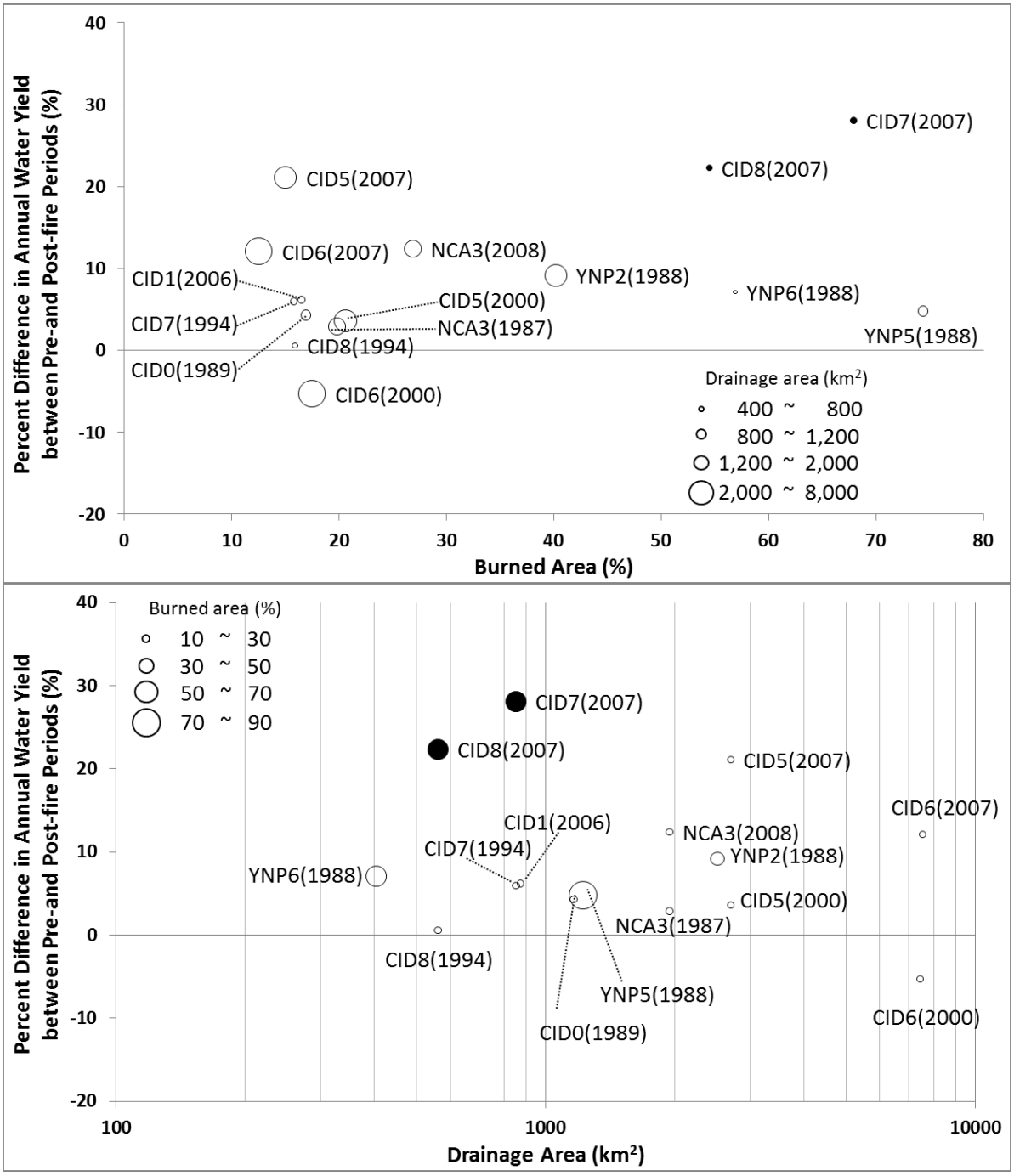


**Figure 2.6** Percent difference in annual water yield between pre- and post-fire periods (A; top panel) as a function of burned area (%) and (B; bottom panel) drainage area ($km^2$). The numbers in parentheses indicate wildfire year. Filled markers, CID7 (2007) and CID8 (2007) indicate statistically significant impact of wildfire.

### 4.4 Budyko Framework with Fu's Equation using $\overline{EI_{FB}}$ and $\overline{DI}$ for pre- and post-fire period

Responses of post-fire annual water yield estimated by the Budyko framework with long-term averaged flow-based evaporative index (averaged $\overline{EI_{FB}}$ and $\overline{DI}$) have similar response as the yearly analysis (Figure 2.7; Table 2.3). Comparisons between the wildfire response at both time scale (yearly) and (long term) show similar prediction in terms of $Q_m$ (Figure 2.8A) and $\omega$ (Figure 2.8B). Long-term time scale approach provides intuitive alteration of water and energy balance and the role of post-fire weather condition in a long-term context, and yearly time scale approach depicts role of climate condition in a short-term context related with water budget within a water year.

**Table 2.3** Summary of post-fire response of annual water yield using Budyko framework. Bold numbers indicate statistically significant wildfire impact from paired watershed analysis. Statistical test for significance of impact of wildfire using long-term average data is not available by accounting single data point for each period.

| Watershed (fire year)* | Drainage Area (km²) | Burned Area (%) | Budyko Framework with Fu's Equation using long-term average data of $\overline{EI_{FB}}$ and $\overline{DI}$ | | | | |
|---|---|---|---|---|---|---|---|
| | | | Pre-fire | Post-fire | Δω | ΔAWY (mm/yr) | ΔAWY (%) |
| CID0 (1989) D | 1163.2 | 16.9 | 1.523 | 1.449 | -0.075 | 38.0 | 6.7 |
| CID1 (2006) W | 874.8 | 16.5 | 1.623 | 1.567 | -0.056 | 20.8 | 5.4 |
| CID5 (2000) D | 2696.6 | 20.6 | 1.894 | 1.813 | -0.080 | 23.0 | 6.3 |
| CID5 (2007) - | 2696.6 | 15.0 | 1.894 | 1.609 | -0.284 | 100.0 | 23.2 |
| CID6 (2000) D | 7451 | 17.5 | 1.885 | 1.946 | 0.061 | -14.8 | -5.3 |
| CID6 (2007) D | 7541 | 12.5 | 1.885 | 1.749 | -0.137 | 39.8 | 12.1 |
| CID7 (1994) - | 853.1 | 15.8 | 1.691 | 1.604 | -0.087 | 36.3 | 7.0 |
| CID7 (2007) - | 853.1 | 67.9 | 1.691 | 1.424 | -0.267 | 125.7 | 25.9 |
| CID8 (1994) - | 561.9 | 15.9 | 1.906 | 1.847 | -0.059 | 18.8 | 3.6 |
| CID8 (2007) - | 561.9 | 54.5 | 1.906 | 1.587 | -0.319 | 116.8 | 23.4 |
| YNP2 (1988) D | 2516.1 | 40.2 | 1.647 | 1.532 | -0.115 | 47.2 | 11.0 |
| YNP5 (1988) - | 1222.3 | 74.4 | 1.436 | 1.384 | -0.051 | 30.9 | 5.0 |
| YNP6 (1988) D | 404.1 | 56.9 | 1.412 | 1.337 | -0.075 | 45.2 | 8.4 |
| NCA3 (1987) D | 1943.1 | 19.8 | 1.758 | 1.686 | -0.072 | 33.5 | 4.5 |
| NCA3 (2008) D | 1943.1 | 26.9 | 1.758 | 1.623 | -0.136 | 63.4 | 9.9 |

* Indicators represent that post-fire weather condition become drier (D), wetter (W) or remained same with pre-fire condition (-).

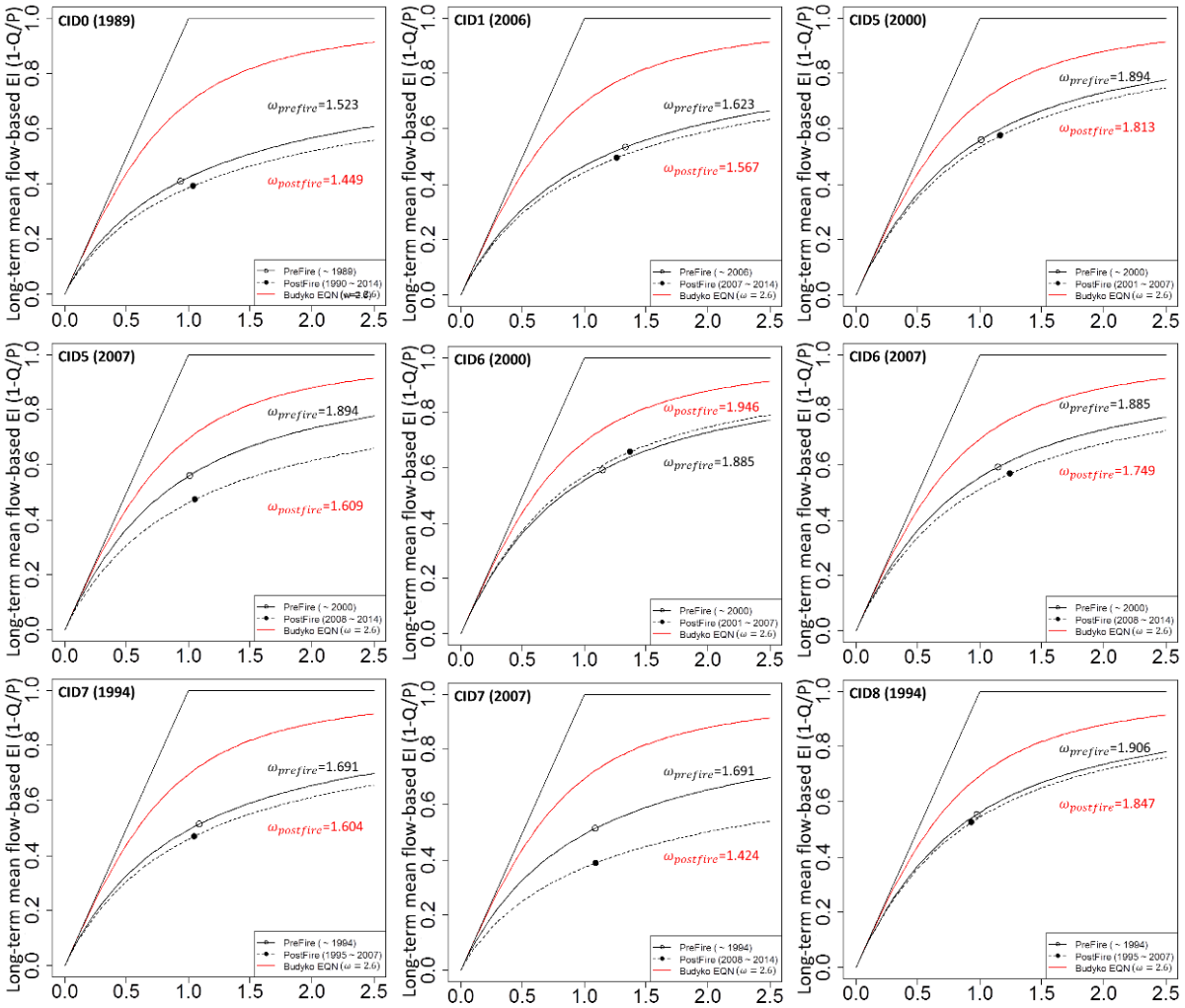


**Figure 2.7** Results of the new analytical approach within the Budyko framework using Fu's equation with long-term average value of $\overline{EI_{FB}}$ and $\overline{DI}$ which were calculated using long-term average of each input variable (i.e. Q, RNY, P) first to average-out the estimation errors reside in P. Numbers in bracelets indicate wildfire year. Open circles and filled circles indicate long-term averaged water and energy balance for pre- and post-fire periods, respectively. Continuous and dashed curves are fitted Fu's equation using non-linear least square method for pre- and post-fire periods, respectively. Red colored curve is a Fu's equation for global Budyko curve with $\omega = 2.6$.

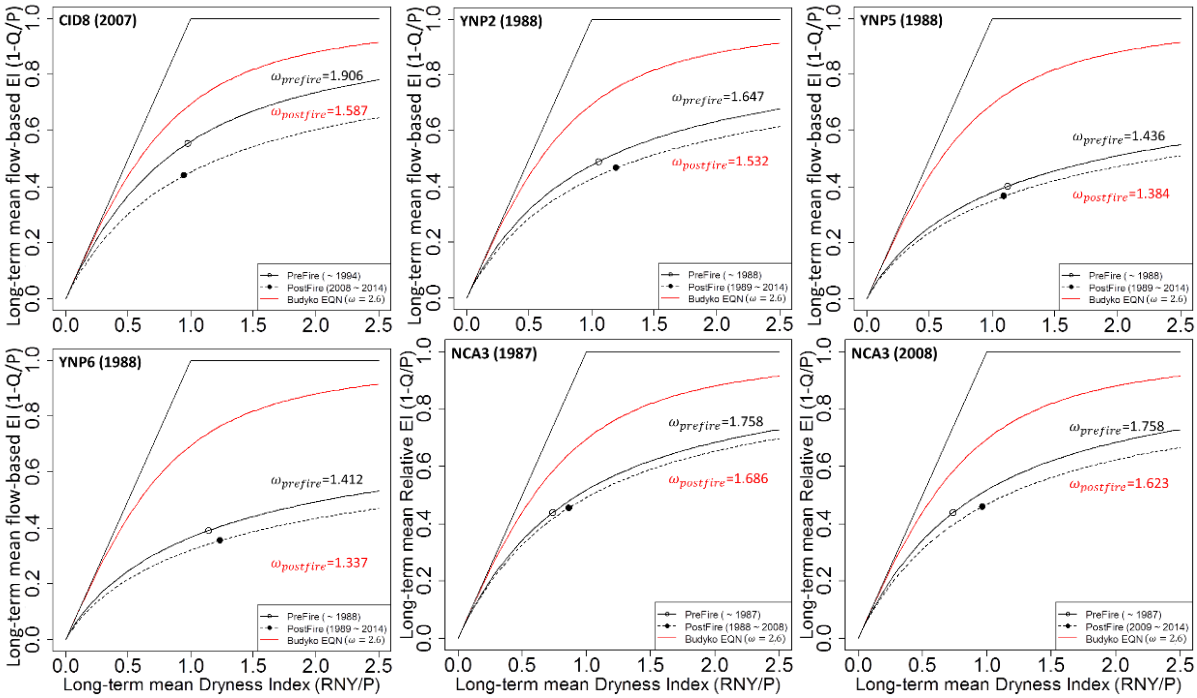


**Figure 2.7** Continue.

The amount of increased post-fire annual water yield was most notable in CID5 (2007), CID7 (2007) and CID8 (2007), where long-term weather condition for post-fire period remains similar to that of the pre-fire period (Figure 2.7; Table 2.3). These watersheds show impact of wildfire without interaction of climate variability, whereas other watersheds experienced both impacts of wildfire and alterations in post-fire climate condition. Watersheds CID1 (2006), CID7 (1994), CID8 (1994) and YNP5 (1988) become wetter during post-fire period (Figure 2.5; Table 2.3). On the other hand, CID0 (1989), CID5 (2000), CID6 (2000), CID6 (2007), YNP2 (1988), YNP6 (1988), NCA3 (1987) and NCA3 (2008) had a drier post- than pre-fire period, and their changes are larger than those in watersheds that become wetter during post-fire period. Post-fire responses of annual water yield in each group support that long-term post-fire weather wet or dry condition mitigated or enhanced the magnitude of impact of wildfire according to the inherent mechanism of post-fire water and energy balance within the Budyko framework, respectively.

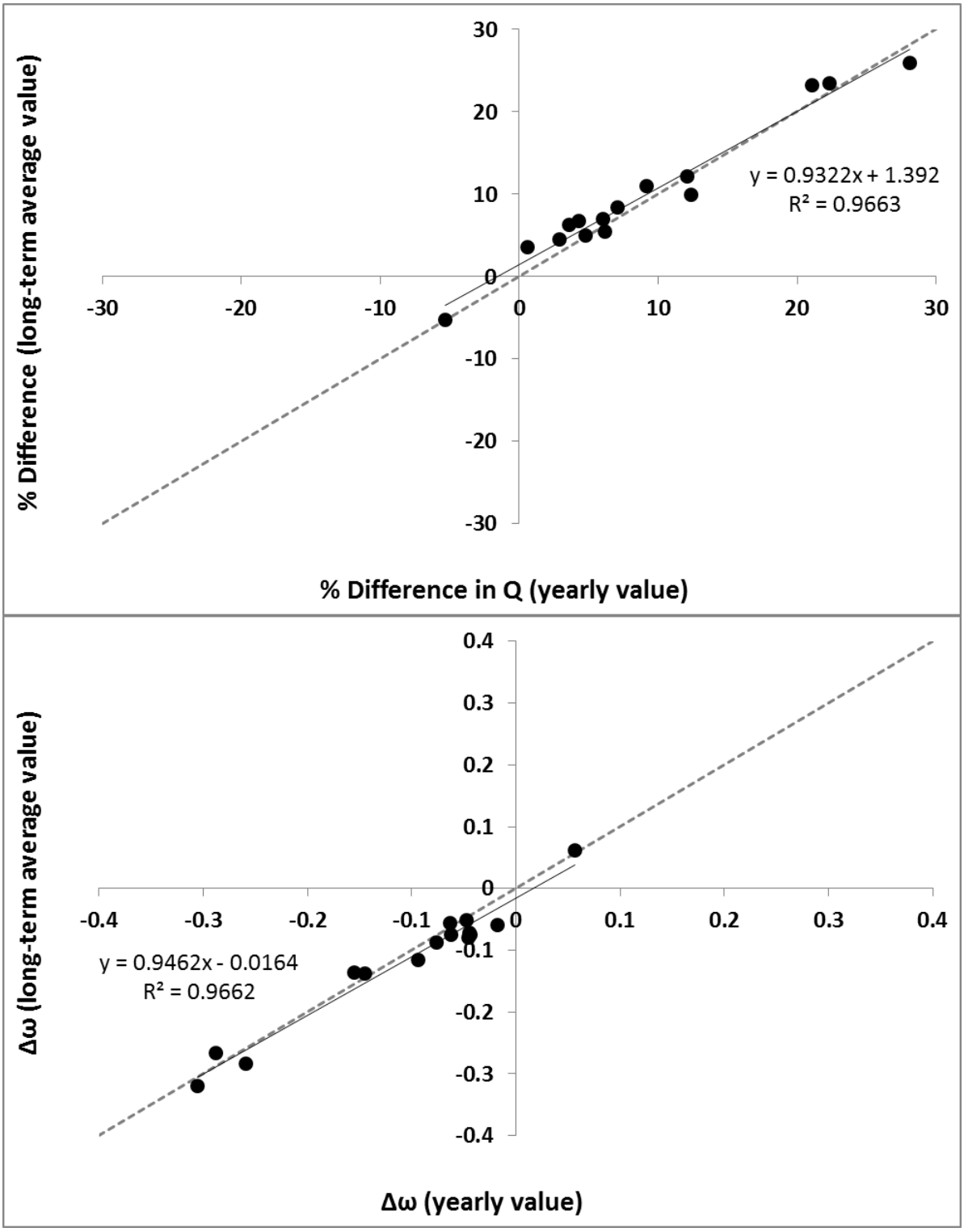


**Figure 2.8** Comparison of post-fire changes in annual water yield (A; left) and empirical parameter (B; right) estimated by the Budyko framework using Fu's equation with (1) yearly time scale (x-axis) and (2) long-term averaged time scale (y-axis) of flow-based evaporative index and dryness index.

The study sites can be categorized as watersheds dominated by snowmelt (watersheds in CID and YNP) or transient of snowmelt and rainfall (NCA3) (Supplementary Figure 2.6). Snowmelt dominant watersheds show overwhelming delay for precipitation-runoff relationship from October to June, and the watershed dominated by transient of snowmelt and rainfall (NCA3) shows masked delayed effect due to significant of rainfall induced discharge with snowmelt discharge from October to June. On the other hand, rainfall dominant watersheds (FLB) do not show snowmelt discharge induced delay throughout water year. FLB (the Suwanee Swamp across Georgia and Florida) was excluded in this study due to existence of undefined water sources (Supplementary Figure 2.7). But, it is shown in Figure 2.9 to illustrate characteristic of water and energy balance of watersheds categorized by dominance of water supply. Watersheds dominated by snowmelt and transient of snowmelt and rainfall are located below the global mean Budyko curve while rainfall dominant watersheds are located above the global mean Budyko curve. And, increase in post-fire annual water yield was detected in dominated by transient of snowmelt and rainfall (NCA3) and snowmelt (CID and YNP) whereas decrease in post-fire annual water yield was detected in rainfall dominant watersheds (FLB). The latter is expected from our hypothesis that regrowth will start quickly in those watersheds reducing Q.

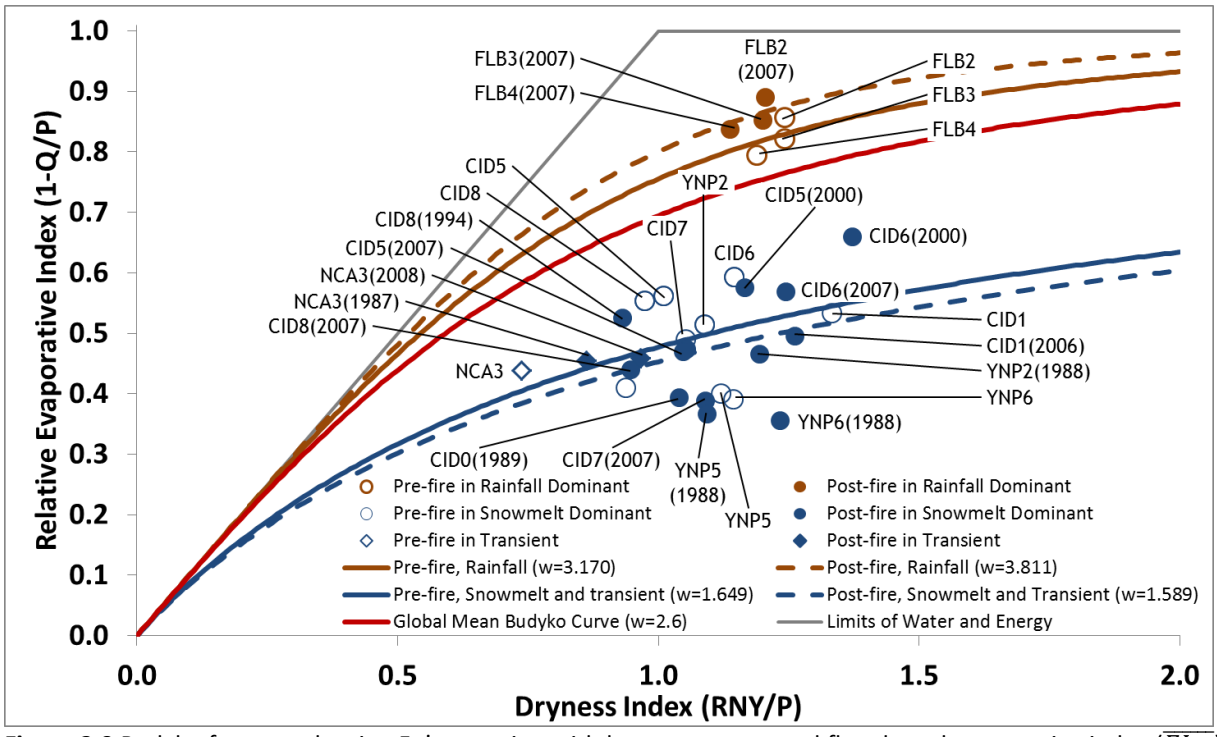


**Figure 2.9** Budyko framework using Fu's equation with long-term averaged flow-based evaporative index ($\overline{EI_{FB}}$) and dryness index ($\overline{DI}$) for pre- and post-fire periods in burned watersheds. Numbers in bracelets indicate wildfire year. Burned watersheds were categorized based on water supply source that dominated by (1) rainfall (FLA and FLB; brown) and (2) snowmelt (CID and YNP; blue) and transient of snowmelt and rainfall (NCA3) considering double mass curve of cumulative precipitation and annual water yield (Supplementary Figure 2.6).

## 5 Conclusions

The Budyko framework has long been applied for the analyses of post-external disturbance (i.e. forest harvest, climate change, dam regulation, irrigation, etc.) response of water and energy balance but wildfire has not been considered as an external disturbance yet. This study employed the Budyko framework for the assessment of the impact of wildfire and interaction of post-wildfire weather condition in large watersheds at both yearly and pre and post-wildfire time scales. It presented an alternative method for the assessment of post-wildfire response of Q especially in large watersheds (500 ~ 8,000 km$^2$) where data is limited and selecting control-paired watershed is challenging. We suggested a flow-based evaporative index ($EI_{FB}$; 1-Q/P) instead of traditional evaporative index ($EI$; AET/P) with steady-state condition. The model with $EI_{FB}$ showed better performance than $EI$ for the Budyko framework using Fu's equation in spatial scale of watersheds ranges from several hundreds to thousands of square kilometers.

Although, the impact of wildfire was statistically significant and increased Q in 2 out of 10 analyzed watersheds, post-wildfire response of Q estimated by both long-term and yearly time scale approaches showed good agreement and an increase in post-wildfire Q in all but one watershed, which experienced fast regrowth right after wildfire. The model also highlighted the significance of post-wildfire weather condition, which has been observed in previous studies. The Budyko framework supported the observation-based finding that wildfire-induced changes in Q are less detectable in watersheds with wetter post- than pre-wildfire conditions but more detectable for the inverse weather conditions. Because of this weather-trend dependence, detection of a general trend in large watershed has been difficult besides the limitation in data.

**References**

Adams HD, Luce CH, Breshears DD, Allen CD, Weiler M, Hale VC, Smith AMS, Huxman TE. 2012. Ecohydrological consequences of drought- and infestation- triggered tree die-off: insights and hypotheses. Ecohydrology, **5**: 145-159. DOI: 10.1002/eco.233.

Bales RC, Molotch NP, Painter TH, Dettinger MD, Rice R, Jeff D. 2006. Mountain hydrology of the western United States. Water Resources Research, **42**: W08432. DOI: 10.1029/2005WR004387.

Bart R, Hope A. 2010. Streamflow response to fire in large catchments of a Mediterranean-climate region using paired-catchment experiments. Journal of hydrology, **388**: 370-378. DOI: 10.1016/j.jhydrol.2010.05.016.

Bart RR. 2016. A regional estimate of postfire streamflow change in California. Water Resources Research, **52**: 1465-1478. DOI: 10.1002/2014WR016553.

Berndt H. 1971. Early effects of forest fire on streamflow characteristics. In: Res. Note PNW-RN-148. Portland, OR: US Department of Agriculture, Forest Service, Pacific Northwest Forest and Range Experiment Station. 11 p, USDA Forest Service, Pacific Northwest Forest and Range Experiment Station.

Brooks KN, Ffolliott PF, Gregersen HM, DeBano LF. 1997. Hydrology and the management of watersheds. Iowa State University Press.

Budyko M. 1974. Climate and Life, 508 pp. Academic Press, New York.

Campbell RE, Baker J, Ffolliott PF, Larson FR, Avery CC. 1977. Wildfire effects on a ponderosa pine ecosystem: an Arizona case study. In: USDA For. Serv. Res. Pap. RM-191. Fort Collins, CO: US Department of Agriculture, Forest Service, Rocky Mountain Forest and Range Experimental Station. 12 p., USDA Forest Service.

Chen X, Alimohammadi N, Wang D. 2013. Modeling interannual variability of seasonal evaporation and storage change based on the extended Budyko framework. Water Resources Research, **49**: 6067-6078. DOI: 10.1002/wrcr.20493.

Choudhury B. 1999. Evaluation of an empirical equation for annual evaporation using field observations and results from a biophysical model. Journal of Hydrology, **216**: 99-110. DOI: 10.1016/S0022-1694(98)00293-5.

Dennison PE, Brewer SC, Arnold JD, Moritz MA. 2014. Large wildfire trends in the western United States, 1984–2011. Geophysical Research Letters, **41**: 2928-2933. DOI: 10.1002/2014GL059576.

Dillon GK, Holden ZA, Morgan P, Crimmins MA, Heyerdahl EK, Luce CH. 2011. Both topography and climate affected forest and woodland burn severity in two regions of the western US, 1984 to 2006. Ecosphere, **2**: 1-33. DOI: 10.1890/ES11-00271.1.

Donohue RJ, Roderick ML, Mcvicar TR. 2007. On the importance of including vegetation dynamics in Budyko's hydrological model. Hydrology and earth system sciences, **11**: 983-995. DOI: 10.5194/hess-11-983-2007.

Donohue RJ, Roderick ML, Mcvicar TR. 2011. Assessing the differences in sensitivities of runoff to changes in climatic conditions across a large basin. Journal of Hydrology, **406**: 234-244. DOI: 10.1016/j.jhydrol.2011.07.003.

Donohue RJ, Roderick ML, Mcvicar TR. 2012. Roots, storms and soil pores: Incorporating key ecohydrological processes into Budyko's hydrological model. Journal of Hydrology, **436**: 35-50. DOI: 10.1016/j.jhydrol.2012.02.033.

Fang K, Shen C, Fisher JB, Niu J. 2016. Improving Budyko curve-based estimates of long-term water partitioning using hydrologic signatures from GRACE. Water Resources Research, **52**: 5537-5554. DOI: 10.1002/2016WR018748.

Feikema PM, Sherwin CB, Lane PNJ. 2013. Influence of climate, fire severity and forest mortality on predictions of long term streamflow: potential effect of the 2009 wildfire on Melbourne's water supply catchments. Journal of Hydrology, **488**: 1-16. DOI: 10.1016/j.jhydrol.2013.02.001.

Fu B-p. 1981. On the calculation of the evaporation from land surface [in Chinese]. Scientia Atmospherica Sinica, **1**: 23–31.

Greve P, Gudmundsson L, Orlowsky B, Seneviratne SI. 2015. Introducing a probabilistic Budyko Framework. Geophysical Research Letters, **42**: 2261-2269. DOI: 10.1002/2015GL063449.

Hallema DW, Sun G, Caldwell PV, Norman SP, Cohen EC, Liu Y, Bladon KD, McNulty SG. 2018. Burned forests impact water supplies. Nature Communications, **9**: 1307. DOI: 10.1038/s41467-018-03735-6.

Hallema DW, Sun G, Caldwell PV, Norman SP, Cohen EC, Liu Y, Ward EJ, McNulty SG. 2017. Assessment of wildland fire impacts on watershed annual water yield: Analytical framework and case studies in the United States. Ecohydrology, **10**: e1794. DOI: 10.1002/eco.1794.

Helvey J. 1980. Effects of a north central Washington wildfire on runoff and sediment production. Journal of the American Water Resources Association, **16**: 627-634. DOI: 10.1111/j.1752-1688.1980.tb02441.x.

Huntington TG. 2006. Evidence for intensification of the global water cycle: review and synthesis. Journal of Hydrology, **319**: 83-95. DOI: 10.1016/j.jhydrol.2005.07.003.

Jeton AE, Watkins SA, Lopes TJ, Huntington J. 2006. Evaluation of precipitation estimates from PRISM for the 1961–90 and 1971–2000 data sets, Nevada. In: USGS Scientific Investigations Report 2005-5291.

Jiang C, Xiong L, Wang D, Liu P, Guo S, Xu C-y. 2015. Separating the impacts of climate change and human activities on runoff using the Budyko-type equations with time-varying parameters. Journal of Hydrology, **522**: 326-338. DOI: 10.1016/j.jhydrol.2014.12.060.

Kuczera G. 1987. Prediction of water yield reductions following a bushfire in ash-mixed species eucalypt forest. Journal of hydrology, **94**: 215-236. DOI: 10.1016/0022-1694(87)90054-0.

Lane PN, Feikema PM, Sherwin C, Peel M, Freebairn A. 2010. Modelling the long term water yield impact of wildfire and other forest disturbance in Eucalypt forests. Environmental Modelling & Software, **25**: 467-478. DOI: 10.1016/j.envsoft.2009.11.001.

Li D, Pan M, Cong Z, Zhang L, Wood E. 2013. Vegetation control on water and energy balance within the Budyko framework. Water Resources Research, **49**: 969-976. DOI: 10.1002/wrcr.20107.

Liang L, Liu Q. 2014. Streamflow sensitivity analysis to climate change for a large water-limited basin. Hydrological Processes, **28**: 1767-1774. DOI: 10.1002/hyp.9720.

Liu Y, Gupta H, Springer E, Wagener T. 2008. Linking science with environmental decision making: Experiences from an integrated modeling approach to supporting sustainable water resources management. Environmental Modelling & Software, **23**: 846-858. DOI: 10.1016/j.envsoft.2007.10.007.

Luce C, Morgan P, Dwire K, Isaak D, Holden Z, Rieman B, Gresswell R, Rinne J, Neville HM, Gresswell R. 2012. Climate change, forests, fire, water, and fish: Building resilient landscapes, streams, and managers. USDA Forest Service.

Martin DA, Moody JA. 2001. Comparison of soil infiltration rates in burned and unburned mountainous watersheds. Hydrological Processes, **15**: 2893-2903. DOI: 10.1002/hyp.380.

McKee TB, Doesken NJ, Kleist J. 1993. The relationship of drought frequency and duration to time scales. In: 8th Conference on Applied Climatology, American Meteorological Society.

Morgan P, Heyerdahl EK, Gibson CE. 2008. Multi-season climate synchronized forest fires throughout the 20th century, northern Rockies, USA. Ecology, **89**: 717-728. DOI: 10.1890/06-2049.1.

Running SW, Mu Q, Zhao M, Moreno A. 2017. MODIS global terrestrial evapotranspiration (ET) product (NASA MOD16A2/A3) NASA earth observing system MODIS land algorithm. In: User's Guide, NASA.

Scott D. 1993. The hydrological effects of fire in South African mountain catchments. Journal of hydrology, **150**: 409-432. DOI: 10.1016/0022-1694(93)90119-T.

Sidman G, Guertin DP, Goodrich DC, Thoma D, Falk D, Burns IS. 2016. A coupled modelling approach to assess the effect of fuel treatments on post-wildfire runoff and erosion. International Journal of Wildland Fire, **25**: 351-362. DOI: 10.1071/WF14058.

Sposito G. 2017. Understanding the Budyko Equation. Water, **9**: 236. DOI: 10.3390/w9040236.

Stoof CR, Vervoort R, Iwema J, Elsen E, Ferreira A, Ritsema C. 2012. Hydrological response of a small catchment burned by experimental fire. Hydrology and Earth System Sciences, **16**: 267-285. DOI: 10.5194/hess-16-267-2012.

van der Velde Y, Vercauteren N, Jaramillo F, Dekker SC, Destouni G, Lyon SW. 2014. Exploring hydroclimatic change disparity via the Budyko framework. Hydrological Processes, **28**: 4110-4118. DOI: 10.1002/hyp.9949.

Vieira D, Fernández C, Vega J, Keizer J. 2015. Does soil burn severity affect the post-fire runoff and interrill erosion response? A review based on meta-analysis of field rainfall simulation data. Journal of hydrology, **523**: 452-464. DOI: 10.1016/j.jhydrol.2015.01.071.

Wang C, Wang S, Fu B, Zhang L. 2016. Advances in hydrological modelling with the Budyko framework: A review. Progress in Physical Geography, **40**: 409-430. DOI: 10.1177/0309133315620997.

Wang D, Hejazi M. 2011. Quantifying the relative contribution of the climate and direct human impacts on mean annual streamflow in the contiguous United States. Water Resources Research, **47**: W00J12. DOI: 10.1029/2010WR010283.

Wang D, Tang Y. 2014. A one-parameter Budyko model for water balance captures emergent behavior in Darwinian hydrologic models. Geophysical Research Letters, **41**: 4569-4577. DOI: 10.1002/2014GL060509.

Wine M, Cadol D. 2016. Hydrologic effects of large southwestern USA wildfires significantly increase regional water supply: fact or fiction? Environmental Research Letters, **11**: 085006. DOI: 10.1088/1748-9326/11/8/085006.

Wine ML, Cadol D, Makhnin O. 2018. In ecoregions across western USA streamflow increases during post-wildfire recovery. Environmental Research Letters, **13**: 014010. DOI: 10.1088/1748-9326/aa9c5a.

Xu X, Yang D, Yang H, Lei H. 2014. Attribution analysis based on the Budyko hypothesis for detecting the dominant cause of runoff decline in Haihe basin. Journal of Hydrology, **510**: 530-540. DOI: 10.1016/j.jhydrol.2013.12.052.

Yang D, Sun F, Liu Z, Cong Z, Lei Z. 2006. Interpreting the complementary relationship in non-humid environments based on the Budyko and Penman hypotheses. Geophysical Research Letters, **33**: L18402. DOI: 10.1029/2006GL027657.

Yang H, Yang D, Lei Z, Sun F. 2008. New analytical derivation of the mean annual water-energy balance equation. Water Resources Research, **44**: W03410. DOI: 10.1029/2007WR006135.

Zhang K, Kimball JS, Nemani RR, Running SW. 2010. A continuous satellite-derived global record of land surface evapotranspiration from 1983 to 2006. Water Resources Research, **46**: W09522. DOI: 10.1029/2009WR008800.

Zhang L, Dawes WR, Walker GR. 2001. Response of mean annual evapotranspiration to vegetation changes at catchment scale. Water Resources Research, **37**: 701-708. DOI: 10.1029/2000WR900325.

Zhang L, Hickel K, Dawes WR, Chiew FHS, Western AW, Briggs PR. 2004. A rational function approach for estimating mean annual evapotranspiration. Water Resources Research, **40**: W02502. DOI: 10.1029/2003WR002710.

Zhang S, Yang H, Yang D, Jayawardena A. 2016. Quantifying the effect of vegetation change on the regional water balance within the Budyko framework. J Geophysical Research Letters, **43**: 1140-1148. DOI: 10.1002/2015GL066952.

Zhou Y, Zhang Y, Vaze J, Lane P, Xu S. 2015. Impact of bushfire and climate variability on streamflow from forested catchments in southeast Australia. Hydrological sciences journal, **60**: 1340-1360. DOI: 10.1080/02626667.2014.961923.

# Appendix A: Supplementary Material for Chapter 1

## Tables

**Supplementary Table 1.1** Gauges station name for Table 1.1. Shaded rows indicate burned watersheds.

| Site | Watershed ID | Gauge ID | Station Name |
|---|---|---|---|
| CID | 0 | 13235000 | South Fork Payette River at Lowman, ID |
| | 1 | 13237920 | Middle Fork Payette River near Crouch, ID |
| | 2 | 13295000 | Valley Creek at Stanley, ID |
| | 3 | 13296500 | Salmon River below Yankee Fork near Clayton, ID |
| | 5 | 13309220 | Middle Fork Salmon River at Middle Fork Lodge near Yellow Pine, ID |
| | 6 | 13310199 | Middle Fork Salmon River at Mouth near Shoup, ID |
| | 7 | 13310700 | South Fork Salmon River near Krassel Ranger Station, ID |
| | 8 | 13313000 | Johnson Creek at Yellow Pine, ID |
| YNP | 0 | 06037500 | Madison River near West Yellowstone, MT |
| | 1 | 06043500 | Gallatin River near Gallatin Gateway, MT |
| | 2 | 06186500 | Yellowstone River at Yellowstone Lake outlet, YNP |
| | 5 | 13010065 | Snake River above Jackson Lake at Flagg Ranch, WY |
| | 6 | 13011500 | Pacific Creek at Moran, WY |
| | 7 | 13011900 | Buffalo Fork above Lava Creek near Moran, WY |
| | 10 | 06280300 | South Fork Shoshone River near Valley, WY |
| NCA | 0 | 11517500 | Shasta River near Yreka, CA |
| | 1 | 11519500 | Scott River near Fort Jones, CA |
| | 2 | 11520500 | Klamath river near Seiad Valley, CA |
| | 3 | 11522500 | Salmon River at Somes Bar, CA |

**Supplementary Table 1.2** Long-term average values of annual baseflow index of burned watersheds.

| Watershed | CID0 | CID1 | CID6 | CID7 | CID8 | YNP0 | YNP6 | NCA3 |
|---|---|---|---|---|---|---|---|---|
| mean BFI | 0.45 | 0.36 | 0.40 | 0.43 | 0.45 | 0.75 | 0.43 | 0.28 |

**Supplementary Table 1.3** All results of linear regression models of the paired watersheds. Bold numbers represent statistically significant coefficients (confidence level>90%).

| Site | Control Water-shed | Burned Watershed (Fire year) | Linear Regression Model | | | | | |
|---|---|---|---|---|---|---|---|---|
| | | | Estimation | | | DF | p-value | Adj. $R^2$ |
| | | | **Intercept** | **a** | **b** | | | |
| | | | [$m^3/s$] | [-] | [$m^3/s$] | | | |
| CID | 2 | 0 (1989) | 0.52 | 3.98 | 1.24 | 41 | <2.2E-16 | 0.954 |
| | | 1 (2006) | -3.70 | 3.03 | -1.91 | 12 | 2.62E-06 | 0.863 |
| | | 6 (2000) | 3.28 | 13.76 | -1.98 | 11 | 4.00E-15 | 0.997 |
| | | 6 (2007) | 2.34 | 13.91 | 5.82 | 11 | 2.89E-08 | 0.950 |
| | | 7 (1994) | -1.42 | 2.88 | 0.46 | 17 | 1.20E-14 | 0.974 |
| | | 7 (2007) | -1.50 | 2.89 | 1.53 | 11 | 6.20E-08 | 0.942 |
| | | 8 (1994) | 0.17 | 1.71 | 0.05 | 34 | <2.2E-16 | 0.948 |
| | | 8 (2007) | 0.57 | 1.64 | 1.06 | 28 | <2.2E-16 | 0.921 |
| | 3 | 0 (1989) | -0.15 | 0.83 | 0.55 | 49 | <2.2E-16 | 0.953 |
| | | 1 (2006) | -3.53 | 0.62 | -2.67 | 11 | 8.81E-07 | 0.906 |
| | | 5 (2000) | -8.55 | 1.84 | 1.19 | 10 | 4.81E-10 | 0.984 |
| | | 5 (2007) | -7.40 | 1.79 | 0.36 | 10 | 4.94E-09 | 0.974 |
| | | 7 (1994) | -3.21 | 0.64 | 0.97 | 19 | 1.41E-14 | 0.962 |
| | | 7 (2007) | -2.76 | 0.63 | 1.12 | 19 | 9.69E-14 | 0.953 |
| | | 8 (1994) | -0.84 | 0.37 | 0.37 | 42 | <2.2E-16 | 0.936 |
| | | 8 (2007) | -0.74 | 0.37 | 1.09 | 42 | <2.2E-16 | 0.930 |
| YNP | 1 | 0 (1988) | 6.38 | 0.35 | -0.28 | 47 | 4.53E-07 | 0.440 |
| | | 2 (1988) | 2.48 | 1.50 | 1.02 | 55 | 4.55E-10 | 0.526 |
| | | 5 (1988) | -3.27 | 1.24 | -0.12 | 27 | 5.76E-07 | 0.630 |
| | | 6 (1988) | -0.70 | 0.33 | 0.58 | 54 | 2.33E-07 | 0.411 |
| | 7 | 0 (1988) | 7.67 | 0.52 | -1.06 | 34 | 5.24E-09 | 0.655 |
| | | 2 (1988) | 1.92 | 2.41 | 0.92 | 43 | <2.2E-16 | 0.902 |
| | | 5 (1988) | -0.33 | 1.70 | 0.77 | 28 | 1.88E-14 | 0.888 |
| | | 6 (1988) | -2.15 | 0.61 | 0.73 | 43 | <2.2E-16 | 0.841 |
| | 10 | 0 (1988) | 9.15 | 0.49 | -0.53 | 42 | 1.26E-04 | 0.317 |
| | | 2 (1988) | 2.45 | 3.08 | 0.59 | 51 | <2.2E-16 | 0.819 |
| | | 5 (1988) | 5.05 | 1.68 | 1.10 | 28 | 1.30E-05 | 0.520 |
| | | 6 (1988) | -1.31 | 0.73 | 0.62 | 51 | 1.34E-13 | 0.675 |
| NCA | 0 | 3 (1987) | 2.02 | 9.58 | -1.19 | 56 | <2.2E-16 | 0.833 |
| | | 3 (2008) | -0.68 | 10.05 | 8.39 | 40 | <2.2E-16 | 0.849 |
| | 1 | 3 (1987) | 10.88 | 2.28 | 1.07 | 56 | <2.2E-16 | 0.956 |
| | | 3 (2008) | 11.29 | 2.26 | 6.30 | 40 | <2.2E-16 | 0.955 |
| | 2 | 3 (1987) | -0.19 | 0.46 | 5.89 | 54 | <2.2E-16 | 0.876 |
| | | 3 (2008) | 0.16 | 0.46 | 12.04 | 38 | <2.2E-16 | 0.880 |

**Supplementary Table 1.4** Changes in landcover composition during post-fire period. CID5(2000), CID5(2007), CID7(1994), CID8(1994), YNP2(1988), YNP5(1988), NCA3(1987) were omitted where impact of wildfire ($b$) was statistically insignificant.

| Watersheds | CID0 | CID1 | CID6 | CID6 | CID7 | CID8 | YNP6 | NCA3 |
|---|---|---|---|---|---|---|---|---|
| (Wildfire year) | (1989) | (2006) | (2000) | (2007) | (2007) | (2007) | (1988) | (2008) |
| Changes in NLCD | 1992 ~2011 | 2006 ~2011 | 2001 ~2006 | 2006 ~2011 | 2006 ~2011 | 2006 ~2011 | 1992 ~2011 | 2006 ~2011 |
| Water body [%] | 0.59 | 0.0 | 0.0 | 0.0 | 0.0 | 0.0 | -0.46 | 0.0 |
| Developed [%] | 0.36 | 0.0 | 0.0 | 0.0 | 0.0 | 0.0 | 0.0 | 0.01 |
| Barren area [%] | -18.67 | 0.0 | 0.01 | 0.0 | 0.0 | 0.0 | -23.99 | 0.01 |
| Tree [%] | -8.80 | -3.53 | -1.60 | -5.62 | -21.93 | -17.07 | -6.93 | -0.07 |
| Shrub [%] | 15.31 | 1.77 | 3.83 | 1.26 | 2.68 | 3.63 | 37.73 | 0.05 |
| Grass and crop [%] | 9.97 | 1.76 | -2.23 | 4.36 | 19.26 | 13.44 | -7.90 | 0.02 |
| Wetland [%] | -0.11 | 0.0 | 0.0 | 0.0 | -0.01 | 0.0 | 1.54 | 0.0 |
| Relative changes in Q [%] | 5.5 | -17.9 | -3.8 | 6.4 | 9.5 | 10.7 | 11.1 | 27.1 |

**Supplementary Table 1.5** Calculations for the analytical model for the post-fire response in annual water yield.

| Watersheds (Wildfire year) | Input variables | | | | | | Relative changes in annual water yield ($\Delta\mathbf{Q}/\boldsymbol{Q_{Pre}}$) [%] | | |
|---|---|---|---|---|---|---|---|---|---|
| | $\boldsymbol{F}$ [%] | $\boldsymbol{EI_{FB,Pre}}$ | $\boldsymbol{c}$ [-] | $\overline{\boldsymbol{P}}_{\boldsymbol{Pre}}$ [mm/yr] | $\overline{\boldsymbol{Q}}_{\boldsymbol{Pre}}$ [mm/yr] | $\boldsymbol{m}$ [%] | PWA | Eq. 4 | Eq. S6 ($\boldsymbol{k} = \mathbf{0.2}$) |
| CID0 (1989) | 0.542 | 0.410 | 0.594 | 1113.1 | 656.4 | 8.80 | 5.5 | 6.0 | 6.7 |
| CID1 (2006) | 0.775 | 0.534 | 0.594 | 761.3 | 354.9 | 3.53 | -17.9 | 2.0 | 3.3 |
| CID5 (2000) | 0.599 | 0.561 | 0.594 | 1054.9 | 462.8 | 0.57 | 3.7 | 0.1 | 0.5 |
| CID5 (2007) | 0.599 | 0.561 | 0.594 | 1054.9 | 462.8 | 7.62 | 1.6 | 1.4 | 6.1 |
| CID6 (2000) | 0.589 | 0.593 | 0.594 | 923.5 | 375.9 | 1.60 | -3.8 | 0.01 | 1.3 |
| CID6 (2007) | 0.589 | 0.593 | 0.594 | 923.5 | 375.9 | 5.62 | 6.4 | 0.04 | 4.4 |
| CID7 (1994) | 0.838 | 0.514 | 0.594 | 1001.8 | 486.8 | 4.41 | 6.7 | 4.5 | 4.3 |
| CID7 (2007) | 0.838 | 0.514 | 0.594 | 1001.8 | 486.8 | 21.93 | 9.5 | 22.3 | 21.6 |
| CID8 (1994) | 0.815 | 0.554 | 0.594 | 1084.2 | 483.4 | 7.30 | 3.0 | 3.5 | 7.0 |
| CID8 (2007) | 0.815 | 0.554 | 0.594 | 1084.2 | 483.4 | 17.07 | 10.7 | 8.3 | 16.4 |
| YNP2 (1988) | 0.490 | 0.489 | 0.594 | 976.9 | 498.8 | 13.72 | 2.5 | 5.5 | 10.1 |
| YNP5 (1988) | 0.426 | 0.401 | 0.594 | 989.1 | 592.9 | 1.07 | 1.6 | 0.6 | 0.8 |
| YNP6 (1988) | 0.491 | 0.391 | 0.594 | 910.0 | 554.3 | 6.93 | 11.1 | 4.5 | 5.1 |

**Figures**

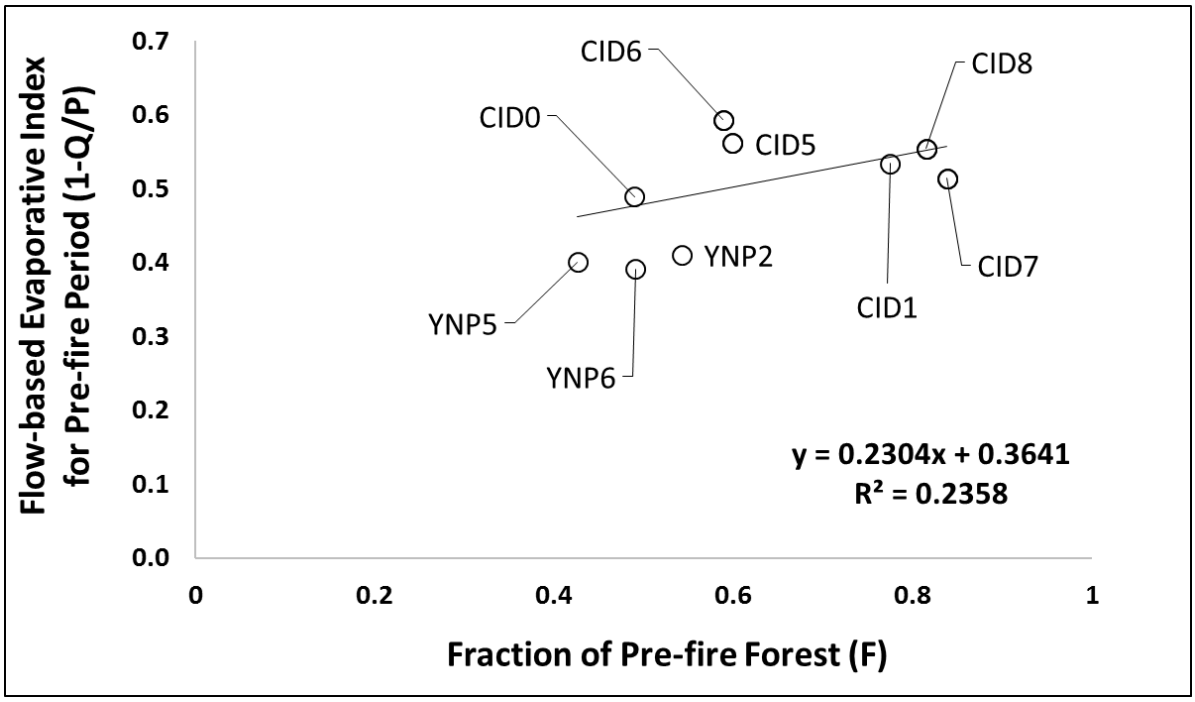


**Supplementary Figure 1.1** Estimation of the empirical coefficient of evaporative capacity of forest ($c$) of study sites by extrapolating the flow-based evaporative index for a watershed that is fully covered by forest ($\mathrm{F} = 1$) thus $c = EI_{F=1} = 0.5941$.

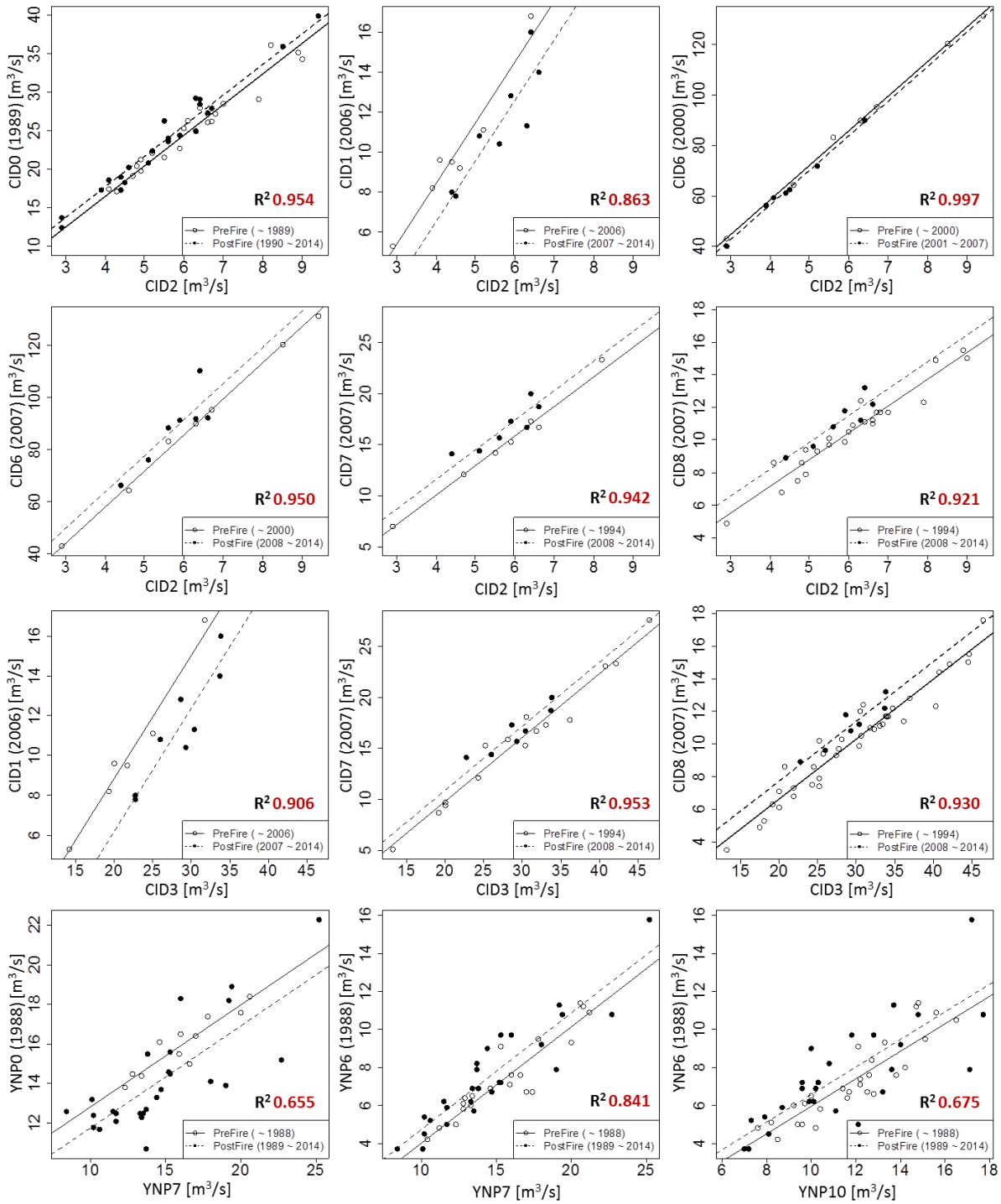


**Supplementary Figure 1.2** All results of linear regression models between burned watersheds (y-axis) and control watersheds (x-axis) (pairs that wildfire impact is insignificant (no fire effect) are excluded from Supplementary Table 1.3). B-Site# and C-Site# indicate burned and control watersheds of each site, respectively. Continuous line and dash line indicate linear regression of paired water yield of pre- and post- wildfire, respectively.

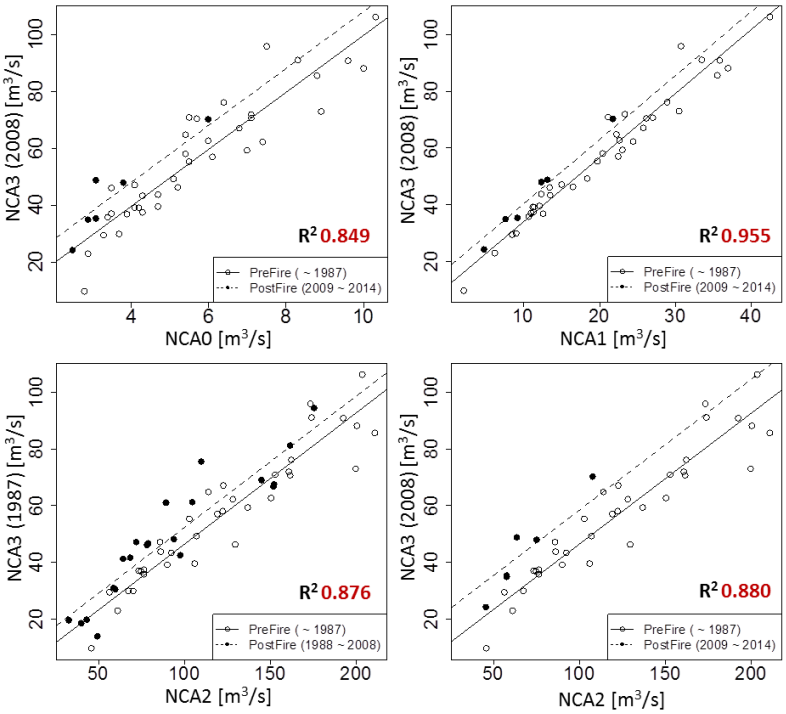


**Supplementary Figure 1.2** Continue.

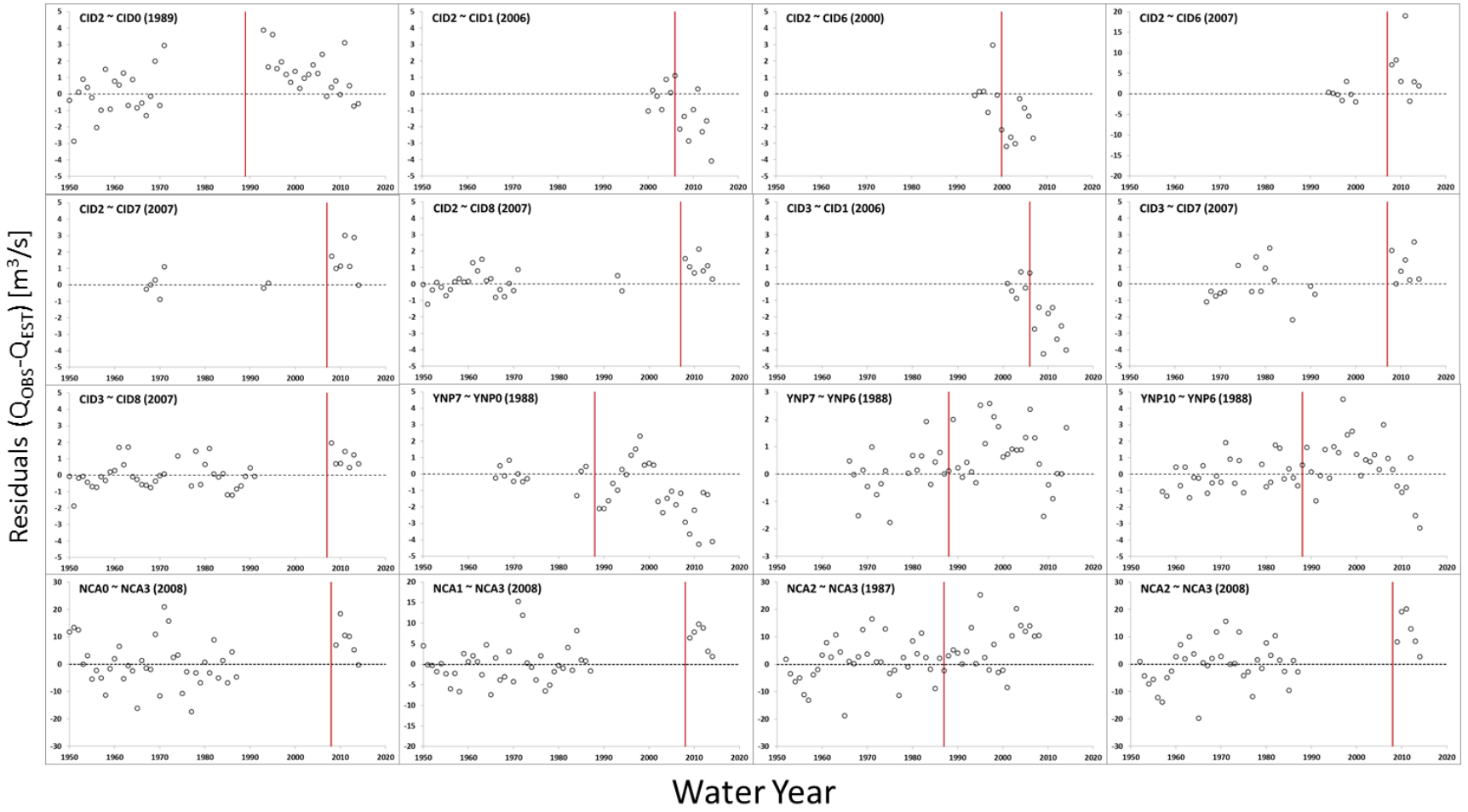


**Supplementary Figure 1.3** Residuals ($Q_{OBS}$ – $Q_{EST}$) between observed discharges ($Q_{OBS}$) and discharges estimated ($Q_{EST}$) by the linear regression model using I=0 of paired watersheds where impact of wildfire was statistically significant with 90% of confidence level from Supplementary Table 1.3. Vertical intercepts indicate major wildfire years, which correspond to numbers in bracelets.

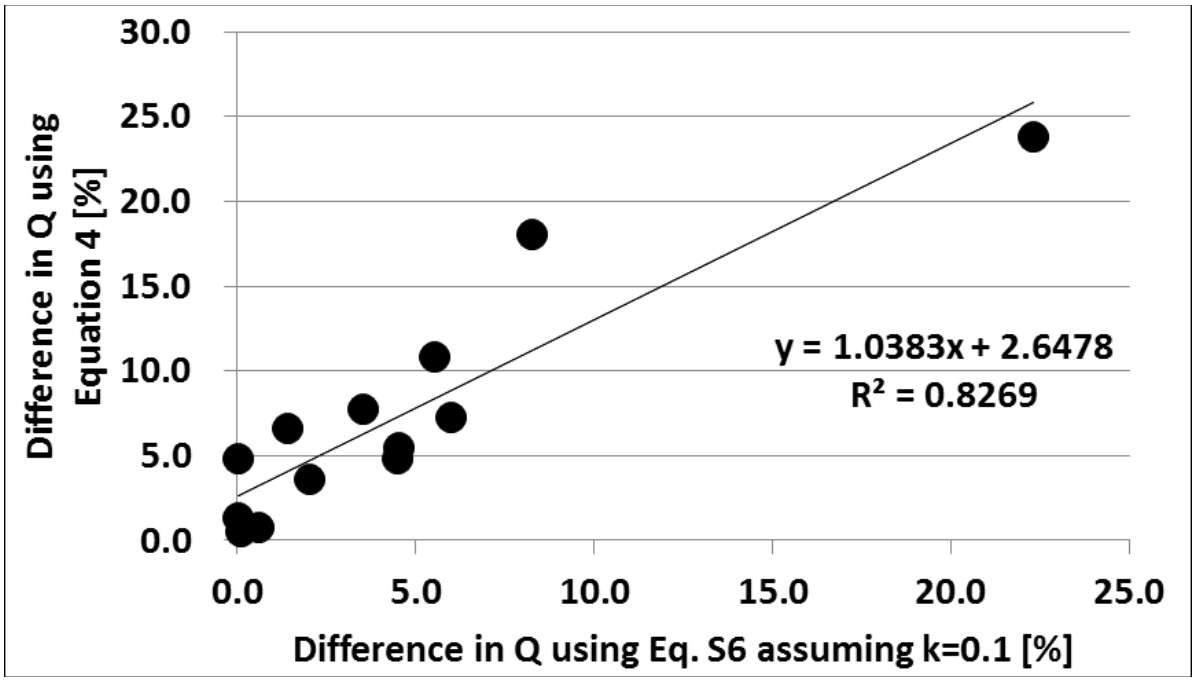


**Supplementary Figure 1.4** Relationship between relative changes in post-fire annual water yield estimated using Equation 1.4 (y-axis) and Supplementary Equation S6 assuming k=0.1 (x-axis).

**Equations**

Relative changes in annual water yield after wildfire ($\Delta Q/Q_{pre}$) is defined as Equation S1.

$$\frac{\Delta Q}{Q_{pre}} = \frac{Q_{post} - Q_{pre}}{Q_{pre}} \quad \text{(S1)}$$

where, $Q_{pre}$ and $Q_{post}$ are annual water yields for pre- and post-fire periods, respectively. Equation S1 can be expressed as Equation S2 by substituting Equation 1.2 and Equation 1.3 into Equation S1.

$$\frac{\Delta Q}{Q_{pre}} = \frac{P-(F-m)cP-\{1-F+m\}kcP-P+FcP+(1-F)kcpP}{P-FcP-(1-F)kcP} \quad \text{(S2)}$$

Where, $ET_f = cP$ and $ET_g = kET_f = kcP$. $P$ is a generic precipitation, which is the same over the watershed to measure the response via the change in landcover composition. If the major cover is forest and short vegetation including shrub, grass and crops then the overall response is due to the change in forested area. Thus, right-hand side of Equation S2 can be divided by $P$, then Equation S2 can be simplified as Equation S3.

$$\frac{\Delta Q}{Q_{pre}} = \frac{mc-mkc}{1-Fc-kc+Fkc} \quad \text{(S3)}$$

Equation S3 can be expressed as a function of permanent tree mortality ($m$), which depicts the hypothesis of this study that changes in evapotranspiration due to permanent tree mortality is one of key factors for the post-fire response of annual water yield (Equation S4):

$$\frac{\Delta Q}{Q_{pre}} = m\left\{\frac{c-kc}{1-Fc-kc+Fkc}\right\} \quad \text{(S4)}$$

Equation S4 can be re-arranged as Equation S5 by adding "+c-c" in denominator.

$$\frac{\Delta Q}{Q_{pre}} = m\left\{\frac{c(1-k)}{-Fc+Fkc+1-kc+c-c}\right\} = m\left\{\frac{c(1-k)}{-Fc(1-k)+c(1-k)+1-c}\right\} \quad \text{(S5)}$$

Numerator and denominator of Equation S5 can be divided by $c(1-k)$ and then written as:

$$\frac{\Delta Q}{Q_{pre}} = m\left\{\frac{1}{1-F+\frac{1-c}{c(1-k)}}\right\} \quad \text{(S6)}$$

Equation S6 supports the hypothesis of this study that post-fire response in annual water yield will be determined by changes in capacity of evapotranspiration of a burned watershed ($c$ and $k$) due to changes in landcover composition after wildfire ($F$ and $m$). However, it is difficult to estimate the relative efficiency of evapotranspiration of short vegetation ($k$), which is site-specific empirical parameter. Thus, Equation S6 is required to be written with other variables that are easier to estimate than the $k$.

To replace $k$ with other variables such as annual water yield and precipitation, let's recall the relationship between total evapotranspiration (left-hand side of Equation S7) and evapotranspiration via forest and short vegetation (right-hand side of Equation S7).

$$ET_{pre} = ET_f + ET_g = FcP_{pre} + (1 - F)kcP_{pre} \quad \text{(S7)}$$

Equation S7 can be divided by $P$ (Equation S8).

$$\frac{ET_{pre}}{P} = EI_{pre} = Fc + (1 - F)kc = Fc + kc - Fkc \quad \text{(S8)}$$

Equation S8 can be substituted into Equation S4 (Equation S9).

$$\frac{\Delta Q}{Q_{pre}} = m\left\{\frac{c(1-k)}{1-EI_{pre}}\right\} \quad \text{(S9)}$$

And, water budget under steady-state condition is written as Equation S10.

$$P_{pre} = ET_{pre} + Q_{pre} \quad \text{(S10)}$$

Equation S7 can be substituted into Equation S10 (Equation S11)

$$P_{pre} = cP_{pre}(F + k - Fk) + Q_{pre} \quad \text{(S11)}$$

Flow-based evaporative index ($1 - \mathrm{Q}_{pre}/\mathrm{P}_{pre}$) corresponds to $EI_{pre}$ under steady-state condition. To define flow-based evaporative index from Equation S11, let's transpose $Q_{pre}$ to the left-hand side and divide Equation S11 by $P_{pre}$ then:

$$1 - \frac{Q_{pre}}{P_{pre}} = EI_{pre} = c(F + k - Fk) \quad \text{(S12)}$$

Equation S12 can be re-arranged for c (Equation S13).

$$c = \frac{EI_{pre}}{F+k-Fk} = \frac{EI_{pre}}{1-(1-F)(1-k)} \quad \text{(S13)}$$

Equation S13 can be written for $(1-k)$ (Equation S14).

$$1-k = \left(1-\frac{EI_{pre}}{c}\right)\frac{1}{1-F} = \frac{c-EI_{pre}}{c}\frac{1}{1-F} = \frac{c-EI_{pre}}{c(1-F)} \quad \text{(S14)}$$

Equation S14 can be substituted into Equation S9 then the $k$ will be removed from the equation of relative changes in post-fire annual water yield (Equation S15).

$$\frac{\Delta Q}{Q_{pre}} = m\left\{\frac{c}{1-EI_{pre}}\frac{c-EI_{pre}}{c(1-F)}\right\} = m\left\{\frac{c-EI_{pre}}{(1-EI_{pre})(1-F)}\right\} = m\left\{\frac{1}{\frac{1-EI_{pre}}{c-EI_{pre}}(1-F)}\right\} \quad \text{(S15)}$$

$EI_{pre}$ from Equation S15 was defined as flow-based evaporative index ($1-\mathrm{Q}_{pre}/\mathrm{P}_{pre}$). Equation S15 can be expressed with $Q_{pre}$ and $P_{pre}$ instead of $EI_{pre}$ through substitution of flow-based evaporative index into Equation S15 (Equation S16).

$$\frac{\Delta Q}{Q_{pre}} = m\left[\frac{1}{(1-F)\frac{Q_{pre}}{P\left\{c-\left(1-\frac{Q_{pre}}{P_{pre}}\right)\right\}}}\right] = m\left\{\frac{1}{(1-F)\frac{Q_{pre}}{cP_{pre}-P_{pre}+Q_{pre}}}\right\} \quad \text{(S16)}$$

Equation S16 can be simplified as Equation 1.4.

$$\frac{\Delta Q}{Q_{pre}} = m\left\{\frac{P_{pre}(c-1)+Q_{pre}}{Q_{pre}(1-F)}\right\} = m\left\{\frac{P_{pre}}{Q_{pre}}\frac{(c-1)}{(1-F)} + \frac{1}{1-F}\right\} \quad (4)$$

From Equation 1.4, the term $P_{pre}-cP_{pre}$ is the amount of water released by the watershed ($Q_{forest}$) if it is fully covered by forest ($F=1$), thus Equation 1.4 could be interpreted as Equation S17.

$$\frac{\Delta Q}{Q_{pre}} = \frac{Q_{post}-Q_{pre}}{Q_{pre}} = \frac{m}{1-F}\left\{\frac{Q_{pre}-Q_{forest}}{Q_{pre}}\right\} \quad (S17)$$

# Appendix B: Supplementary Material for Chapter 2

## Tables

**Supplementary Table 2.1** Gauges and station name of burned watersheds.

| Site | Watershed ID | Gauge ID | BFI | Station Name |
|---|---|---|---|---|
| CID | 0 | 13235000 | 0.45 | South Fork Payette River at Lowman, ID |
| | 1 | 13237920 | 0.36 | Middle Fork Payette River near Crouch, ID |
| | 5 | 13309220 | 0.38 | Middle Fork Salmon River at Middle Fork Lodge near Yellow Pine, ID |
| | 6 | 13310199 | 0.40 | Middle Fork Salmon River at Mouth near Shoup, ID |
| | 7 | 13310700 | 0.42 | South Fork Salmon River near Krassel Ranger Station, ID |
| | 8 | 13313000 | 0.45 | Johnson Creek at Yellow Pine, ID |
| YNP | 0 | 06037500 | 0.75 | Madison River near West Yellowstone, MT |
| | 2 | 06186500 | 0.48 | Yellowstone River at Yellowstone Lake outlet, YNP |
| | 5 | 13010065 | 0.45 | Snake River above Jackson Lake at Flagg Ranch, WY |
| | 6 | 13011500 | 0.43 | Pacific Creek at Moran, WY |
| NCA | 3 | 11522500 | 0.28 | Salmon River at Somes Bar, CA |

**Supplementary Table 2.2** Linear regression models of the representative paired watersheds considering the fitting power (adjusted $R^2$) in case of more than one control watersheds for each burned watershed. Bold numbers represent statistically significant coefficients (confidence level>90%). DF indicates number of data points used for regression model.

| Site | Control Water-shed | Burned Watershed (Fire year) | Linear Regression Model | | | | | |
|---|---|---|---|---|---|---|---|---|
| | | | Estimation | | | DF | p-value | Adj. R2 |
| | | | **Intercept** [m3/s] | **a** [-] | **b** [m3/s] | | | |
| CID | 2 | 0 (1989) | 0.52 | 3.98 | 1.24 | 41 | <2.2E-16 | 0.954 |
| | | 6 (2000) | 3.28 | 13.76 | -1.98 | 11 | 4.00E-15 | 0.997 |
| | | 6 (2007) | 2.34 | 13.91 | 5.82 | 11 | 2.89E-08 | 0.950 |
| | 3 | 1 (2006) | -3.53 | 0.62 | -2.67 | 11 | 8.81E-07 | 0.906 |
| | | 7 (2007) | -2.76 | 0.63 | 1.12 | 19 | 9.69E-14 | 0.953 |
| | | 8 (2007) | -0.74 | 0.37 | 1.09 | 42 | <2.2E-16 | 0.930 |
| YNP | 7 | 6 (1988) | -2.15 | 0.61 | 0.73 | 43 | <2.2E-16 | 0.841 |
| NCA | 1 | 3 (2008) | 11.29 | 2.26 | 6.30 | 40 | <2.2E-16 | 0.955 |

**Supplementary Table 2.3** Summary of Budyko framework using linear equation ($EI = (k + \Delta k) \times DI$) with evaporative index ($AET/P$) and dryness index ($RNY/P$) from 1984 to 2014. Bold numbers indicate statistically significant estimations with 90% of confidence level rejecting a null hypothesis that $k_{prefire} = k_{postfire}$. Negative and positive difference between post-fire and pre-fire, $\Delta_k$, indicate increase and decrease in annual water yield after wildfire, respectively.

| Watershed (wildfire year) | Burned Area [%] | $k$ | | | Adjusted $R^2$ | |
|---|---|---|---|---|---|---|
| | | Pre-fire | Post-fire | $\Delta k$ | Pre-fire | Post-fire |
| CID0 (1989) | 16.9 | 0.344 | 0.340 | -0.004 | 0.995 | 0.997 |
| CID1 (2006) | 16.5 | 0.406 | 0.408 | 0.002 | 0.997 | 0.996 |
| CID5 (2000) | 20.6 | 0.362 | 0.352 | -0.010 | 0.996 | 0.992 |
| CID5 (2007) | 15.0 | 0.362 | 0.319 | -0.043 | 0.996 | 0.997 |
| CID6 (2000) | 17.5 | 0.353 | 0.343 | -0.010 | 0.996 | 0.990 |
| CID6 (2007) | 12.5 | 0.353 | 0.308 | -0.045 | 0.996 | 0.996 |
| CID7 (1994) | 15.8 | 0.340 | 0.338 | -0.002 | 0.997 | 0.995 |
| CID7 (2007) | 67.9 | 0.340 | 0.323 | -0.017 | 0.997 | 0.997 |
| CID8 (1994) | 15.9 | 0.359 | 0.363 | 0.004 | 0.997 | 0.994 |
| CID8 (2007) | 54.5 | 0.359 | 0.330 | -0.029 | 0.997 | 0.998 |
| YNP2 (1988) | 40.2 | 0.426 | 0.418 | -0.008 | 0.998 | 0.998 |
| YNP5 (1988) | 74.4 | 0.376 | 0.344 | -0.032 | 0.998 | 0.996 |
| YNP6 (1988) | 56.9 | 0.375 | 0.354 | -0.021 | 0.996 | 0.998 |
| NCA3 (1987) | 19.8 | 0.4445 | 0.4447 | 0.0002 | 0.998 | 0.997 |
| NCA3 (2008) | 26.9 | 0.4445 | 0.430 | -0.015 | 0.998 | 0.997 |

## Figures

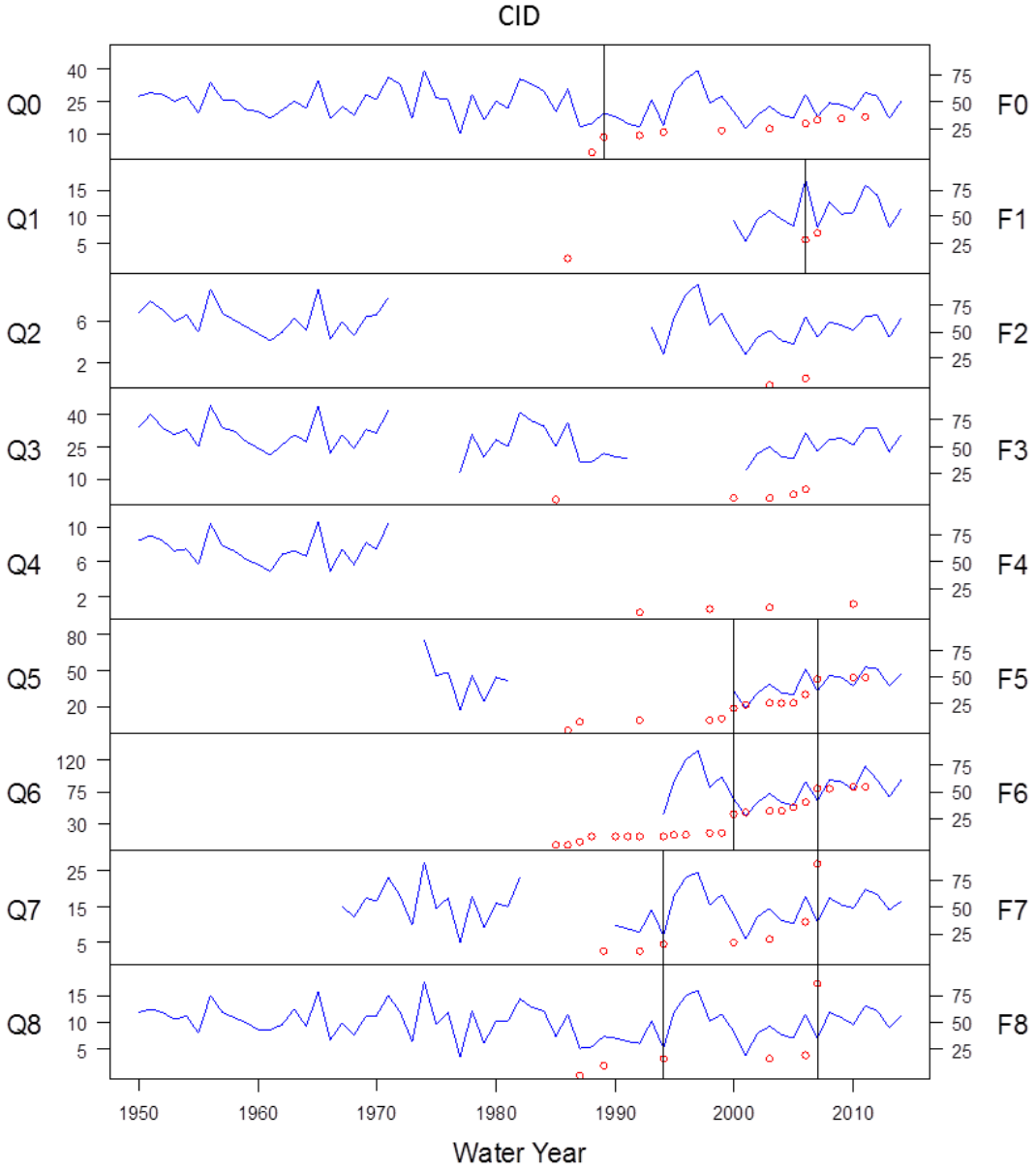


**Supplementary Figure 2.1** Annual water yield (Q [m3/s]; blue-line) and cumulative percent burned area (F [%]; red-dot) of the study sites CID. Vertical reference lines indicate major wildfire years. 16.9% of CID0 was burned in 1989; 16.5% of CID1 was burned in 2006; 20.6% and 15.0% of CID5 was burned in 2000 and 2007; 17.5% and 12.5% of CID6 was burned in 2000 and 2007; 15.8% and 67.9% of CID7 was burned in 1994 and 2007; and 15.9% and 54.5% of CID8 was burned in 1994 and 2007.

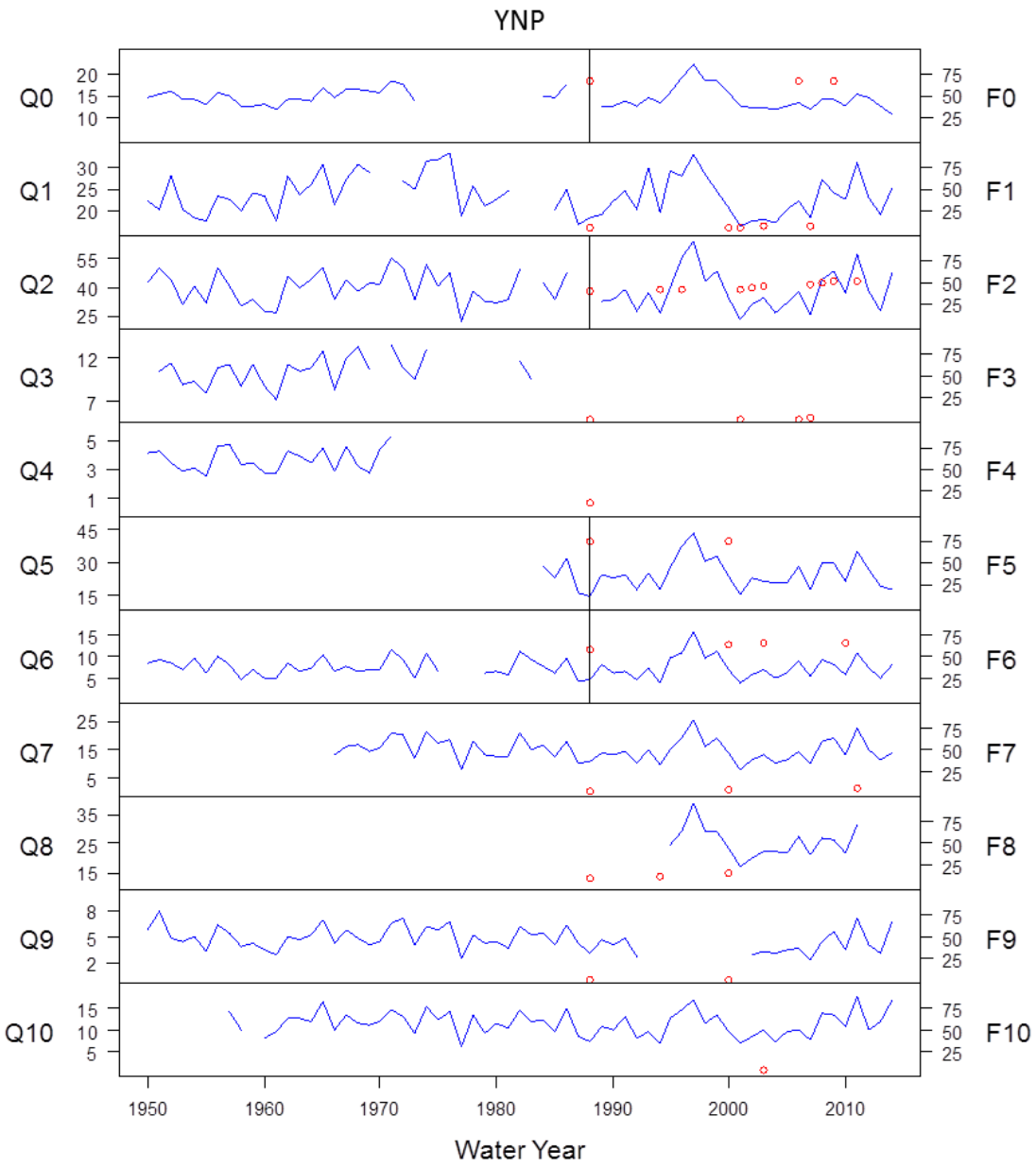


**Supplementary Figure 2.2** Annual water yield (Q [m3/s]; blue-line) and cumulative percent burned area (F [%]; red-dot) of the study sites YNP. Vertical reference lines indicate major wildfire years. 40.2% of YNP2, 74.4% of YNP5 and 56.9% of YNP6 were burned in 1988.

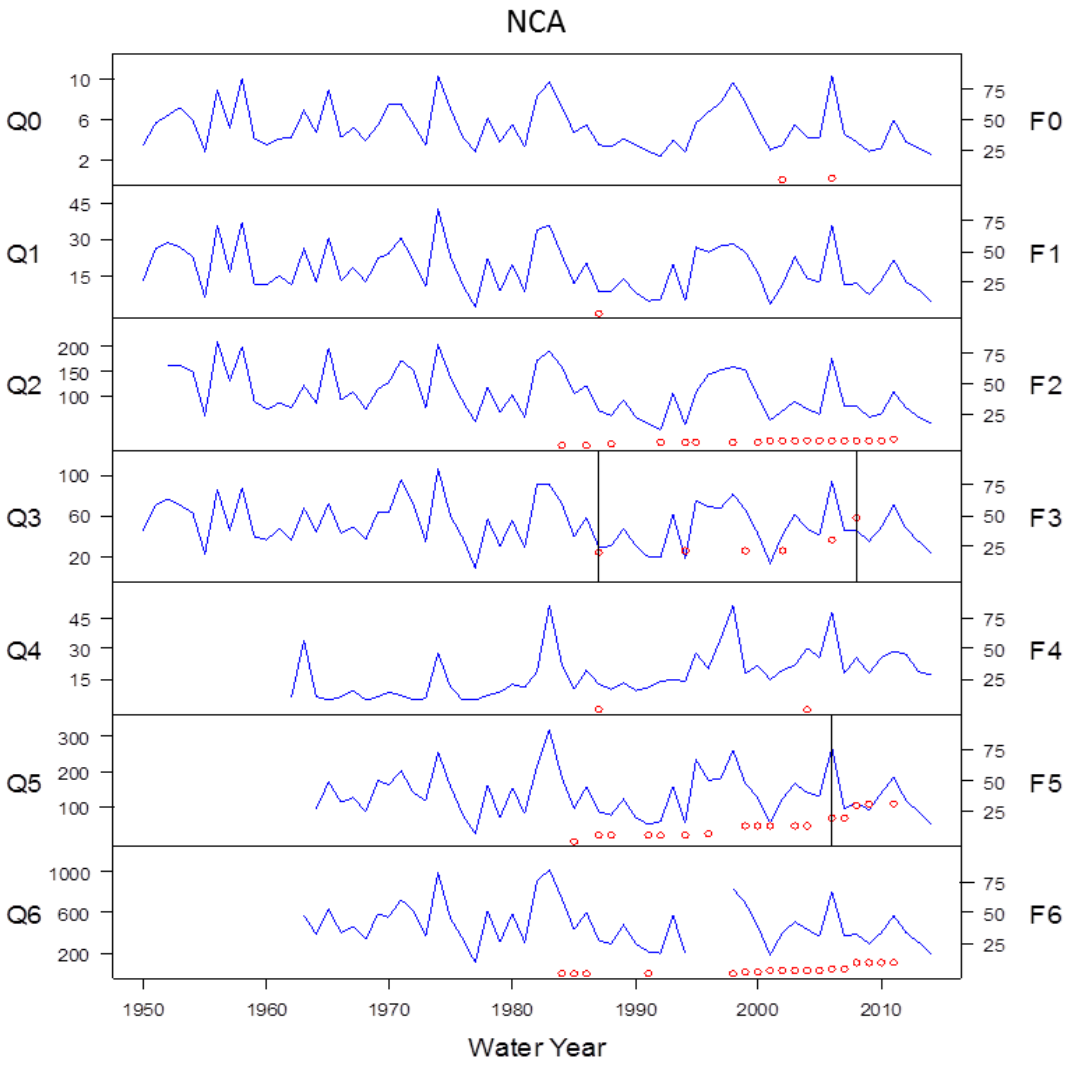


**Supplementary Figure 2.3** Annual water yield (Q [m3/s]; blue-line) and cumulative percent burned area (F [%]; red-dot) of the study sites NCA. Vertical reference lines indicate major wildfire years. 26.9% of NCA3 was burned in 1987 and 2008.

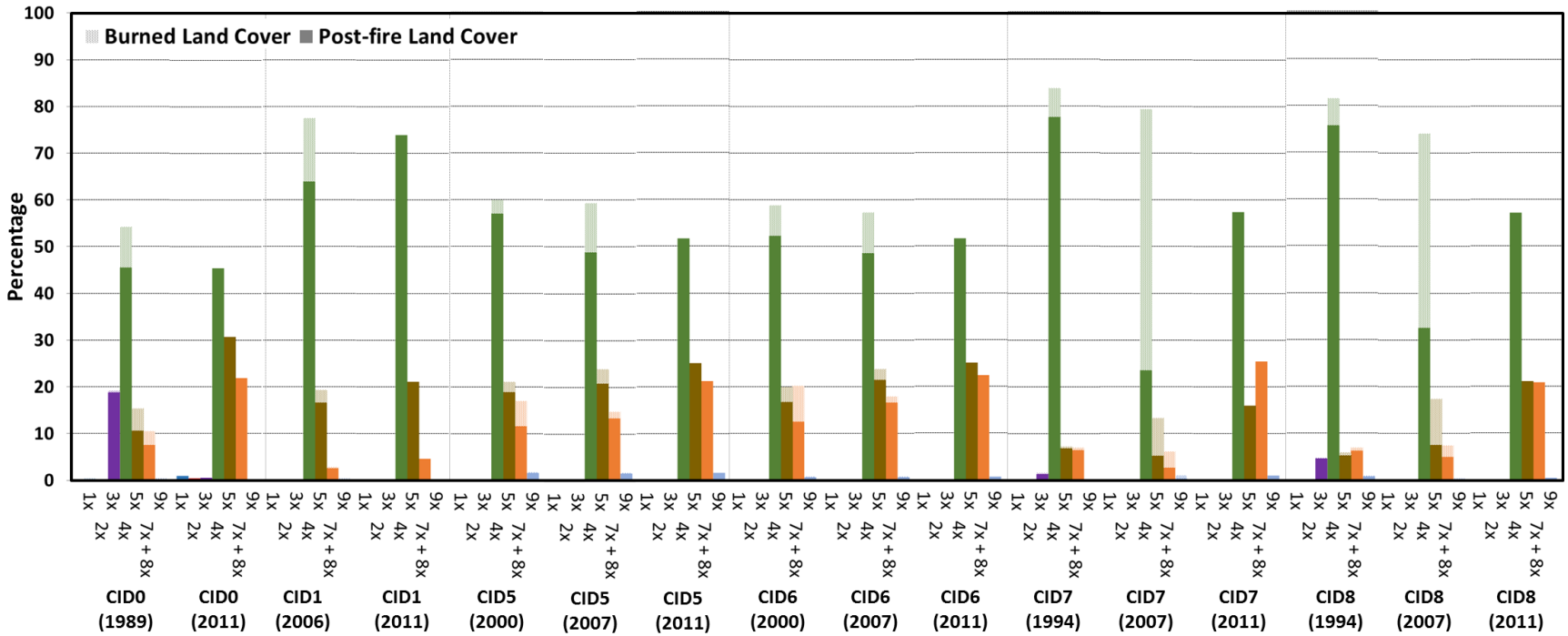


**Supplementary Figure 2.4** Fraction of burned and unburned land cover type and land cover composition after wildfire which is available recent observation in CID. Solid colored and mosaic bars are percentage of unburned and burned land cover type after wildfire, respectively. Numbers in parenthesis indicate major fire year at each burned watershed. NLCD 1992 was used for wildfires in 1987, 1988, 1989 and 1994; NLCD 2001 was used for wildfire in 2000; NLCD 2006 was used for wildfires in 2006, 2007 and 2008. 1x (blue): water body and perennial snow, 2x (red): developed area, 3x (purple): barren, 4x (green): forest, 5x (brown): shrubland, 7x+8x (orange): grassland and cultivated crop, 9x (sky blue): wetlands.

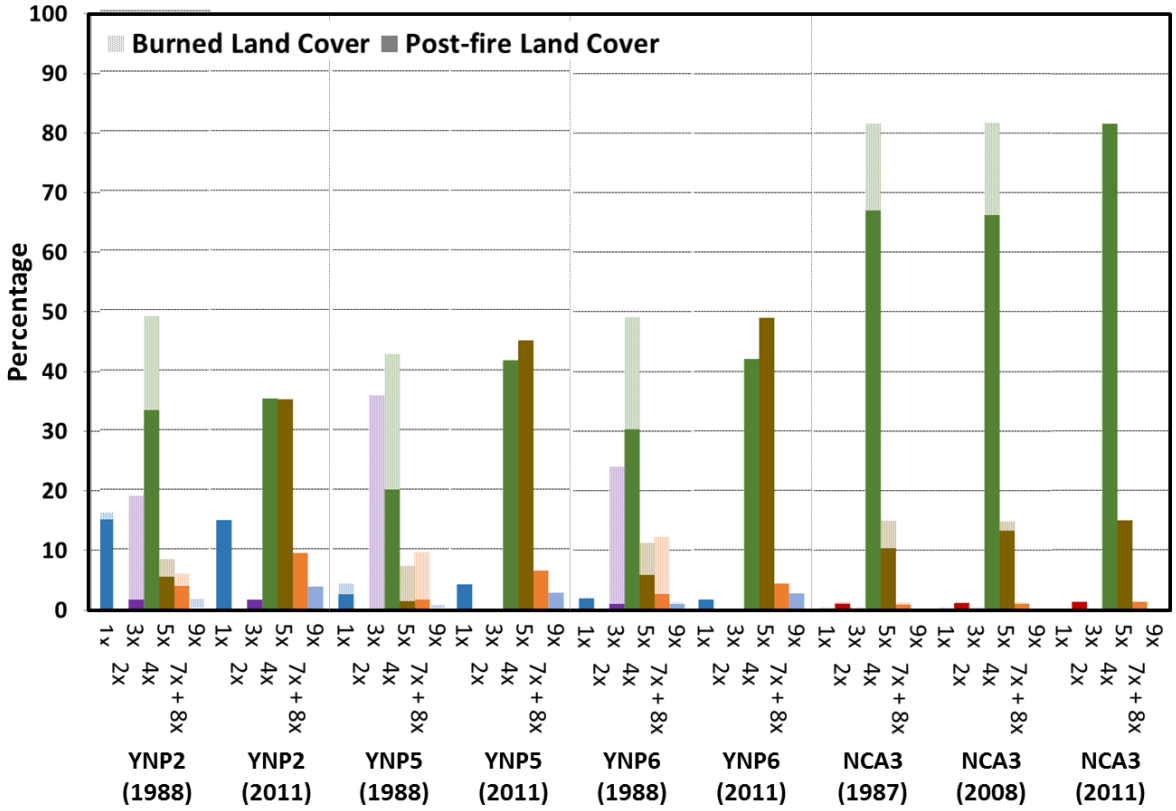


**Supplementary Figure 2.5** Fraction of burned and unburned land cover type and land cover composition after wildfire which is available recent observation in YNP and NCA. Solid colored and mosaic bars are percentage of unburned and burned land cover type after wildfire, respectively. Numbers in parenthesis indicate major fire year at each burned watersheds. NLCD 1992 was used for wildfires in 1987, 1988, 1989 and 1994; NLCD 2001 was used for wildfire in 2000; NLCD 2006 was used for wildfires in 2006, 2007 and 2008. 1x (blue): water body and perennial snow, 2x (red): developed area, 3x (purple): barren, 4x (green): forest, 5x (brown): shrubland, 7x+8x (orange): grassland and cultivated crop, 9x (sky blue): wetlands.

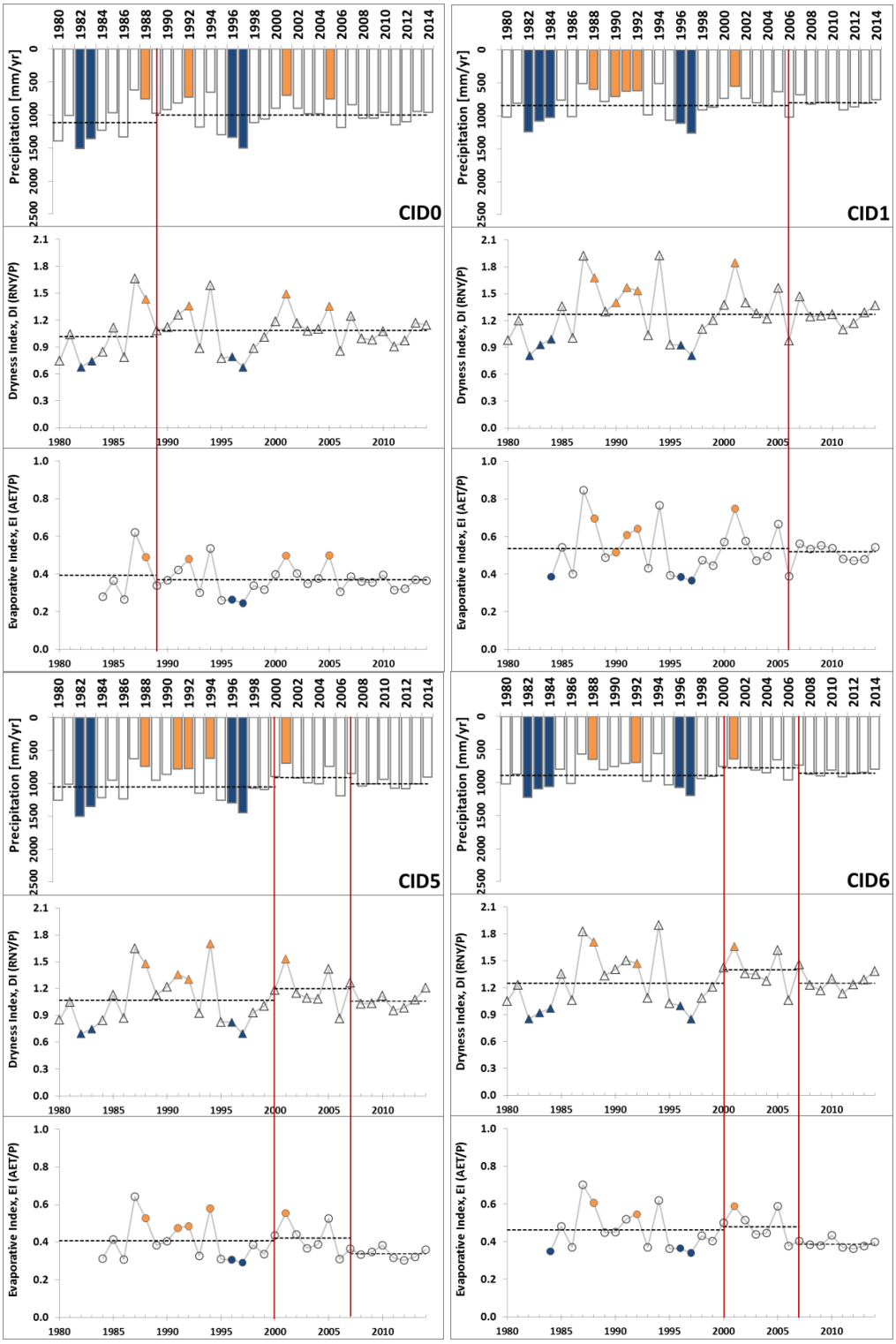


**Supplementary Figure 2.6** Precipitation (P, mm/year), dryness index (RNY/P) and evaporative index (AET/P) from WY 1980 to WY 2014 (x-axis). Vertical intercepts indicate wildfire year. Dashed lines indicate average of each variable for pre- and post-fire periods. Blue, orange colored and opened markers indicate wet (SPI>=1), dry (SPI=<-1) and normal (-1<SPI<1) water year according to SPI (Standardized Precipitation Index; (McKee *et al.*, 1993)), respectively.

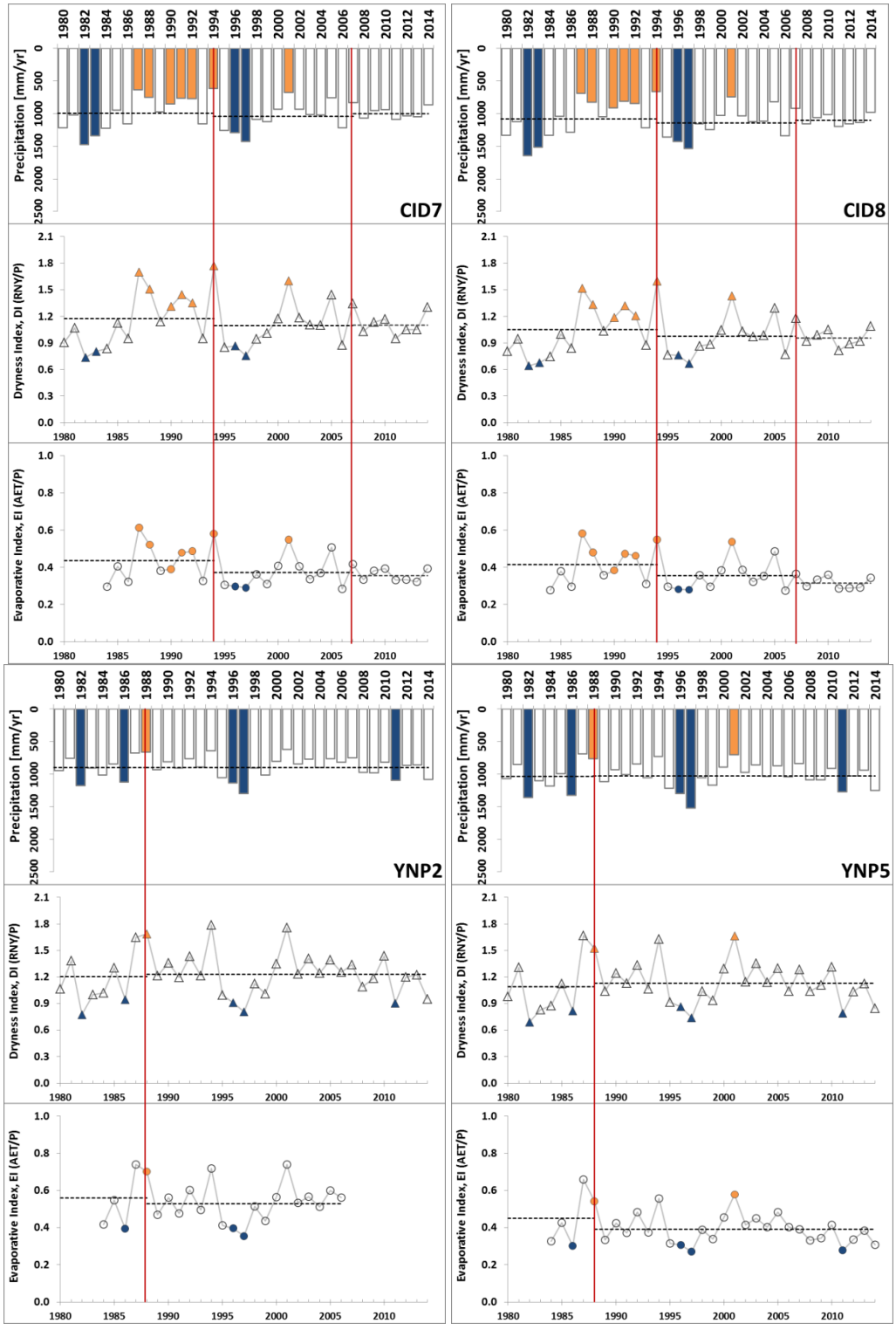


**Supplementary Figure 2.6** Continue.

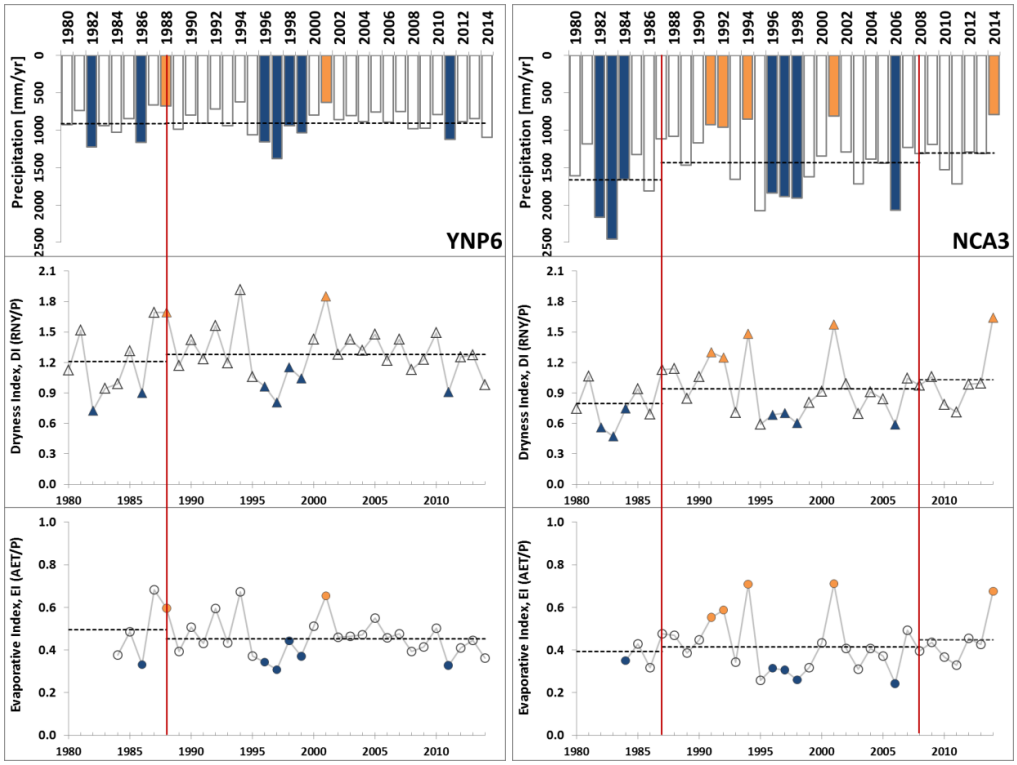


**Supplementary Figure 2.6** Continue.

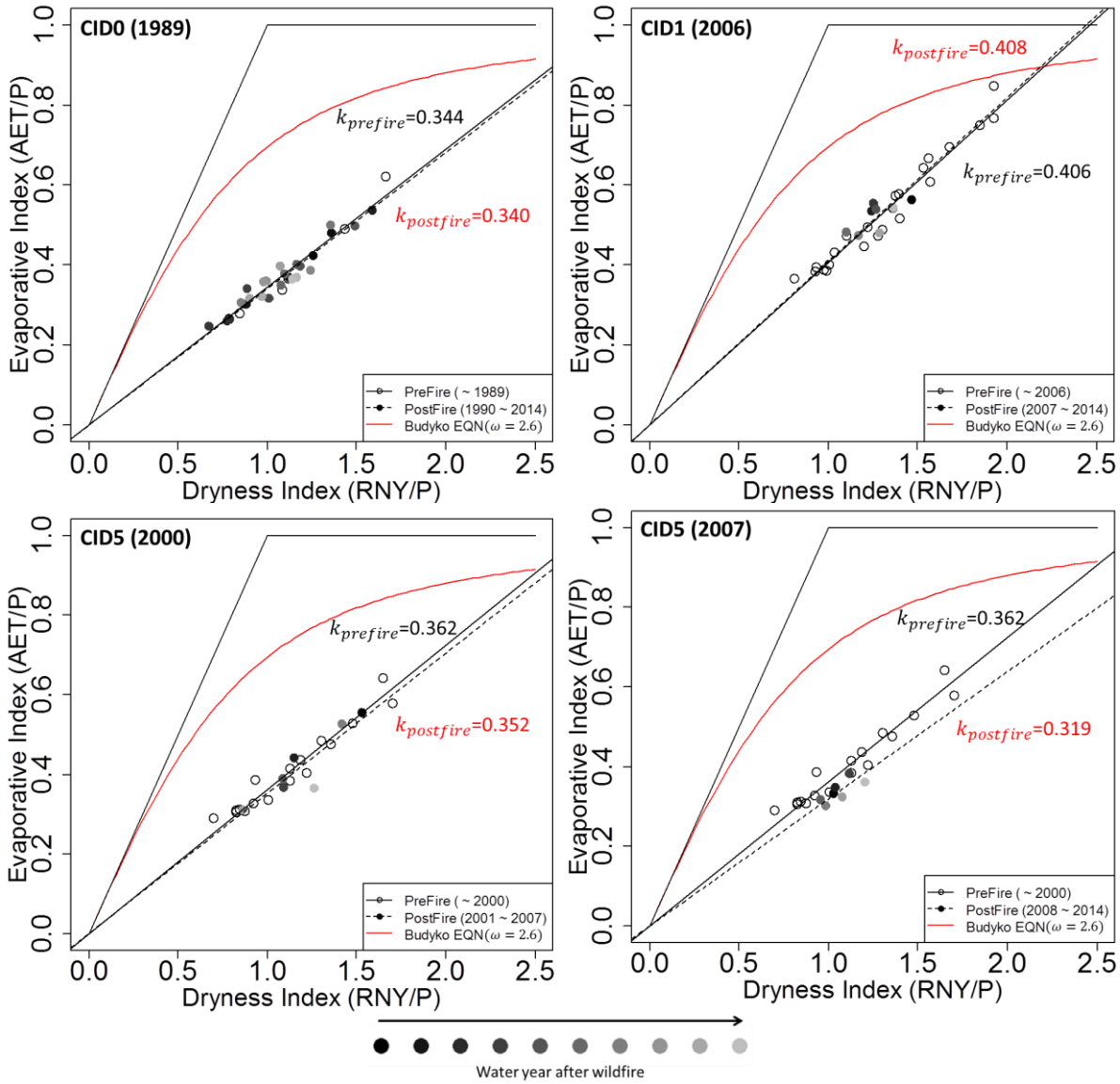


**Supplementary Figure 2.7** Budyko framework using linear equation with evaporative index ($AET/P$) and dryness index (RNY/P) from 1984 to 2014 in burned watersheds where wildfire effects on annual water yield were statistically significant from paired watershed analysis. Numbers in bracelets indicate wildfire year. Open circles and filled circles indicate scatter between EI and DI during pre- and post-fire period, respectively. Continuous and dashed lines are fitted linear equation ($EI = (k + \Delta k) \times DI$) using least square method for pre- and post-fire period, respectively. $k$ and $\Delta k$ are empirical parameter of the linear model for the water and energy balance and wildfire induced changes in empirical parameter, respectively. Red colored curve is a Fu's equation for original Budyko framework with $\omega = 2.6$.

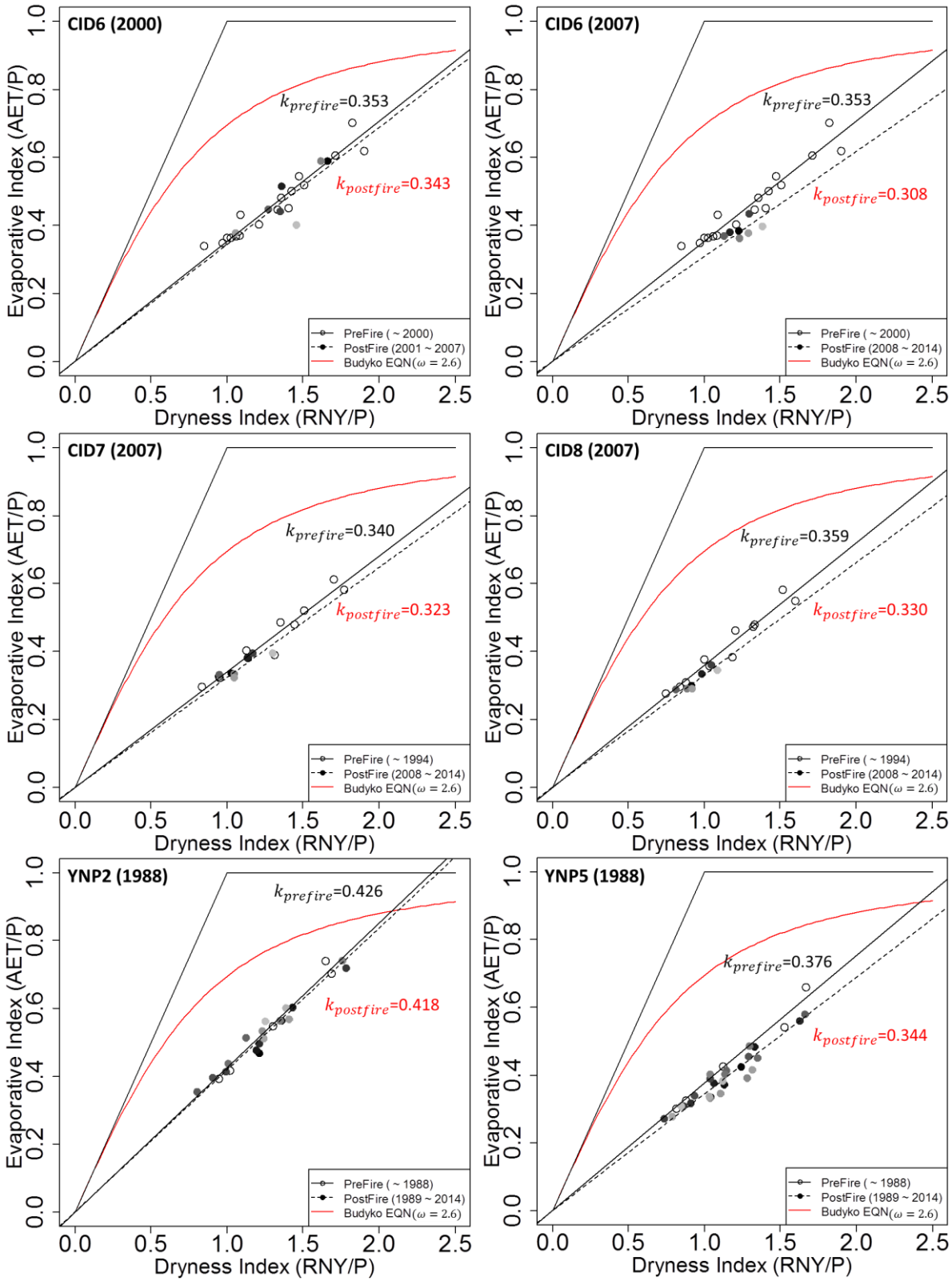


**Supplementary Figure 2.7** Continue.

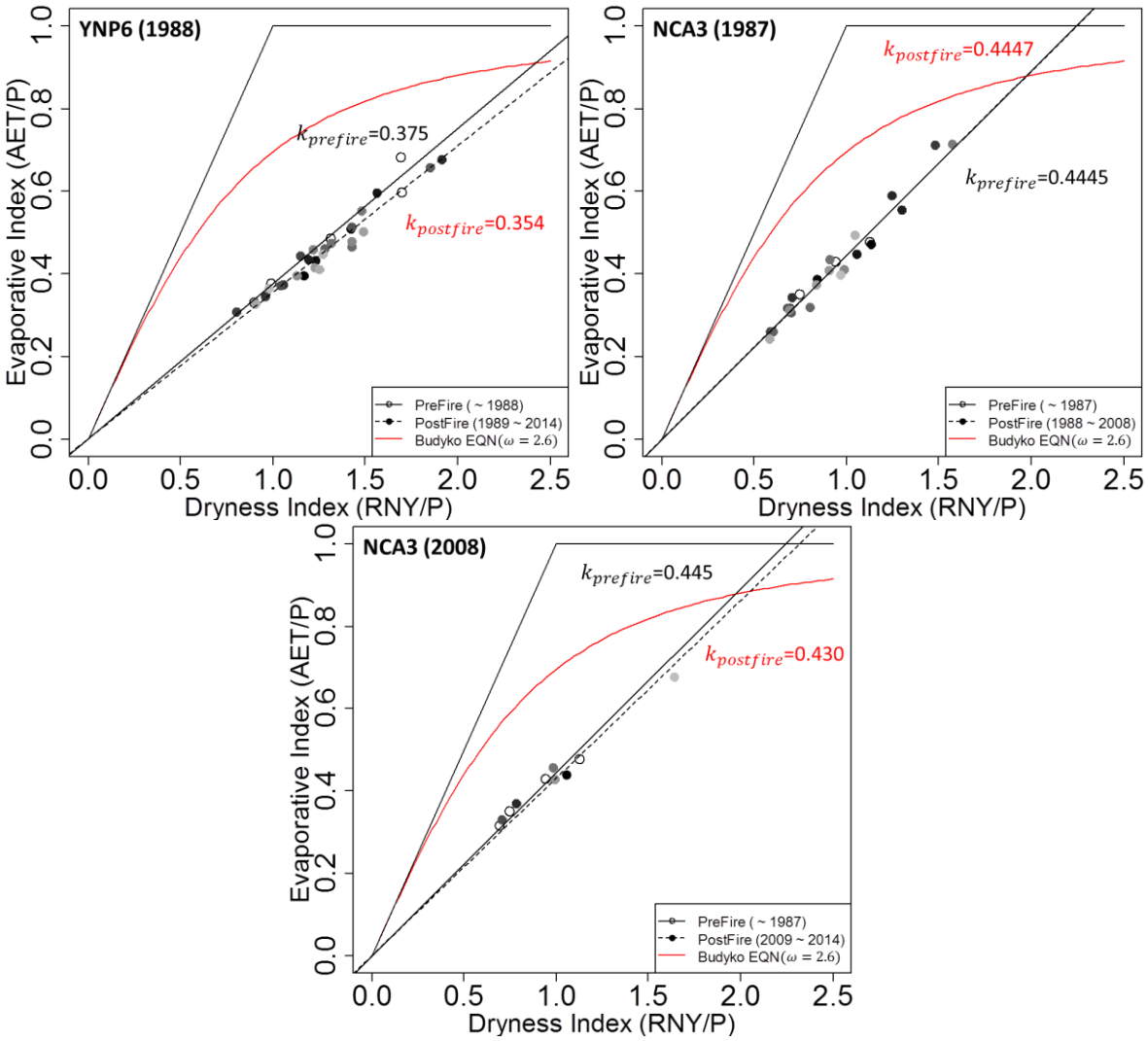


**Supplementary Figure 2.7** Continue.

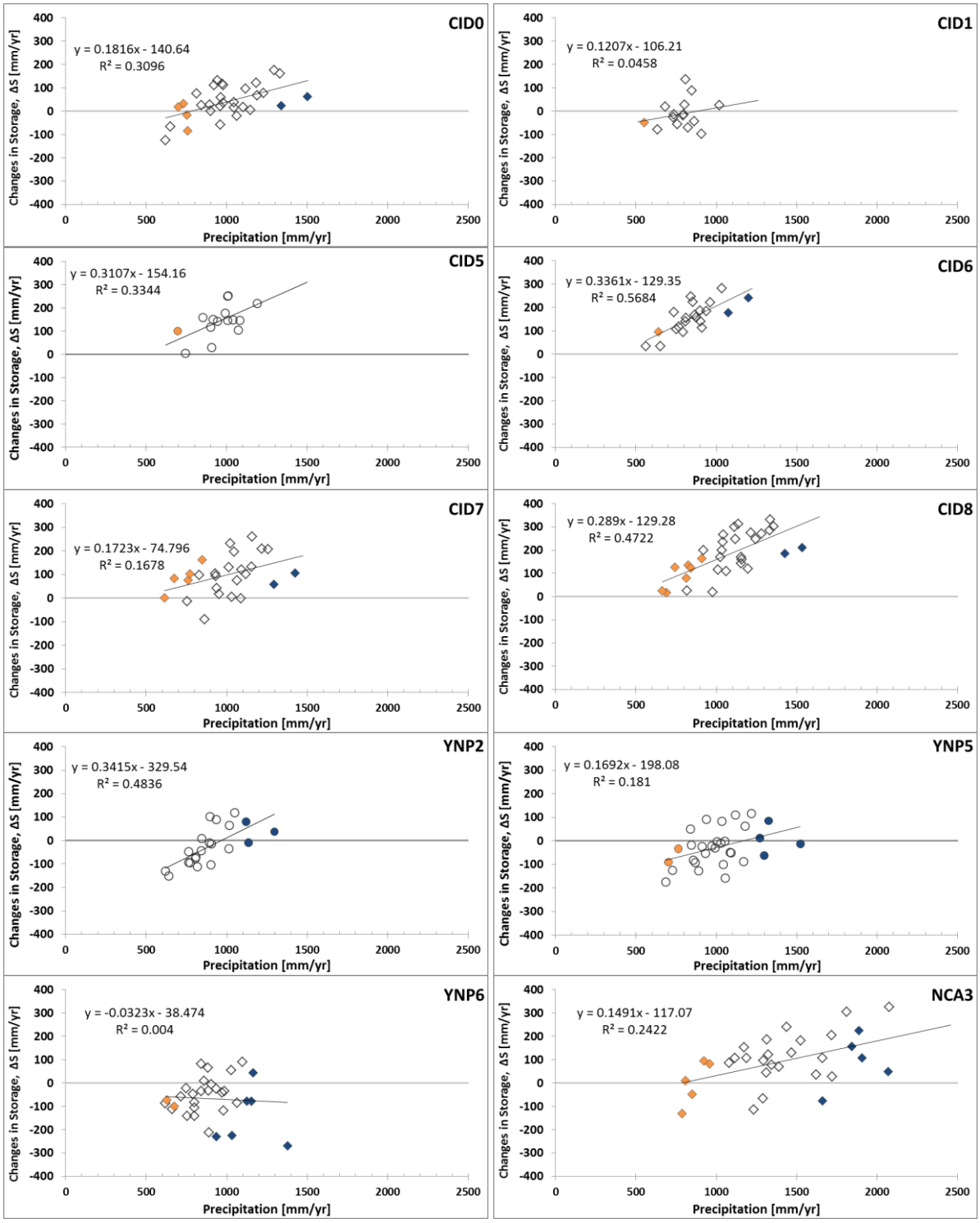


**Supplementary Figure 2.8** Changes in storage (P-Q-AET) following precipitation of burned watersheds. Orange and blue colored markers represent dry or wet water year based on SPI.

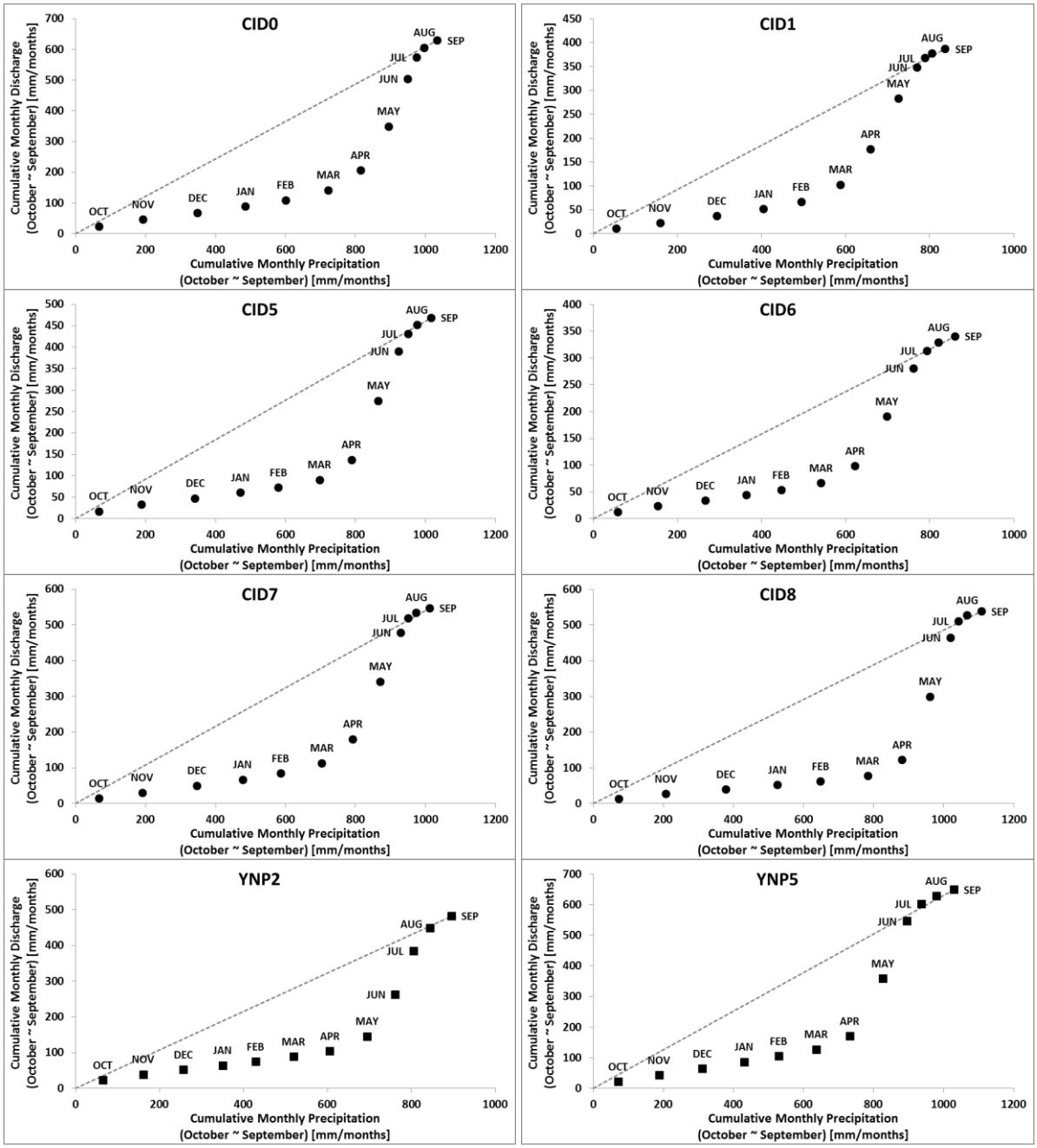


**Supplementary Figure 2.9** Double mass curves of cumulative precipitation and annual water yield of monthly mean value through the study period (WY 1980 ~ WY 2014).

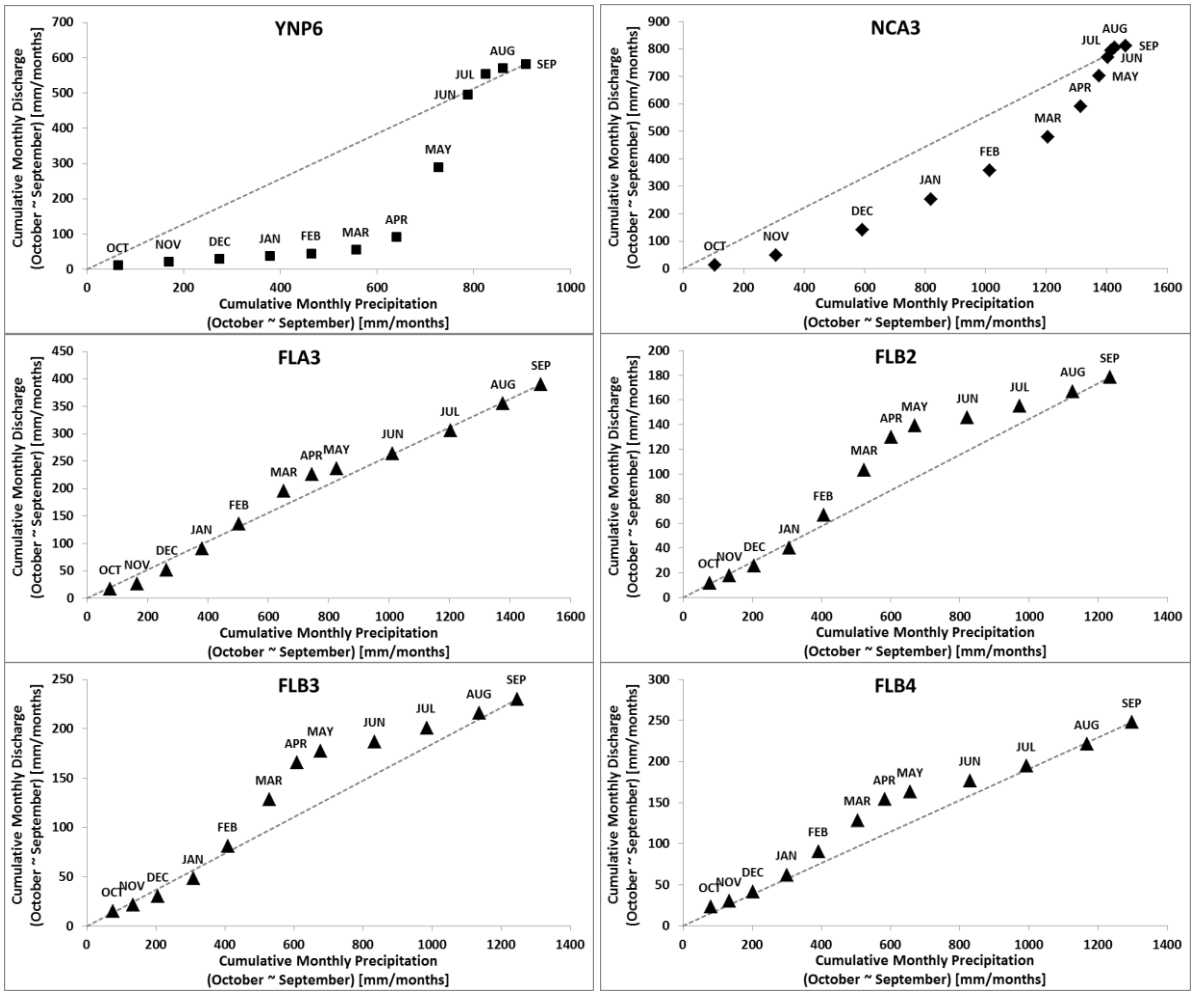


**Supplementary Figure 2.9** Continue.

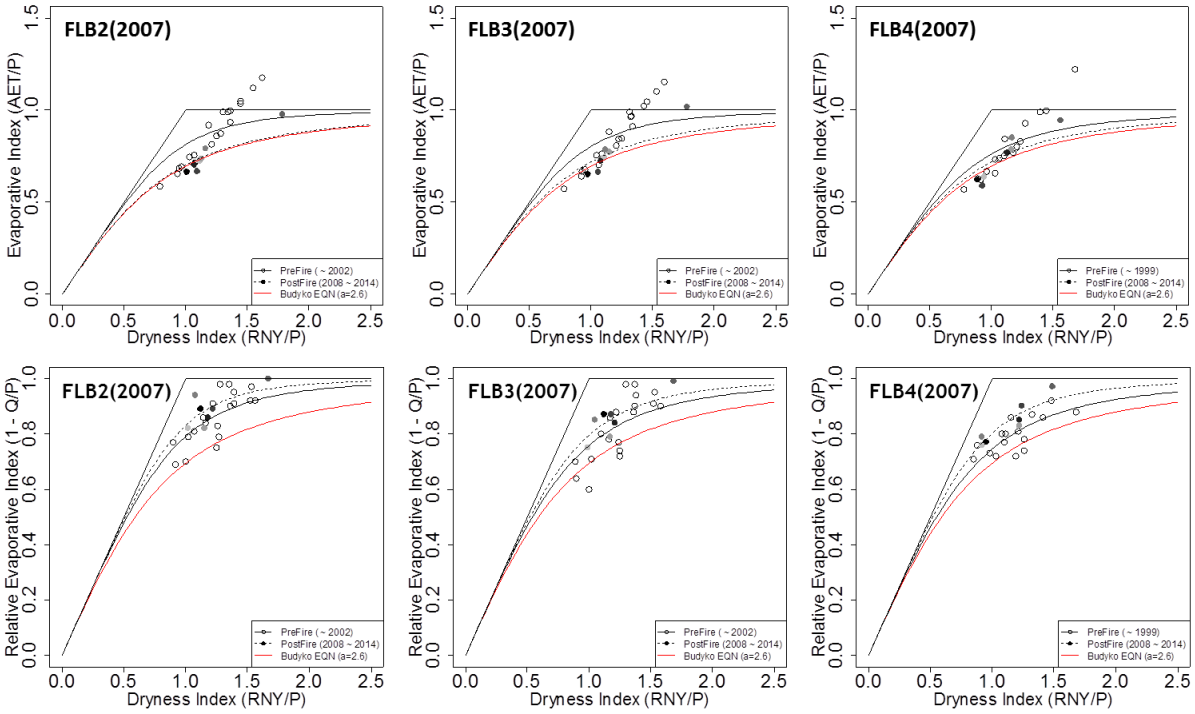


**Supplementary Figure 2.10** Budyko framework using Fu's equation with yearly time scale of evaporative index (AET/P) and dryness index (RNY/P) (Top panel) and with yearly time scale of flow-based evaporative index (1-Q/P) and dryness index (RNY/P) (bottom panel).